UNIVERSIDAD POLITÉCNICA DE MADRID

ESCUELA TÉCNICA SUPERIOR
DE INGENIEROS DE TELECOMUNICACIÓN

MÁSTER UNIVERSITARIO EN INGENIERÍA DE TELECOMUNICACIÓN

TRABAJO FIN DE MÁSTER

DESIGN OF A CLOSED-LOOP NEUROSTIMULATION SYSTEM FOR THE TREATMENT OF CEREBROVASCULAR DISORDERS.

Almudena Calatrava Moreno

2026

MÁSTER UNIVERSITARIO EN INGENIERÍA DE TELECOMUNICACIÓN

TRABAJO FIN DE MÁSTER

Título: **Design of a closed-loop neurostimulation system for the treatment of cerebrovascular disorders.**

Autor: Dña. Almudena Calatrava Moreno

Tutor: D. Alvaro Araujo Pinto

Departamento: Departamento de Ingeniería Electrónica.

MIEMBROS DEL TRIBUNAL

Presidente: D. José Manuel Pardo Muñoz

Vocal: D. Alberto Almendra Sánchez

Secretario: D. Pablo Ituero Herrero

Suplente: Dña. Jimena Olivares Roza

Los miembros del tribunal arriba nombrados acuerdan otorgar la calificación de: 10.

Madrid, a 20 de febrero de 2026

UNIVERSIDAD POLITÉCNICA DE MADRID

ESCUELA TÉCNICA SUPERIOR DE INGENIEROS DE TELECOMUNICACIÓN

MÁSTER UNIVERSITARIO EN INGENIERÍA DE TELECOMUNICACIÓN

TRABAJO FIN DE MÁSTER

DESIGN OF A CLOSED-LOOP NEUROSTIMULATION SYSTEM FOR THE TREATMENT OF CEREBROVASCULAR DISORDERS.

ALMUDENA CALATRAVA MORENO

2026

RESUMEN

El presente trabajo se desarrolla en el marco del proyecto STRIKE. Este proyecto es el resultado de una colaboración entre el B105 Electronic Systems Lab de la Universidad Politécnica de Madrid, el Laboratorio de Neuro-computación y neuro-robótica de la Universidad Complutense de Madrid y la empresa Bioactive Surfaces S.L. STRIKE tiene como objetivo integrar tres técnicas durante la recuperación del ictus: la implantación de células mesenquimales, la estimulación magnética transcraneal y la estimulación del nervio vago en la rama auricular.

El objetivo principal de este Trabajo Fin de Máster es el diseño de un sistema de neuroestimulación en bucle cerrado capaz de realizar la estimulación eléctrica y, de forma simultánea, la monitorización de señales fisiológicas para el control adaptativo de dicha estimulación.

Para alcanzar este objetivo, se han desarrollado cuatro módulos que conforman el sistema: un módulo de adquisición de señales electrofisiológicas como el electrocardiograma o el electroencefalograma; un módulo de procesado de señales, encargado de la extracción y el análisis de parámetros relevantes de la señal del electrocardiograma; un módulo de estimulación eléctrica, responsable de implementar las estrategias de control de la estimulación; y un módulo de comunicaciones con el dispositivo, que permite la recepción de datos de adquisición y la actualización de parámetros.

El desarrollo del sistema se ha llevado a cabo a través de las siguientes fases: análisis de datos experimentales, diseño y validación del algoritmo de procesado, estudio de los dispositivos electrónicos disponibles, programación de los módulos de adquisición, estimulación y comunicaciones, el diseño y construcción de un prototipo funcional y finalmente, el diseño de experimentos y la ejecución en diferentes escenarios para la validación del dispositivo.

El resultado es un sistema preliminar de neuroestimulación adaptable y configurable, que facilita las tareas de estimulación y control en proyectos como STRIKE.

SUMMARY

This work is developed within the framework of the STRIKE project. This project is the result of a collaboration between the B105 Electronic Systems Lab of the Universidad Politécnica de Madrid, the *Grupo de Neuro-computación y neuro-robótica* of the Universidad Complutense de Madrid and the company Bioactive Surfaces S.L. This project aims to integrate three techniques during stroke recovery: mesenchymal cell implantation, transcranial magnetic stimulation and vagus nerve stimulation in the auricular branch.

The main objective of this Master's Thesis is the design of a closed-loop neurostimulation system capable of performing electrical stimulation and, simultaneously, the monitoring of physiological signals for the adaptive control of said stimulation.

To achieve this objective, four modules have been developed to constitute the system: an electrophysiological signal acquisition module, capable of acquiring biological signals such as the electrocardiogram or electroencephalogram; a signal processing module, responsible for the extraction and analysis of relevant parameters from the electrocardiogram signal; an electrical stimulation module in charge of implementing stimulation control strategies; and a device communication module, which enables the reception of acquired data and the updating of system parameters.

The development of the system has been carried out through the following phases: analysis of experimental data, design and validation of the processing algorithm, study of the available electronic devices, programming of the acquisition, stimulation and communications modules, the design and construction of a functional prototype and finally, the design of experiments and execution in different scenarios for the validation of the device.

The result is a preliminary adaptable and configurable neurostimulation system, which facilitates stimulation and control tasks in projects such as STRIKE.

PALABRAS CLAVE

Electrocardiograma, señales biológicas, electrofisiología, dispositivo biomédico, estimulación, nervio vago, ictus, ictus isquémico, sistema embebido, INTAN, MSP430, código abierto, BLE, SPI.

KEYWORDS

Electrocardiogram, biological signals, electrophysiology, biomedical device, stimulation, vagus nerve, stroke, ischemic stroke, embedded system, INTAN, MSP430, open source, BLE, SPI.

AGRADECIMIENTOS

A mamá, por la paciencia y el respeto.

A papá, por intentar entenderlo.

A los dos, por dejarme elegir y darme la oportunidad de formarme, eternamente agradecida.

A Ode, porque siempre serás mi hermano.

A los abuelos, los cuatro, porque sé que estáis orgullosos.

A Carmen, por ser y por estar.

A Araujo, por el esfuerzo.

Al B105, por todo lo que me sigue dando y lo que queda por dar.

Al equipo de STRIKE, porque la ciencia va pasito a pasito.

Al Cheeto, por seguir formando equipo.

A la Fira, por un “vfale” más.

Y a mí, porque hemos cerrado otra etapa.

Enhorabuena Almudena de 18, lo has conseguido.

INTEX OF CONTENT

FIGURES

ABBREVIATIONS

ABVN	Auricular Branch Vagus Nerve
AC	Alternating Current
ADC	Analog to Digital Converter
ANS	Autonomic Nervous System
ASIC	Application Specific Integrated Circuit
aVNS	Auricular Vagus Nerve Stimulation
BLE	Bluetooth Low Energy
BPM	Beats Per Minute
CCS	Code Composer Studio
CED	Cambridge Electronic Design
CNS	Central Nervous System
CSV	Comma Separated Values
CTB	Centro de Tecnología Biomédica
CVA	Cerebrovascular Accident
cVNS	Cervical Vagus Nerve Stimulation
DC	Direct Current
DSP	Digital Signal Processing
ECG/EKG	Electrocardiogram / Elektrocardiogram
EEG	Electroencephalogram
FIR	Finite Impulse Response
FSM	Finite State Machine
GUI	Graphical User Interface
HAL	Hardware Abstraction Layer
HW	Hardware
IIR	Infinite Impulse Response
LSB	Least Significant Bit
MSB	Most Significant Bit
NCP	NeuroCybernetic Prosthesis
OSR	Oversampling Ratio
PCB	Printed Circuit Board
PNS	Peripheral Nervous System
SD16	Sigma Delta of 16 bits
SNS	Somatic Nervous System
SPI	Serial Peripheral Interface
SW	Software
tDCS	Transcranial Direct Current Stimulation
TMS	Transcranial Magnetic Stimulation
UCM	Universidad Complutense de Madrid
UPM	Universidad Politécnica de Madrid
VNS	Vagus Nerve Stimulation
WHO	World Health Organization
WPI	World Precision Instruments

1. INTRODUCTION AND OBJECTIVES

This chapter presents an introduction explaining the project where this work has been developed and the objectives established for this work.

1.1. INTRODUCTION

This section provides an overview of the STRIKE project and its context. It begins by describing the project's purpose and introduces the multidisciplinary team and collaborating institutions involved. The text also outlines the methodology adopted and specifies the organizational structure and workflow. Finally, it presents the scientific background on stroke, its clinical relevance, and the therapeutic strategies explored in STRIKE, as well as the rationale for integrating the techniques under a closed-loop monitoring approach. The structure of the report is presented at the end of this section.

1.1.1. STRIKE PROJECT

The present work has been carried out within the framework of the STRIKE project, which falls under the category of oriented research, as its primary objective is the resolution of a specific problem: the treatment of ischemic stroke. This research area is aligned with one of the priority themes established in the "Plan Estatal de Investigación Científica y Técnica y de Innovación 2021-2023" [1].

INTRODUCTION

Stroke, or cerebrovascular accident, is a brain disorder that causes a partial or total reduction of blood flow to the brain. This neurological condition is the second leading cause of death worldwide and, in Spain, it is the primary cause of death among women and the third among men [2] [3]. Furthermore, it is the main cause of disability in Spain, where 50% of patients suffer long-term sequelae or die. For these reasons, despite its incidence having decreased in recent years, the increasing average age of the population and the rise in life expectancy make stroke an ever-growing problem.

Currently, therapies focus on reperfusion (restoration of blood flow) to the penumbra areas (or affected regions) within a very limited time window of approximately 4.5 hours from the onset of the stroke [4] [5]. After this initial phase, physical rehabilitation is carried out. Since neurological recovery is limited, it is essential to continue researching new strategies to complement existing treatments, aiming to protect and repair the consequences of this condition [6].

PROJECT TEAM

The project team is composed of a multidisciplinary group that includes electronic engineers, materials engineers, physicists, biologists, among others, all working under the framework of the project from the Comunidad de Madrid MINA-CM (P2022/BMD-7236). The MINA-CM initiative aims to develop biomedical neurotechnologies for R+D+I applications focused on nervous system pathologies, as well as enhancing brain capabilities and interconnection through physical and functional interfaces. These objectives are pursued through multidisciplinary and inter-institutional collaborations.

The STRIKE project originates from the collaboration between research groups from Universidad Complutense de Madrid (UCM), Universidad Politécnica de Madrid (UPM), and the company Bioactive Surfaces S.L.

This project is being carried out at the following locations:

- B105 Electronic Systems Lab, Departamento de Ingeniería Electrónica (DIE), UPM.
- Centro de Tecnología Biomédica (CTB - UPM), affiliated with UPM.
- Laboratories of the Neuro-computación and Neuro-robótica group at UCM.

METHODOLOGY

Throughout the development of this project, the SCRUM methodology has been employed. SCRUM is an agile framework designed to manage complex projects through iterative and incremental development. It emphasizes collaboration, adaptability, and continuous improvement by organizing work into short cycles called sprints, where teams plan, execute, and review tasks to deliver value progressively.

The working team consists of five members: the Scrum Master (Dr. Alvaro Araujo), the Product Owner (Dr. Atocha Guedán), and the development team (Ana Carretero, Flor Negrete and Almudena Calatrava).

Within this framework, each participant defines the tasks to be completed before the next meeting or sprint (held every two weeks in this case), estimating the time required for each task. A total of 35 sprints were carried out during the development of the present work, starting on the 25th of September 2024 and concluding on the 3rd of February 2026.

PROJECT PARTS

The STRIKE project seeks to evaluate the synergistic effects of three treatments for this disease: transcranial magnetic stimulation, implantation of mesenchymal stem cells encapsulated in silk fibroin, and electrical stimulation of the auricular branch of the vagus nerve. The overall objective of the project is to study the impact of these three approaches on immune response modulation and brain recovery in cases of cerebral ischemia.

TRANSCRANIAL MAGNETIC STIMULATION (TMS)

Transcranial Magnetic Stimulation (TMS) is a non-invasive procedure that causes magnetic fields to stimulate neurons in the brain. Within the STRIKE project, two types of devices have been distinguished: single-coil systems with adjustable pulse parameters and multichannel systems that employ multiple coils to improve control over field orientation and colocation. It should be noted that the use of TMS in humans has already been validated [7].

MESENCHYMAL STEM CELL IMPLANTATION

Numerous studies have demonstrated that stem cell implantation promotes functional recovery and supports brain repair and protection [8] [9] [10]. To enhance cell survival, research is being conducted on their encapsulation within biomaterial scaffolds. In the STRIKE project, scaffolds are fabricated using silk fibroin and mesenchymal stem cells are employed as therapeutic approach for ischemic stroke, based on positive results obtained in murine models.

AURICULA VAGUS NERVE STIMULATION (AVNS)

Bioelectronic medicine is emerging as an alternative to pharmaceutical treatments for multiple diseases. In recent years, vagus nerve stimulation (VNS) has gained significant interest, and stimulation of its auricular branch (aVNS) is considered a promising therapy in humans [11].

The present work focuses on auricular vagus nerve stimulation, which is further detailed in section 2.2.3 Vagus Nerve Stimulation.

CLOSED-LOOP APPROACH

Both vagus nerve stimulation [12] [13] [14] and mesenchymal stem cell implantation [5] [15] [16] [17] have demonstrated immunomodulatory capabilities, producing anti-inflammatory effects and promoting greater neuronal recovery in stroke models. Auricular vagus nerve stimulation is proposed in this project as an additional mechanism to stem cell implantation.

Encapsulation of mesenchymal stem cells in silk fibroin gels increases their survival rate [18] [19] [20]. Moreover, advances have been made in the use of transcranial magnetic stimulation for both prediction and post-stroke treatment [21]. Based on this premise, the aim is for both stimulation

techniques to influence the metabolism of implanted mesenchymal stem cells, enhancing their anti-inflammatory and neuroprotective effects in a cerebral stroke model.

To verify the efficacy of electrical and magnetic stimulation, it is necessary to monitor their impact on the subject. This requires the acquisition of neurological and electrocardiographic signals to assess the physiological response in real time. Such information enables the development of personalized treatments for each patient, depending on their individual response to stimulation, thereby optimizing the therapeutic effect.

1.1.2. STRUCTURE OF THE REPORT

The structure of this work is divided into eight chapters. The first chapter presents the conceptual framework, introducing the fundamental biological concepts, including stroke, the vagus nerve, and the electrocardiogram, as well as the requirements to be fulfilled by the prototype developed in this work. The second chapter describes the system design, starting with the overall closed-loop architecture and continuing with the hardware and software designs. The third chapter presents the implementation of the closed-loop system from both hardware and software perspectives. The fourth chapter presents the test conducted to verify the correct operation of the device. The fifth chapter describes the experiments designed for the validation of the prototype. The sixth chapter presents the experimental results obtained for the validation of the prototype. The seventh chapter presents the conclusions and future research directions. Finally, the last chapter defines five appendices, which include ethical, economic, social and environmental aspects, as well as the configuration functions designed for the INTAN device and the results of the experiments conducted throughout the development of this work.

1.2. OBJECTIVES

The primary objective of this work is to design and develop a closed-loop, adaptable system that enables the execution and analysis of experiments involving vagus nerve stimulation in its auricular branch on rodents (mouse), within the scope of the STRIKE project.

1.2.1. SPECIFIC OBJECTIVES

To achieve this goal, the following specific objectives have been established:

1. To define the functional and technical requirements of a closed-loop neurostimulation system aligned with the needs of the STRIKE project.
2. To establish generic specifications for electrical stimulation and biological signal acquisition systems applicable to related research projects.
3. To design a modular closed-loop system architecture for electrical stimulation and physiological signal monitoring.
4. To develop configurable hardware and software solution for stimulation and acquisition based on commercial and custom electronic components.
5. To validate the correct operation of the proposed system through experimental characterization and testing within the STRIKE project framework.

1.2.2. TASKS

The following tasks were carried out in order to accomplish the defined objectives:

1. Analysis of the STRIKE project requirements and derivation of system specifications.
2. Identification of common needs in related electrical stimulation and biological signal acquisition projects.
3. Study of the INTAN device operation and identification of the configuration and control functions required.
4. Implementation and verification of the INTAN configuration and control functions.
5. Design of the functional modules of the closed-loop system and definition of their responsibilities.
6. Analysis and implementation of pending configuration functions of the MSP430 within the Hardware Abstraction Level, including the timing module.
7. Electronic design implementation using a prototyping platform.
8. Software development to enable the integrated operation of the closed-loop system.
9. Verification of the prototype functionality and characterization of stimulation and acquisition performance.
10. Design of validation experiments for hardware connections and software implementation.
11. Execution of the defined experiments for system validation.
12. Analysis of the experimental results obtained within the STRIKE project.

2. CONCEPTUAL FRAMEWORK

This chapter contains four sections, the first one presents the main concepts of stroke disease: what it is, what types there are, what are the phases or stages of this disease and what treatments exist.

In the second part, the main concepts of the vagus nerve are presented, starting with an anatomical context to locate it and its characteristics, the types of stimulation that exist and the relationship that this stimulation has with stroke recovery are also presented.

The third section presents the electrocardiogram, beginning with an explanation of the anatomy of the heart and the formation of the electrocardiogram signal. This biological signal is of great relevance in the context of vagus nerve stimulation, as such stimulation can induce variations in the characteristics of the electrocardiogram.

Finally, the requirements are presented at a general level, as well as the requirements that must be met when generating the stimulation (depending on the type of experiments to be carried out), and the acquisition requirements.

2.1. STROKE

This section presents the main concepts associated with stroke, including its primary classification, the stages of treatment, and the existing therapeutic approaches.

2.1.1. DEFINITION, TYPES AND STAGES

Stroke, or cerebrovascular accident (CVA), results from a disruption in cerebral blood circulation that temporarily or permanently alters the functioning of one or more regions of the brain [22].

In 2019, the World Health Organization (WHO) identified stroke as the second leading cause of death worldwide, accounting for 11% of all deaths [23]. It is the most common disease among individuals over 55 years of age and one of the main causes of functional disability in the adult population. Among stroke survivors, one-third experience permanent sequelae or physical and cognitive impairments [24].

There are several types of stroke depending on the underlying cause of the lesion. Figure 1 illustrates a classification scheme for stroke types. The primary classification divides strokes into two categories: ischemic stroke and hemorrhagic stroke. The difference between these two types lies in the cause of the interruption of blood flow to the brain [25].

- Ischemic stroke occurs when a clot or debris obstructs blood flow to the brain.
- Hemorrhagic stroke occurs when a blood vessel ruptures, causing bleeding in the brain region.

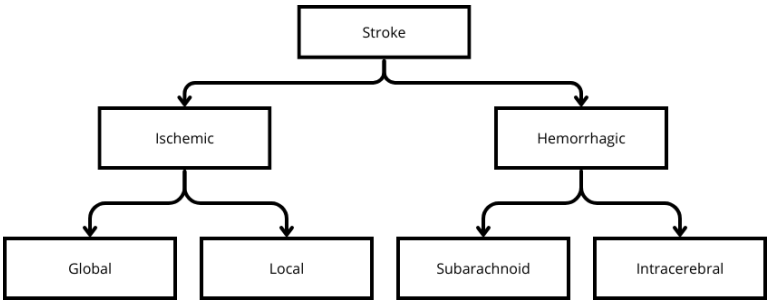

Figure 1 Classification of stroke types.

More than 80% of strokes are ischemic in origin [24]. The immediate consequences on brain tissue depend on the degree of blood flow reduction, which can lead to rapid cell death (infraction). When cerebral ischemia occurs, cellular destruction begins and may evolve into a hemorrhagic stroke due to delayed reperfusion (restoration of blood flow).

This work focuses on ischemic stroke. The rationale behind this choice lies in its high prevalence and clinical relevance, as presented a high percentage (80%) of all strokes are ischemic in origin.

Consequently, research on ischemic stroke addresses the largest patient population affected by this condition and offers the greatest potential for impact in terms of therapeutic innovation and recovery strategies.

There are three stages in the stroke rehabilitation process, depending on the time elapsed since the onset of the condition [24]. Figure 2 illustrates a basic timeline of the phases involved in stroke treatment. The most critical phase is the acute phase, where the medical interventions and measures taken during the initial hours will determine the chances of recovery.

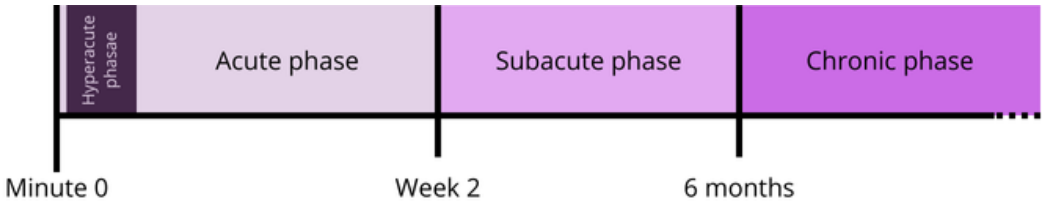

Figure 2 Basic chronology when stroke treatment.

2.1.2. TREATMENTS

Depending on the type of stroke being treated, different therapeutic strategies are employed [26]. In this section, only the treatments for ischemic stroke are discussed, as this type is the focus of the study.

For ischemic stroke, treatment is divided into two distinct phases [26]. In the initial phase, the primary goal is to achieve reperfusion, or restoration of blood flow, as quickly as possible to minimize the extent of brain damage [27]. Among the treatments used during this stage are intravenous thrombolysis and mechanical thrombectomy [26].

In addition to these therapies, there are other approaches known as Neuromodulation Therapies, such as transcranial direct current stimulation (tDCS) [28] and Transcranial Magnetic Stimulation (TMS) which seek to exploit neuronal plasticity (the brain's ability to recover and reorganize neural connections) [29].

2.2. VAGUS NERVE

This section presents the basic biology fundamentals related to the vagus nerve, with the aim of providing the necessary context to understand the role of the vagus nerve in the work within the STRIKE project.

2.2.1. ANATOMICAL CONTEXT

The nervous system is primarily composed of two types of cells: neuronal cells (neurons) and glial cells. The vertebrate nervous system, and therefore the human nervous system, is anatomically classified into two groups: the central nervous system (CNS) and the peripheral nervous system (PNS). Figure 3 shows a diagram representing the CNS and the different branches of the PNS. The CNS and PNS communicate with the brain through cranial nerves (or cranial pairs) and with the spinal cord via spinal nerves [30]. In addition to anatomical classification, there is another classification based on functionality: the autonomic nervous system (ANS) and the somatic nervous system (SNS).

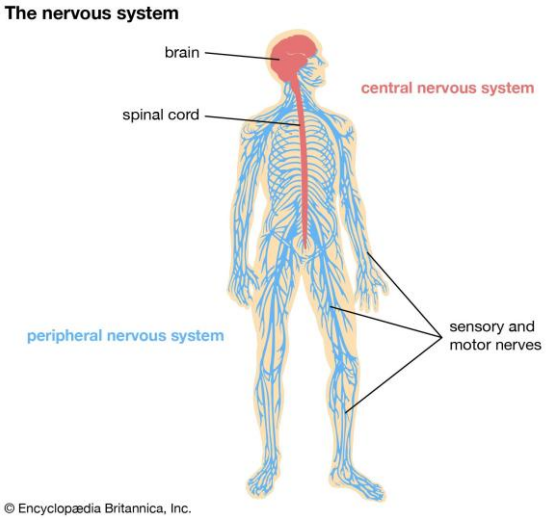

Figure 3 Human nervous system.

2.2.2. CHARACTERISTICS

The vagus nerve belongs to the tenth cranial pair (cranial nerve X) and is the longest cranial nerve in the nervous system. It originates in the medulla oblongata of the brainstem and exits the skull, dividing into two main branches: the superior trunk and the inferior trunk [31].

The branch of interest for this work is the Auricular Branch of the Vagus Nerve (ABVN), located in the cymba of the ear. Figure 4 illustrates the anatomy of the human ear, highlighting in purple the ABVN region.

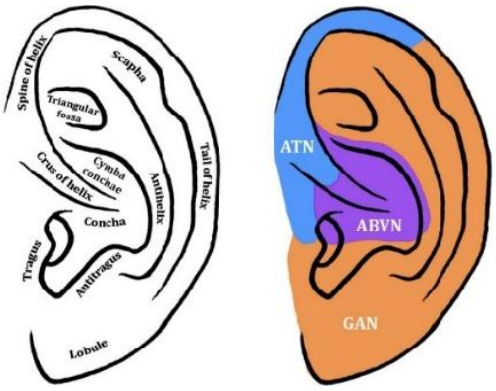

Figure 4 Ear's anatomy. ABVN: Auricular Branch of Vagus Nerve (in purple). ATN: Auricular Temporal Nerve. GAN: Great Auricular Nerve.

The vagus nerve contains two different fiber tracts. Approximately 20% of the fibers are efferent, responsible for transmitting signals from the brain to the organs, thereby regulating their activity. The remaining 80% are afferent fibers, which transmit sensory signals from the body to the brain. Thanks to these two types of fibers and their functions, the vagus nerve serves as a bidirectional communication channel between the brain and the body [31].

2.2.3. VAGUS NERVE STIMULATION

Vagus Nerve Stimulation (VNS) refers to any technique that stimulates the vagus nerve, ranging from manual massage over the carotid artery to electrical stimulation [32].

Studies conducted during the 1930s and 1940s on electrical VNS demonstrated that this type of stimulation influenced brain electrical activity, even producing anticonvulsant effects [33]

From this point onward, the term VNS will refer exclusively to electrical stimulation. This technique is employed for therapeutic purposes in the treatment of refractory epilepsy, treatment-resistant chronic depression [34], chronic headaches and obesity [35].

CERVICAL REGION

Depending on the region of the vagus nerve targeted for stimulation, different physiological effects are observed. Below, two regions of the vagus nerve that can be stimulated are presented, along with some devices used for stimulation in these areas.

Stimulation on the right cervical region has been shown to reduce convulsive activity in both animals and humans [36]. Devices such as CardioFit INOVATE-HF system (BioControl Medical Ltd, Yehud, Israel) are used for the treatment of heart failure [37]. This device connects invasively to the right cervical vagus nerve.

On the other hand, left cervical stimulation, which is the most common clinical application, is used to treat seizures caused by epilepsy [35]. This typically involves the surgical implantation for a programmable pulse generator, such as the NeuroCybernetic Prosthesis (NCP) systems (Cyberonics, Inc. Houston, TX, USA) [38].

An example of a non-invasive stimulation device approved by the European Union for treating headaches, migraines, and other conditions is gammaCore (electroCore LLC, Basking Ridge, NJm USA) [39].

Figure 5 shows the CardioFit device and the AspireSR and SenTiva devices, and the non-invasive gammaCore device.

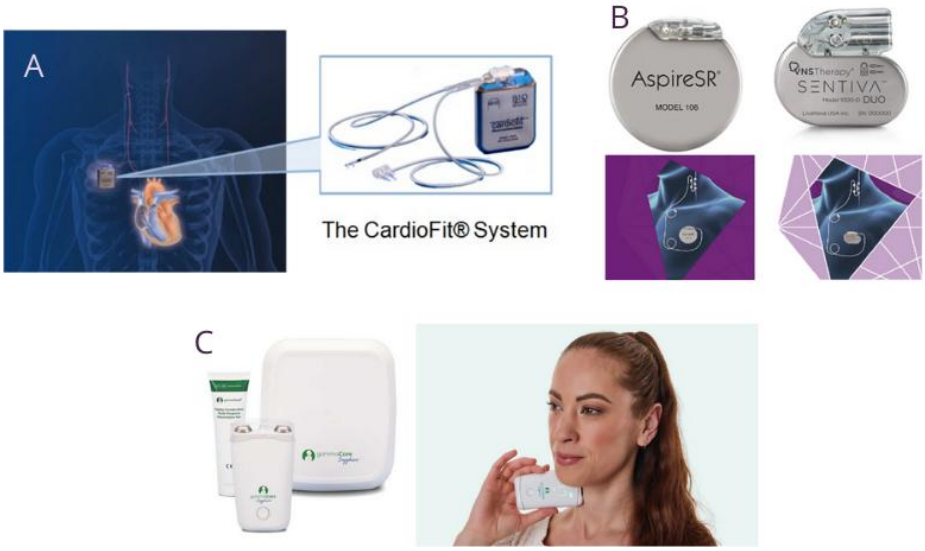

Figure 5 Devices used for VNS. A: CardioFit System [37]. B: AspireSR and SenTiva [38]. C: gammaCore [39].

2.3. ELECTROCARDIOGRAM

In this work, the electrocardiogram (ECG) is employed as a tool to monitor cardiac responses during vagus nerve stimulation (VNS) in rodents. Understanding the physiological basis of cardiac electrical activity and the technical aspects of ECG acquisition is essential for interpreting these responses.

In his section, first, the electrical anatomy of the heart is described. Next, the electrocardiogram is introduced as a tool for recording cardiac activity. Then, a review of the methods of acquiring electrocardiogram signals in rodents is introduced. Finally, the relationship between electrocardiogram measurements and vagus nerve stimulation is presented, highlighting the changes in heart rate observed during its application.

2.3.1. HEART

The heart is the organ responsible for pumping blood throughout the body [40]. The movements of the heart occur due to electrical impulses that originate and propagate through its conduction system. This system can be compared to a network of cables transmitting microcurrents in an organized manner [40]. Figure 6 presents a diagram of the heart's electrical conduction system.

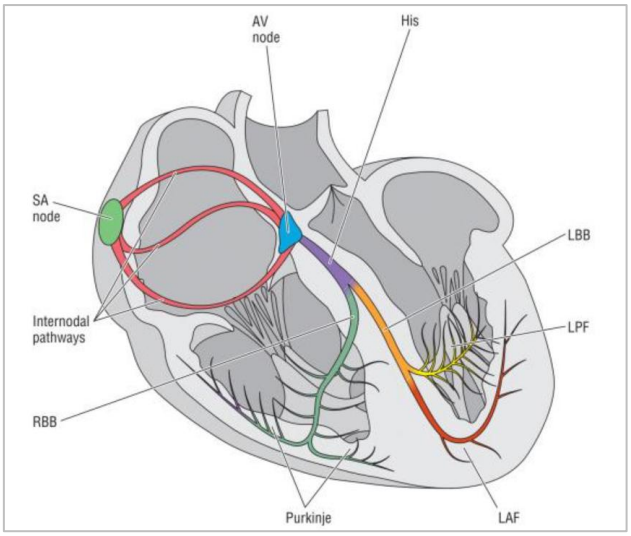

Figure 6 Electrical anatomy of the heart.

2.3.2. ELECTROCARDIOGRAM

The electrocardiogram (ECG or EKG, from German *Electrokardiogram* in reference to its inventor William Einthoven) is considered one of the main diagnostic tests in medicine. It is a graphical representation of the heart's electrical activity over time. This electrical activity reveals deflections (ECG waves) corresponding to the propagation of electrical impulses through the heart's structures [41].

PARAMETERS AND INTERPRETATION

A typical ECG displays the repetition of three main electrical events: atrial depolarization (P wave), ventricular depolarization (QRS complex), ventricular repolarization (T wave) [42].

This set of waves is shown in Figure 7-A. It is important to note that conclusions drawn from human ECG analysis cannot be fully extrapolated to other animals (in this work, the animals of interest are rodents, specifically mice) [43] [42]. Additionally, depending on the type of anesthesia used, the parameters presented in this section may be affected [42]. Figure 7-B illustrates the relationship between the ECG signal and atrial/ventricular depolarization and repolarization times.

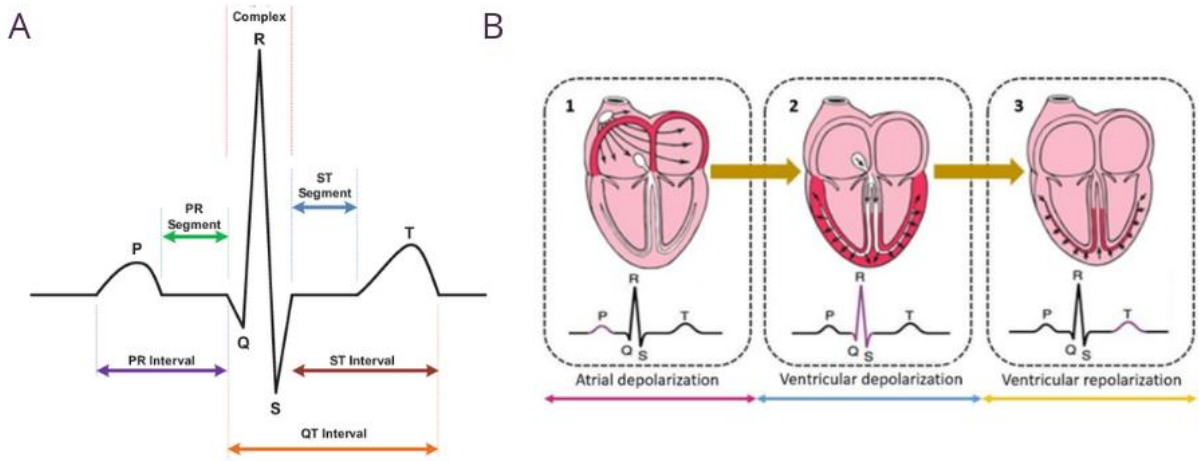

Figure 7 A: Heart beat shape and parts. B: Heart beat relation to depolarization and repolarization [44] [45].

HEART RATE AND RR INTERVAL

Heart rate represents the number of heart contractions during a specific period of time. Typically, one minute is used as a reference, resulting in beats per minute (BPM) [42].

OTHER INDICATORS

For the development of this work, additional parameters have been analyzed, such as P wave duration, PR interval, QRS complex, ST segment, T wave duration and QT interval. Variations in these indicators over time allow for the diagnosis of conditions such as myocardial infraction, pulmonary embolism, and channelopathies, among others [42] [46].

2.3.3. ELECTROCARDIOGRAM MEASUREMENTS

There are several techniques available for recording ECG signals in laboratory animals, ranging from 1 to 12 channels. Most studies employ the Lead II method [42].

INVASIVE METHODS

Invasive ECG recording methods are the most commonly used in experiments with anesthetized rodents. To obtain Lead II measurements, electrodes are placed under the skin of the forelimbs (both left and right) and on the right hind limb. The advantages of this method include the ability to replicate measurements across different subjects and the high quality of recorded signals. However, the main drawback is that the measurements are affected by the effects of anesthesia [42].

An invasive ECG acquisition method that avoids the anesthesia-related issue is telemetry, which involves the subcutaneous implantation of transmitters. These transmitters send the recorded data to receivers located outside the rodent's cage. This technique allows data collection from freely moving animals, although measurements can be affected by electrode displacement or animal movement [47].

NON-INVASIVE METHODS

One example of a non-invasive ECG recording method is the use of jackets fitted with internal electrodes for rodents. The advantages of this approach include its lower cost compared to telemetry and its ability to record signals in conscious animals. However, the main limitation lies in the difficulty of consistently positioning the electrodes across different animals and experimental iterations, as well as signal alterations caused by animal movement [48].

Another non-invasive method consists of placing the animal in a tunnel where its paws rest on ECG sensors [49], using devices similar to the one shown in Figure 8.

Figure 8 Emka Technologies device for non-invasive ECG acquisition in conscious rodents [50].

2.3.4. RELATIONSHIP BETWEEN ECG MEASUREMENTS AND VAGUS NERVE STIMULATION

ECG parameters have been studied in detail because, in vivo experiments, ECG signal analysis is intended to serve as a method for verifying the presence of vagus nerve stimulation. Studies have demonstrated that heart rate varies significantly depending on whether vagus nerve stimulation is applied. During electrical stimulation of the vagus nerve, a decrease in beats per minute is observed [51] [52]. Figure 9 shows an example of ECG measurements recorded before, during, and after VNS in a rodent [51].

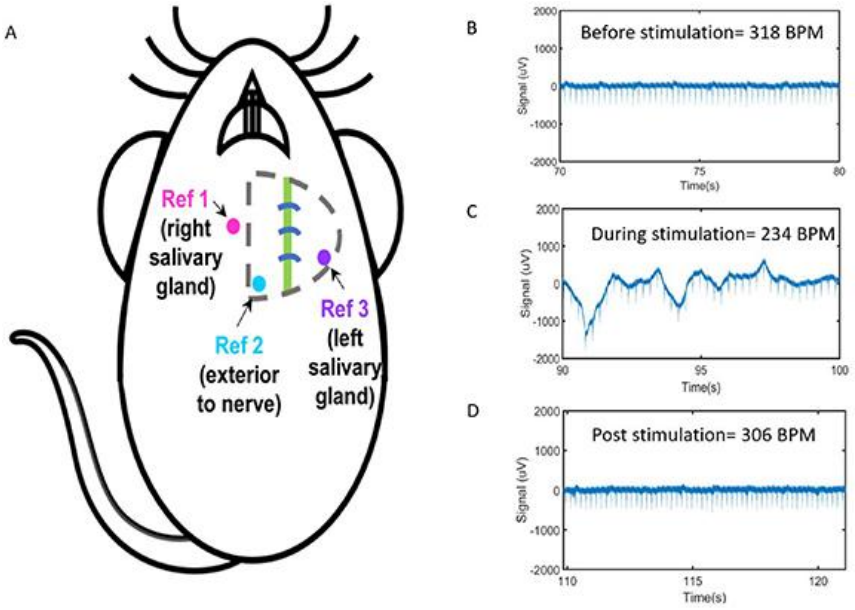

Figure 9 ECG bpm analysis one minute before, during and after VNS on a rat [51].

2.4. REQUIREMENTS

This section presents the requirements established prior to the design and implementation of the prototype, where three types of requirements are defined: general, stimulation-related (depending on the type of experiment to be conducted), and acquisition-related.

GENERAL REQUIREMENTS

The general requirements are as follows:

- The designed device must be:
  - Intuitive for users who will operate the system during experiments without prior knowledge of its design.
  - Compact and light weight, ensuring minimal space requirements and easy portability.
  - Easily configurable without the need for detailed understanding of the underlying design.
- Each module should be independently modifiable and easily replaceable.
- The design must be robust to ensure the proper execution of all activities.
- The design should be versatile and applicable to various projects.
- Wireless operation must be supported.
- The design must be able to stimulate and acquire biological signals.
- When operating only with stimulation, it must be able to work in low power mode.

STIMULATION REQUIREMENTS

Two types of experiments have been considered for stimulation requirements:

- Type A Experiments: These correspond to the STRIKE project, where only the stimulation feature is used. Stimulation is continuous over time (on the order of seconds), with prolonged rest periods (on the order of minutes).
- Type B Experiments: These involve both stimulation and acquisition features, testing all modules operating simultaneously. In these experiments, stimulation consists of single pulses or pulse trains (approximately 5 – 10 pulses) repeated every second for periods of about one minute.

The stimulation parameters in terms of timing and current for both experiment types are defined below.

TYPE A EXPERIMENTS: STRIKE

In this type of experiment, only the stimulation feature is employed. To better illustrate the definition of stimulation parameters, Figure 10 shows the stimulation waveform.

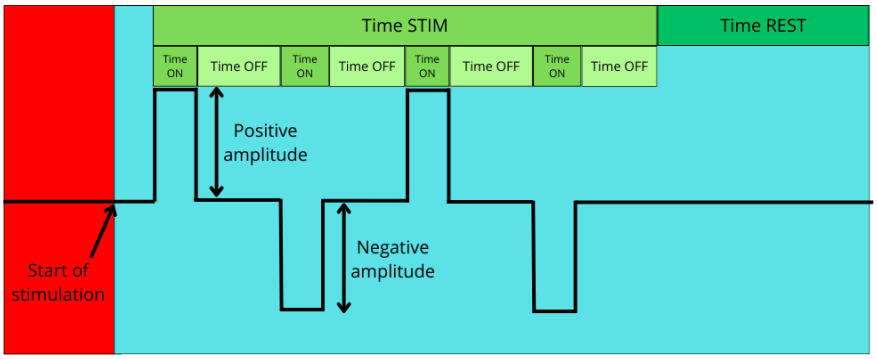

Figure 10 Stimulation parameters definition.

The stimulation characteristics used in these experiments vary depending on the referenced literature [31] [53]. For this work, stimulation requirements have been defined based on experiments currently conducted at CTB:

- Stimulation must be configurable to be bipolar or unipolar.
- Pulse width (Time ON) is 0.5ms.
- Stimulation frequency is 20 Hz. This frequency is calculated in between two Time ON parameters.
- Stimulation duration (Time STIM) is 30 seconds.
- Rest time between stimulations (Time REST) is 5 minutes.
- Amplitude (Positive amplitude and Negative amplitude) is +-0.5 mA.

TYPE B EXPERIMENTS

In this type of experiment, both stimulation and acquisition features are employed. Acquisition requirements will be detailed later.

The stimulation characteristics defined for Type B Experiments are related to another project conducted at the B105 Electronic Systems Lab (VISNE). In this project, two stimulation modes are used: One Shot and Pulse Train. Figure 11 illustrates the difference between these two modes.

The stimulation requirements for Type B experiments are as follows:

- The system must allow configuration for either a single pulse (One Shot) or a pulse train, as shown in Figure 11.
- Stimulation must be unipolar.
- Current must be less than 100 uA. This requirement is based on the fact that VISNE currently applies stimulation in the Thalamic region with currents above 100 uA, and the goal is to observe neurological responses to lower currents.
- Pulse duration (Time ON) must be 1 ms.
- Stimulation frequency is 1 Hz (Time STIM + Time REST).
- The setup should allow integration of other stimulation modalities (e.g. visual stimulation), not only electrical stimulation.

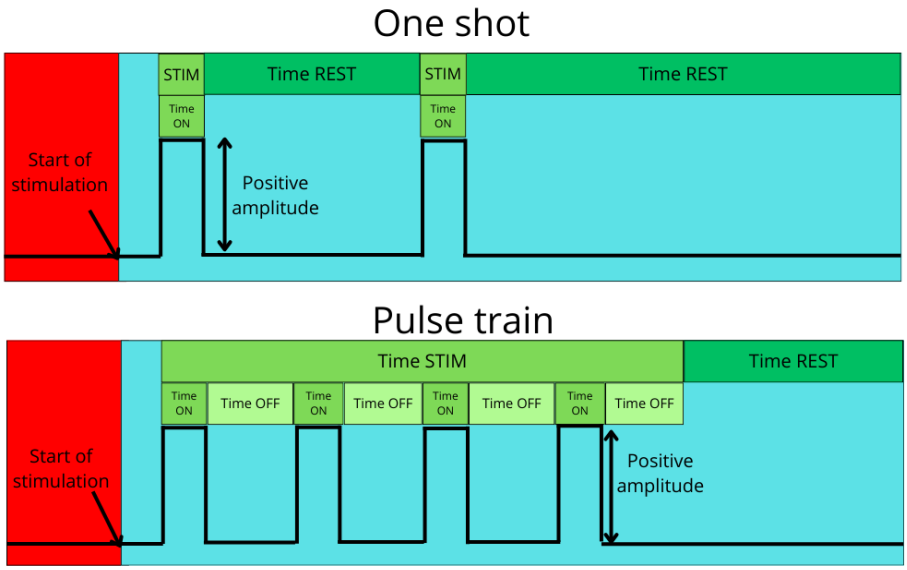

Figure 11 One shot vs Pulse train stimulation definition.

ACQUISITION REQUIREMENTS

Acquisition requirements are only defined for Type B Experiments, based on the actual parameters employed at those experiments:

- The system must be capable of sampling two channels simultaneously.
- Sampling frequency must be equal or greater than 2 kHz.
- Variations from 50µV to 150µV should be observed.

In Figure 12 an example of capture from electrical activity after a stimulation is shown. The signal is captured with a sampling frequency of 2.048 kHz. The vertical values vary from 10 µV to 80 µV. In other measurements those variations go up to 150 µV.

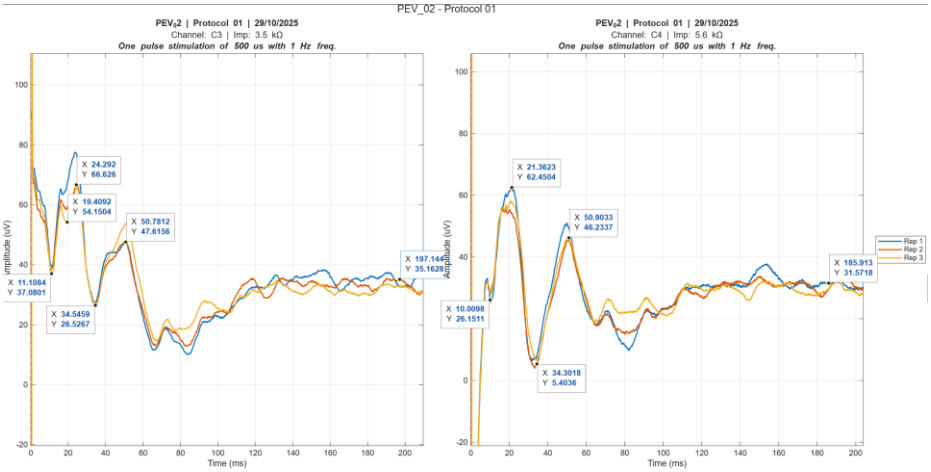

Figure 12 Example of capture for Type B Experiment [54].

Having established the fundamental concepts required to understand the STRIKE project and the set of requirements guiding the development of the closed-loop system, the following chapter introduces the design of the proposed solution. This begins with a comprehensive description of the overall closed-loop architecture and is subsequently followed by detailed presentations of the hardware and software designs.

3. DESIGN

This chapter describes the designs of the different modules that make up the device developed in this work. First, the system design is presented, detailing the components for each of the modules. Also, the protocol created for the control of the interactions is shown. Subsequently, the hardware design, including the components used is presented. Finally, the software design with the definition of all the finite state machines is also presented, including the signal processing module justifying the use of each filtering stage and showing the evolution of the signal analysis throughout the different phases of processing.

3.1. SYSTEM DESIGN

This section defines the parts of modules that constitute the closed-loop system, detailing the activities performed by each module and the components that make them up. Additionally, the control protocol that enables the interaction among the different modules is presented.

3.1.1. CLOSED-LOOP DESIGN

The closed-loop design has been implemented through the definition of several modules, each performing distinct functions.

- Stimulation module: responsible for generating stimulation waveforms with user-defined characteristics.
- Acquisition module: responsible for acquiring biological signals required for each experiment, meeting user-defined sampling frequency, and filtering specifications.
- Communications module: responsible for transmitting the configuration parameters from the user device to the system, including both stimulation and acquisition modules, and receiving acquired data for subsequent visualization and analysis. This module includes a graphical interface to facilitate parameter definition and communication.
- Signal processing module: processes signals (in this case, ECG) and extracts relevant parameters for subsequent analysis. This module also includes a graphical interface to simplify processing tasks.

Figure 13 shows a schematic representation of the connections between the modules that make up the designed closed-loop system. The diagram identifies the components and protocols associated with each module. In the following sections, the functionalities of each module and the characteristics of their components will be described in detail.

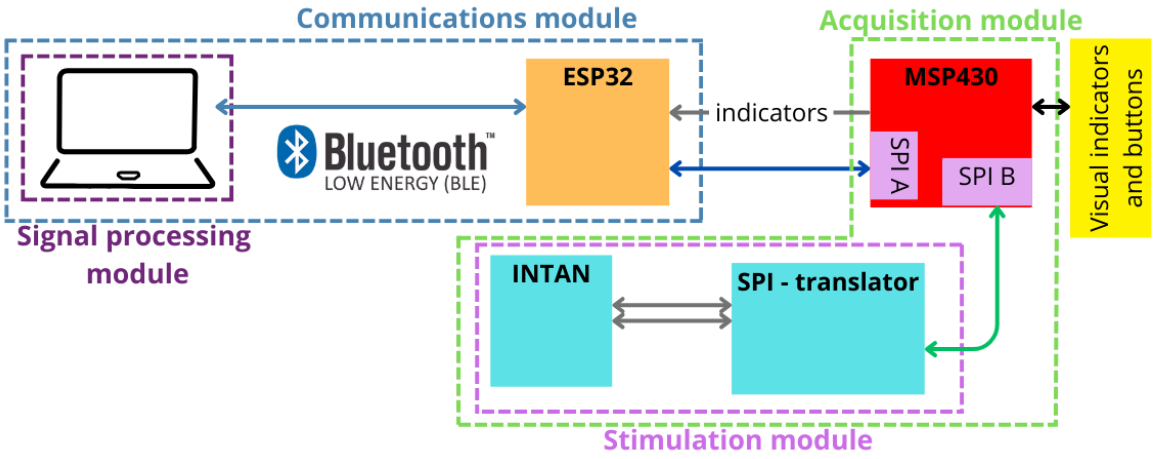

Figure 13 Connection map.

To develop stimulation and acquisition modules, one or two devices capable of performing these tasks (either jointly or separately) are required.

In this work, INTAN devices [55] were selected as it integrates low-noise multichannel acquisition and constant-current stimulation within a single device, reducing hardware complexity and ensuring precise synchronization between signal recording and stimulation. A more detailed description of this device is presented in section 3.2.2.

To operate this device, it is necessary to send a series of read or write commands via differential SPI (Serial Peripheral Interface), specifying in each case which register should be accessed and, in the case of write operations, the value to be assigned. These commands and the description of each register's functionality are detailed in the datasheet [56].

STIMULATION AND ACQUISITION MODULE

For the stimulation and acquisition modules, INTAN has been chosen as the interface between the experimental subject and the system. Furthermore, an additional device (a microcontroller) is required to send programming commands to INTAN via SPI.

In this case, a microcontroller from Texas Instruments, specifically the MSP430FG479 [57], was selected. This choice was motivated by several factors:

- It integrates a set of 16-bit ADCs (Analog to Digital Converters), which would allow the inclusion of additional acquisition modules independent of INTAN in future developments.
- It supports low-power operation while providing clock frequencies high enough to achieve precise sampling rates.
- It includes a timer system, enabling accurate control of stimulation timing. Each time stimulation parameters need to be updated, the microcontroller sends new configurations to INTAN via SPI.

Since the microcontroller responsible for sending commands via SPI does not include a differential SPI interface, it is necessary to incorporate a device that converts standard SPI to differential SPI: in this case the SN65LVDT41PWR [58] is used.

COMMUNICATIONS MODULE

Communication between the user's portable device and the stimulation/acquisition system is implemented using Bluetooth Low Energy (BLE). This protocol was chosen because it meets the required timing and bandwidth specifications. Additionally, BLE (with Python) facilitates the development of user-friendly interfaces for updating stimulation and acquisition parameters and allows real-time communication of stimulation events to the user.

BLE enables point-to-point wireless communication between devices without requiring additional infrastructure, simplifying configuration and reducing system complexity. Also, it is optimized for transmitting small, frequent packets, which aligns with the type of information exchanged in this work: updating stimulation and acquisition parameters while providing immediate notification of stimulation status.

Another key reason for selecting BLE is its low energy consumption, which is lower than other technologies such as Wi-Fi. Additionally, BLE provides broad compatibility with most operating systems and mobile devices, facilitating the integration of the developed prototype with other devices and applications.

SIGNAL PROCESSING MODULE

Within the STRIKE project, several iterations of the ECG analysis algorithm were developed due to the lack of significant results in initial experiments and the lack of knowledge of knowing what kind of variation we were looking for.

The latest iteration includes two different approaches for analyzing heart rate (beats per minute), to account for potential variability in results across experiments. It also incorporates the analysis of other relevant cardiac signal metrics.

The first approach is based on a custom algorithm that calculates BPM by detecting R-peaks. As the information provided by this approach is equivalent to the one given by the second approach, it will not be explained in further detail.

The second approach adapts the algorithm proposed by Pan-Tompkins [59] [60], modifying filter frequencies and configuration parameters to account for the differences between mouse and human heart rates.

This module includes a graphical user interface that allows intuitive configuration of filter frequencies and other parameters.

3.1.1. CONTROL PROTOCOL DESIGN

To ensure that the modules know when to perform actions and interact with each other, considering the presence of multiple components in the design, a control protocol has been developed to regulate the interactions between the MSP430 and the ESP32 that form the system. The control protocol is shown in Figure 14.

The color code represents in green the data acquired from the INTAN ADC's, in red the new parameters sent from ESP32 to MSP430, and in purple the stimulation instructions updates. Later, during the state machine presentation, the function of each of these signals is explained. Next, each design is explained along with its respective state machines.

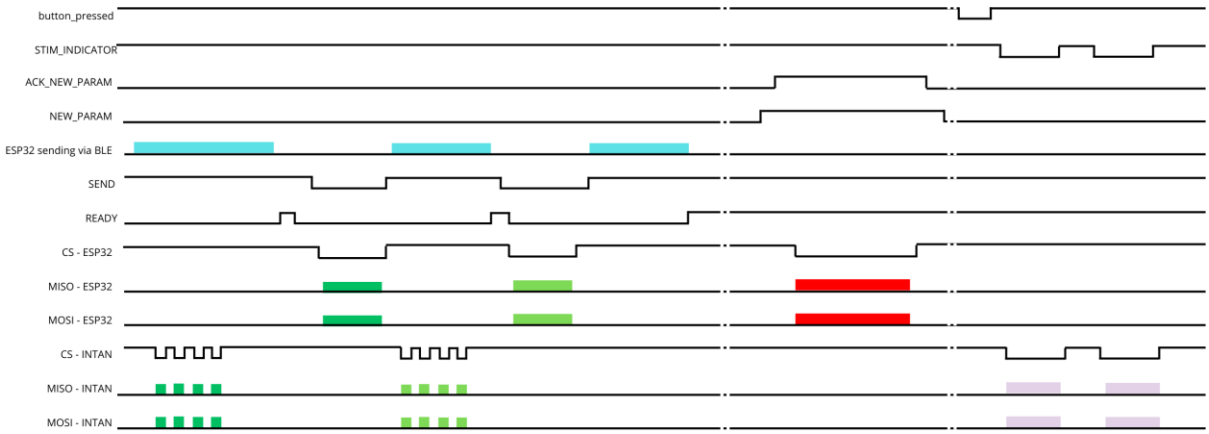

Figure 14 Signals control protocol design.

3.2. HARDWARE DESIGN

This section provides a detailed description of the devices integrated into the modules outlined in the previous section.

3.2.1. PERSONAL DEVICE (LAPTOP)

This device provides the user with the necessary interfaces to analyze the signals obtained during the processing stage and to visualize the results through a graphical interface. It also allows for configuring stimulation and acquisition parameters, sending these configurations to the ESP32. Communication between the personal device and the ESP32 is carried out using the BLE protocol. Additionally, the device receives data acquired by the ESP32 and displays it graphically.

In addition, this device is employed to perform the signal processing required for the execution of STRIKE experiments.

3.2.2. INTAN RHS2116

The INTAN RHS2116 is an Application-Specific Integrated Circuit (ASIC) for biomedical applications developed by Intan Technologies [56]. It is designed for multichannel bioelectrical signal acquisition and current-controlled electrical stimulation. In the proposed system, this device acts as the acquisition and stimulation module and is directly responsible for interfacing with biological tissue. Figure 15 shows the INTAN device.

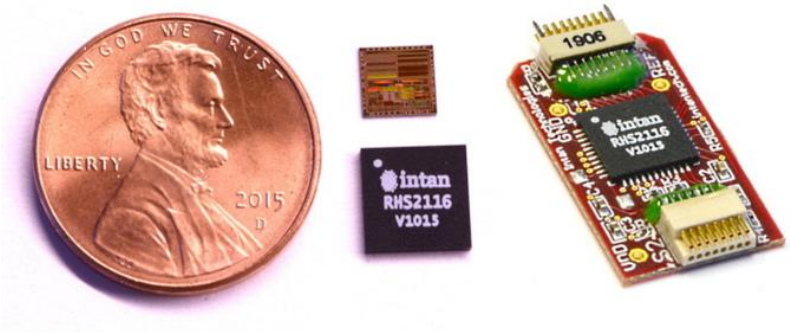

Figure 15 INTAN RSH2116 [55].

The RHS2116 integrates 16 independent channels, each equipped with low-noise amplifiers, configurable analog filters, and a constant-current generator for stimulation. This architecture enables the combination of physiological signal recording (such as ECG or EEG) and electrical stimulation within a single device, thereby reducing external hardware complexity and improving synchronization between acquisition and stimulation.

Regarding acquisition, the RHS2116 incorporates both AC and DC coupled amplifiers with configurable gain, along with a 16-bit analog-to-digital converter optimized for low-amplitude signals. The device allows configuration of both high-pass and low-pass filters and includes a Digital Signal Processing (DSP) module that applies digital filters to remove offsets and unwanted signal components. These features are particularly relevant in biomedical applications, where signal quality is critical.

The stimulation module of RHS2116 is based on constant-current generators capable of delivering positive and negative pulses over a wide current range, typically from tens of nanoamperes up to the milliampere range. Stimulation can be configured in unipolar or bipolar modes.

Communication with the RSH2116 is performed through a differential Serial Peripheral Interface (SPI) which provides high noise immunity and is well suited for environments where very low-amplitude analog signals coexist with digital switching. The device responds to different types of commands (WRITE, READ, and CONVERT), which allow configuration of internal registers, initiation of analog-to-digital conversions, and retrieval of acquired data. The timing of these operations is controlled by an external controller, in this case the MSP430, which acts as the system

master. Later on, the configuration functions developed for the correct functioning of the INTAN RHS2116 will be explained.

3.2.3. SN65LVDT41PWR

The SN65LVDT41PWR [58] is a hardware block that translates conventional SPI signals into differential SPI and vice versa. It is required to adapt communication between the MSP430 and the INTAN circuit. While standard SPI uses single-ended signals referenced to ground, the INTAN employs differential SPI interface designed to improve noise immunity and signal integrity, particularly in biomedical environments and applications involving low-amplitude signals.

Figure 16 shows the 3D design of the Printed Circuit Board (PCB), which includes the required connectors and the SN65LVDT41PWR.

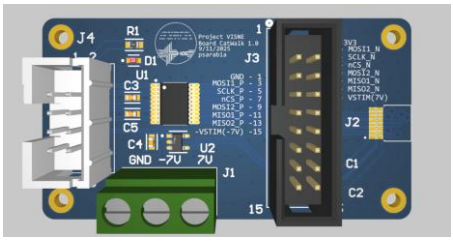

Figure 16 3D design for SN65LVDT41PWR.

3.2.4. MSP430FG479

The MSP430FG479 is an ultra-low-power microcontroller developed by Texas Instruments [57], widely used in biomedical and instrumentation applications due to its energy efficiency and integration of high-precision analog peripherals. Figure 17 shows the development board MSP-TS430PN80 [61] designed for the microcontroller MSP430FG479.

This device constitutes the functional core of the system, acting as the master with respect to both the ESP32 and the INTAN circuit. It is responsible for storing received configuration parameters, managing acquisition and stimulation timing, and generating the required commands for SPI communication with the INTAN.

One of the main reasons for selecting the MSP430FG479 is the inclusion of 16-bit sigma-delta analog-to-digital converters (SD16), which are particularly well suited for acquiring bioelectrical signals such as ECG or EEG. This capability allows the system to operate in two modes: using the INTAN as the acquisition device or directly using the internal ADCs of the MSP430, thus providing design flexibility.

In addition, the MSP430 includes two independent SPI communication modules, enabling simultaneous communication with different external devices without interference. Its low-power operating modes are critical for the stimulation module design, allowing the system behavior to adapt depending on the presence or absence of the ESP32.

Figure 17 MSP-TS430PN80 for MSP430FG479.

3.2.5. ESP32-S3 FEATHER TFT

The ESP32-S3 Feather TFT is a low-power microcontroller developed by Adafruit [62] and uses an Espressif [63] microcontroller. In this work, it functions as the communication node and gateway

between the MSP430 and the user's personal device (computer). Figure 18 shows an image of this microcontroller.

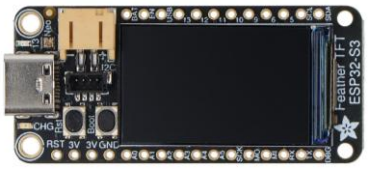

Figure 18 ESP32-S3 Feather TFT.

Its main features include integrated Bluetooth Low Energy (BLE) connectivity, multiple communication interfaces such as SPI, and high capacity for concurrent task processing. These characteristics make the device suitable for simultaneously managing the reception of configuration parameters, forwarding acquisition data, and supervising stimulation execution.

Within the proposed architecture, the ESP32-S3 acts as an intermediary, receiving stimulation and acquisition parameters from the computer via BLE and forwarding them to the MSP430 through SPI. It also transparently relays the data received from the MSP430 back to the computer via BLE.

3.2.6. POWER SUPPLIES

The power supplies allow configuration of the two voltage rails required by the INTAN: a +3.6 V supply for the logic circuitry and a +-7V (maximum) supply for the stimulation circuitry. Figure 19 shows both power supplies: the upper one is configured to deliver 3.6V, while the lower one provides a symmetric 6.8V supply.

Figure 19 Power supplies.

3.2.7. INDICATORS

During the implementation, a set of visual indicators and pushbuttons have been added to be able to control and comply with the design. For example, a button has been included that allows to indicate when a stimulation experiment is started. 3 LEDs have also been added that allow control and visual awareness of the status of the system.

3.3. SOFTWARE DESIGN

This section presents the software design developed for each of the modules that compose the system. The behavior and internal logic of these modules are described using Finite State Machines (FSM), which provide a structured and intuitive representation of their operation. The FSMs corresponding to each module are introduced and explained throughout this section.

The modules addressed in this section are the following:

- Acquisition module: implemented in two configurations, using the INTAN device or the MSP430 microcontroller as the acquisition system.
- Stimulation module: designed to operate in two modes, a standard mode and a low-power mode, depending on system requirements and hardware availability.
- Communications module: detailing the communication technology employed, the design principles that govern its operation, and the functionality of the application developed to update system parameters.
- Signal Processing Module: describing the spectral analysis performed to justify the design choices adopted for this module, together with the processing steps required to extract relevant information from the acquired signals.

Together, these designs establish software architecture that enables the coordinated operation of the overall system and supports its closed-loop functionality.

3.3.1. ACQUISITION MODULE

The acquisition module is responsible for obtaining biological signals. The device can be used in two configurations depending on how the parameters are obtained. On one hand, the system can be configured so that the MSP430 ADCs acquire the biological signal values, or it can be configured so that the INTAN device performs this acquisition.

Additionally, the use of the ECG acquisition system employed at CTB for the STRIKE project experiments is also considered, allowing testing individually the stimulation module developed.

INTAN IN ACQUISITION MODE

When INTAN is used as the acquisition interface for biological signals, it is necessary to configure its internal filters via SPI write commands (WRITE) to specific registers. Each parameter and register description is provided in the datasheet [56]. Some relevant characteristics of this device in acquisition mode include:

- It allows reading both continuous (DC) and alternating (AC) signal values using two different types of amplifiers.
- All channels (16 in total) share the amplifier configuration.
- It offers two selectable high-pass filters with dynamically adjustable cutoff frequencies, without requiring reconfiguration.
- It includes a low-pass filter to eliminate high-frequency components.
- Digital Signal Processing (DSP) functionality can be enabled or disabled.
- Channel value readings are triggered by the convert command (CONVERT).
- Timing for readings is controlled by the external device sending commands.

Figure 20 illustrates how the CONVERT command works and when conversion and data transmission occur. As shown, additional logic is required to identify channel values for two commands after the CONVERT command is issued [56].

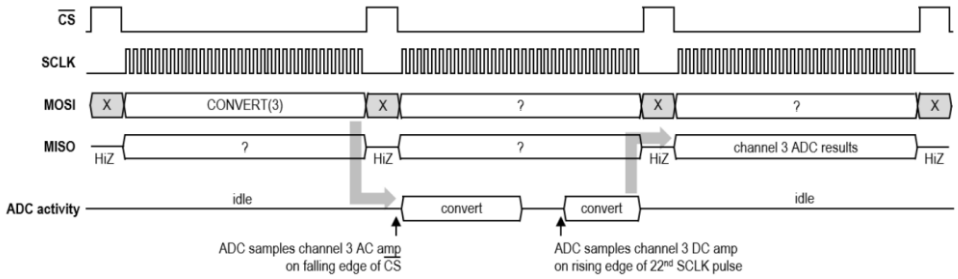

Figure 20 Diagram of commands send and response logic for INTAN technologies [56].

The structure of the CONVERT command is shown in Figure 21. It consists of two parts: one defines the flags to activate or deactivate, and the other specifies the channel to read. The response to the CONVERT command is also shown in Figure 21, where the Most Significant Bits (MSB) represent the AC value of the requested channel, while the Least Significant Bits (LSB) represent its DC value.

Additionally, if channel 63 (out of range of the number of channels) is requested, the device performs consecutive readings of channels as many times as CONVERT(63) commands are sent. This feature is leveraged to implement functionalities such as conversion of N consecutive channels.

Command: CONVERT(C) – Run analog-to-digital conversion on channel C

MSB 31	30	29	28	27	26	25 – 22	21 – 16	LSB 15 – 0
0	**0**	**U**	**M**	**D**	**H**	**0000**	**C[5:0]**	**00000000 00000000**

Result:

MSB 31 – 16	15 – 10	LSB 9 – 0
A[15:0]	**000000**	**W[9:0]**

Figure 21 CONVERT command structure for INTAN technologies [56].

FSMS FOR ACQUISITION MODULES

Figure 22 shows two Finite State Machines (FSMs) designed for the acquisition module. The left FSM represents the main behavior of the MSP430, which includes five states. The right state machine corresponds to one of the states in the main FSM (SD – 1.1), describing the process for sending data obtained from an INTAN channel using the CONVERT command and forwarding its obtained value to the ESP32.

Initially, the design included sending only one CONVERT command per channel and forwarding the response via SPI. However, during implementation, it was observed that a significant time was spent waiting for BLE transmission of the acquired data. To optimize this, the BLE transmission time was used to acquire additional samples, thereby increasing the sampling frequency. As a result, instead of sending only one CONVERT command per channel, up to 10 commands are now sent. The outcome of this implementation is presented in chapter 5. The states of the machines are explained below.

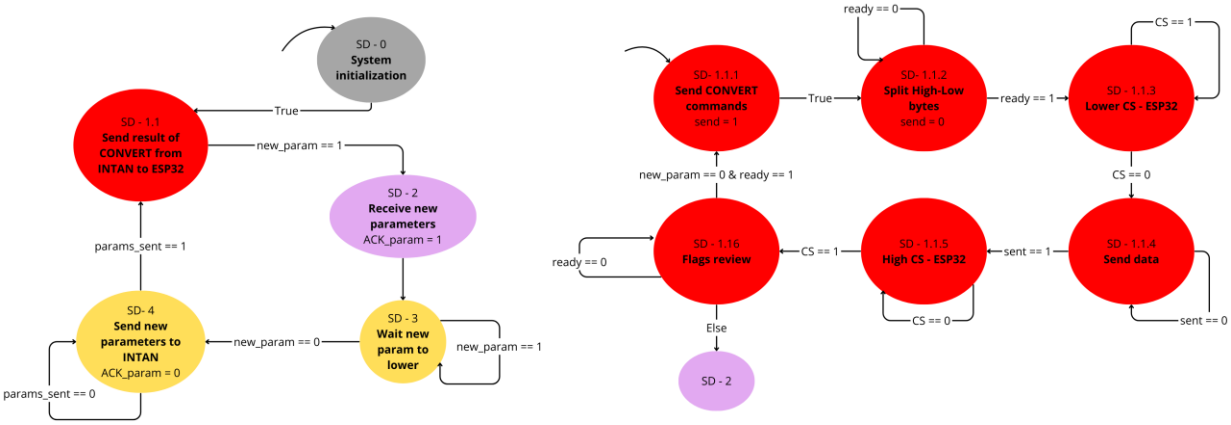

Figure 22 FSM for MSP430 in active mode with INTAN as acquisition module.

MAIN MSP430 FSM

- SD – 0: Initial state, where the system is configured (clocks, timers, and communication interfaces).
- SD – 1.1: State for sending data obtained via the CONVERT command. The logic of the SEND and READY signals presented in Figure 14 is applied in this state of the FSM.
    - SD-1.1.1: Sending the CONVERT commands.
    - SD-1.1.2: Splitting the two bytes obtained from the conversion into separate bytes. This is necessary because MSP430 uses 8-bit SPI registers, requiring two separate transmissions.
    - SD-1.13 to SD1.1.5: Protocol for sending the converted data along with the channel identifier header via SPI to the ESP32. This includes lowering the Chip Select pin and transmitting all required packets.
- SD – 1.2 to SD-1.3: Receiving new parameters. When the ESP32 receives new parameters via BLE, it raises a flag called *new_param*, which signals the MSP430 that updates are available. Pin-based logic ensures proper control of parameter updates.
- SD – 1.4: Sending updated parameters to INTAN. A full reconfiguration of all register values is performed. Although optimization could involve updating only changed values, full reconfiguration ensures correction of any previous transmission errors.

MSP430 IN ACQUISITION MODE

The MSP430 includes a set of 16-bit SD16-type ADCs [57]. This type of ADC is commonly used in biomedical devices. For this reason (among others), the MSP430FG479 model was selected in a previous project. In this work, the design of the biological signal acquisition circuit (electrocardiographic: ECG and electroencephalographic: EEG) developed in that project [64] is leveraged, as it may be useful for future integration into this device.

Consequently, a dedicated FSM was designed to use the MSP430 ADC as the acquisition system. Figure 23 shows the FSM design for the MSP430-based acquisition system: the left diagram illustrates the main state machine, including integration with stimulation (which will be described later), while the right diagram depicts the state machine related to sampling the corresponding SD16 channel.

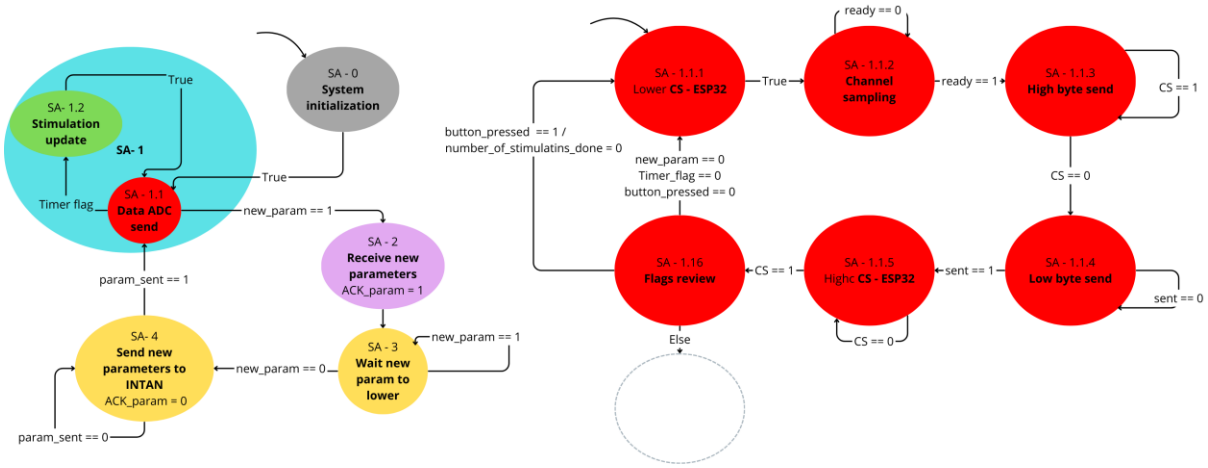

Figure 23 FSM for MSP430 in active mode with stimulation update and MSP430 as acquisition module.

The description of the acquisition states is similar to that presented for INTAN-based acquisition. The main difference lies in reading the ADC register: instead of requesting the value via CONVERT command, the value is directly obtained from the MSP430 memory register.

Additionally, the protocol for sending data to the ESP32 begins by lowering the Chip Select pin, followed by sampling and transmitting the value through the channel.

Apart from this, the operation remains the same, including parameter updates, which in this case involve updating stimulation parameters.

3.3.2. MODULE FOR ELECTRICAL STIMULATION

The electrical stimulation module has been designed to provide precise and configurable electrical stimulation in closed-loop experiments, ensuring compatibility with the INTAN device and the MSP430 microcontroller, but also considering easy and fast substitution of the components.

Here, the operational principles and the implementation details of the stimulation subsystem, including the configuration of INTAN in stimulation mode, the definition of the stimulation patterns, and the logic of the operating modes are described.

INTAN IN STIMULATION MODE

The INTAN device can be used as a stimulator by configuring each of its channels to operate as an independent stimulation source. Channel configuration combinations allow individual stimulation with fixed currents ranging from 10 nA to 1.27 mA. Furthermore, both positive and negative stimulation can be configured independently by writing to different registers [56].

INTAN does not include an internal timing system; therefore, stimulation timing control is managed by an external microcontroller, in this case the MSP430.

STIMULATION PATTERN

The stimulation pattern designed below is presented in the requirements in section 2.4. In this case, only the pattern used in Stimulation Type A (STRIKE project) is described in detail, as its adaptation for Stimulation Type B is straightforward. This pattern includes two distinct intervals:

- Stimulation Time (STIM): During which the stimulation waveform is updated.
- Rest Time (REST): During which stimulation remains off.

The FSMs related to this stimulation pattern are explained below.

OPERATING MODE

When designing the stimulation module, two configurations were considered depending on the devices connected to the system. As the MSP430 has the possibility to work on low power mode, this feature is leveraged in the design. The stimulation module was designed so that, depending on whether the ESP32 is connected, the system operates in low-power mode or not. To detect the presence of the ESP32 (which prevents low-power operation), the ESP32_connected pin is used, as will be shown in section 4.1.

The logic for selecting the operating mode is presented in Figure 24. The process always begins with the configuration of the general MSP430 modules. Then, depending on whether the ESP32 is present, the following configurations are applied:

- SD16 (or INTAN) in acquisition mode.
- SPI interface for communication with the ESP32.
- Timer configured by polling or by interruption.

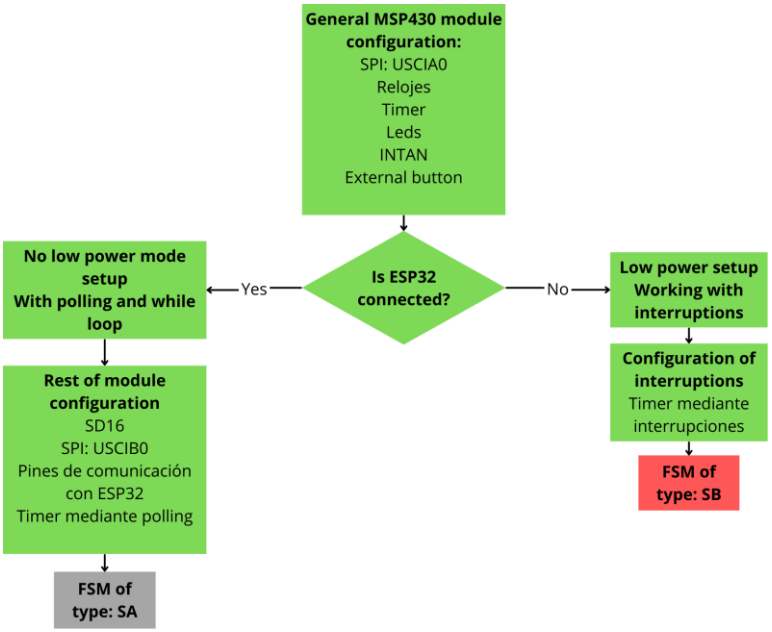

Figure 24 Decision map and configurations of low power.

Depending on the path selected in Figure 24, one state machine or another will be initialized. Both state machines are shown in Figure 25. The left state machine corresponds to the active mode configuration, which is initialized when the ESP32 is connected, while the low-power mode state machine is initialized when the ESP32 is not connected. The explanation of the states for each FSM is provided below.

It is important to note that both FSM operate with a common and critical signal (STIM_INDICATOR), which enables the addition of other stimulation types (such as visual stimulation) by activating this signal at low level, as shown in Figure 14.

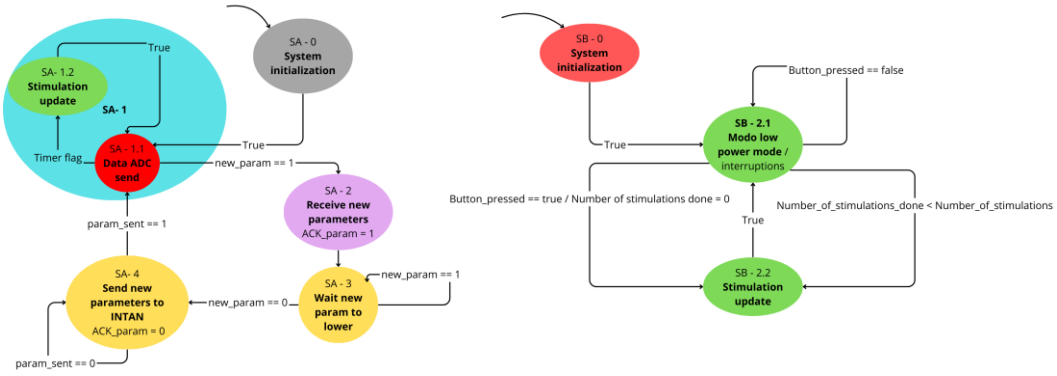

Figure 25 FSM of the MSP430 comparison between low power design (right) and active mode (left).

MSP430 IN ACTIVE MODE

The state machine on the left of Figure 25 represents the behavior of the MSP430 when the ESP32 is connected. Additionally, Figure 26 shows the state machines related to stimulation update (on the left) and stimulation waveform update (on the right).

These state machines describe the stimulation behavior illustrated in Figure 10 which shows the stimulation waveform used in the STRIKE project. For the other stimulation type, the resulting state machines are similar, except for the removal of two states (ON_N and OFF_N) due to their simplicity. Therefore, they are not explained in this section.

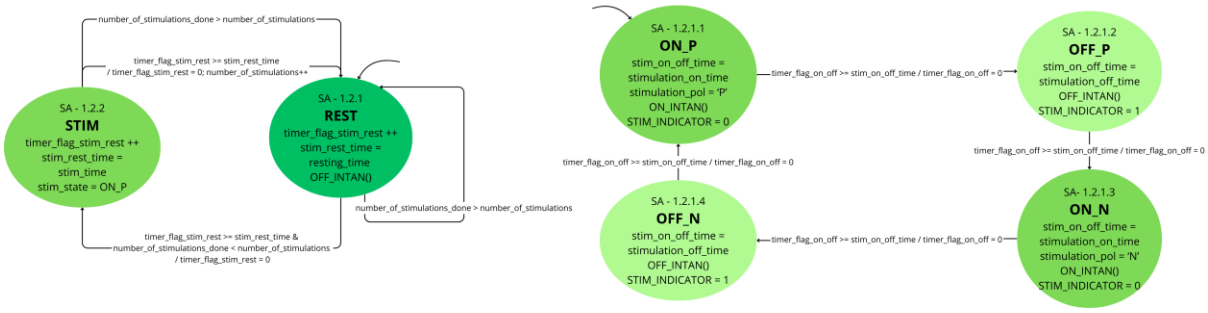

Figure 26 FSMs for stimulation pattern control.

The states of the FSM in active mode are described as follows:

- SA – 0: Initializes the modules that configure the general operation of the MSP430 in active mode.
- SA – 1.1: Handles the transmission of the biological signal value to be acquired, either through the MSP430 or INTAN. The stimulation pattern does not start until an external button is pressed.
- SA – 1.2: When the timer counter reaches the corresponding limit value (*timer_flag*), stimulation is updated using the state machine shown in Figure 26.
    - SA – 1.2.1 (REST): Stimulation is in rest state, with the stimulation off.
    - SA – 1.2.2 (STIM): Stimulation is active: the waveform is updated if necessary, the timer is the module of the MSP430 in charge of controlling the time components.
        - SA-1.2.2.1 (ON_P): Waveform is in positive stimulation. STIM_INDICATOR is activated (low level).
        - SA-1.2.2.2 (OFF_P): Waveform is off after positive stimulation. STIM_INDICATOR is deactivated (high level).
        - SA-1.2.2.3 (ON_N): Waveform is in negative stimulation. STIM_INDICATOR is activated (low level).
        - SA-1.2.2.4 (OFF_N): Waveform is off after negative stimulation. STIM_INDICATOR is deactivated (high level).
- SA – 2 to SA – 3: When the *new_param* flag is received via ESP32, parameters are updated.
- SA – 4: Sends updated parameters to INTAN. A full reconfiguration of all register values is performed. Although optimization could involve updating only changed values, full reconfiguration ensures correction of any previous transmission errors.

MSP430 IN LOW-POWER MODE

The state machine on the right in Figure 25 represents the behavior of the MSP430 when the ESP32 is disconnected. This machine is simpler than the one used in active mode. The states are described as follows:

- SB – 0: Initializes the modules that configure the general operation of the MSP430 in low-power mode. Unlike active mode, after configuring all parameters, the system switches to low-power operation and uses interruptions to update any needed parameter or send commands to the INTAN.
- SB – 2.1: The system enters sleep mode and enables interrupts. The predefined stimulation pattern in the basic program does not start until the user presses an external button.
- SB – 2.2: When a timer interrupt occurs, stimulation parameters are updated using the same stimulation pattern and FSMs presented in active mode.

3.3.3. STIMULATION AND ACQUISITION INTEGRATION

Figure 25 illustrates the configuration of the MSP430 in acquisition mode, integrating the states of the stimulation and acquisition states in the FSM. This integration was straightforward thanks to the prior work carried out during the development of the previous work [64]. The equivalent integration using the INTAN device is presented and explained below.

Figure 27 shows the FSM resulting from this integration. The main difference compared to Figure 25 lies in the use of INTAN as the acquisition system instead of the MSP430. Additionally, Figure 14 depicts the signal protocol design that enables simultaneous operation of both stimulation and acquisition modules.

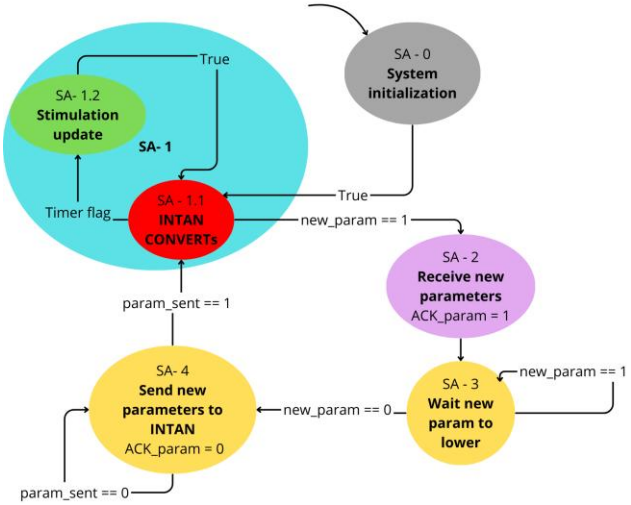

Figure 27 FSM including stimulation and acquisition modules.

3.3.4. COMMUNICATIONS MODULE

To implement the communications module, a BLE connection is established between the user's personal device (a laptop in this case) and the ESP32. For this purpose, two components were designed: a state machine for the ESP32 operation and an application for parameter and data reception and update on the personal device.

USE OF BLE

The technology employed for communication between the user's personal device (laptop) and the ESP32 is Bluetooth Low Energy (BLE). This choice is based on system characteristics and real-time operation requirements.

BLE enables point-to-point wireless communication between the computer and the ESP32 without requiring additional infrastructure, simplifying configuration, and reducing system complexity. Furthermore, BLE is optimized for transmitting small, frequent packets, which align with the type of information exchanged in this work: updating stimulation and acquisition parameters while providing immediate notification of stimulation status.

Another key reason for selecting BLE is its low energy consumption, which is lower than other technologies such as Wi-Fi. Regarding transmission capacities, the BLE packets allow up to 250 Bytes of transmission. Considering 10 samples of two channels (as it is the maximum number of channels used in this work), with 3 packets of 8 Bytes each, 240 Bytes of information are sent. This quantity fits perfectly with the BLE restrictions.

Additionally, BLE provides broad compatibility with most operating systems and mobile devices, facilitating the integration of the developed prototype with other devices and applications.

ESP32 STATE MACHINE

The state machine governing ESP32 behavior, shown in Figure 28, does not vary depending on whether INTAN or MSP430 is used as the acquisition device. The states are as follows:

- SG – 1: Data obtained from the MSP430 is forwarded via BLE. To perform this transmission, the SEND pin must be active (low level). When this condition is met, if the ESP32 is ready to forward data, the READY signal will also be active (low level). While performing other tasks

(such as BLE transmission), the READY signal remains inactive (high level). This behavior is shown in Figure 14.

- SG – 2 and SG – 3: If a new set of parameters is received via BLE, a flag (*RX_BT*) is raised, initialing the parameter communication protocol from the ESP32 to the MSP430. The received data is stored in the SPI queue, and the system waits for the MSP430 to acknowledge the presence of new parameters.
- SG – 4 and SG – 5: The system waits until the MSP430 has completed receiving and updating all parameters, after which the ESP32 flags are reset.

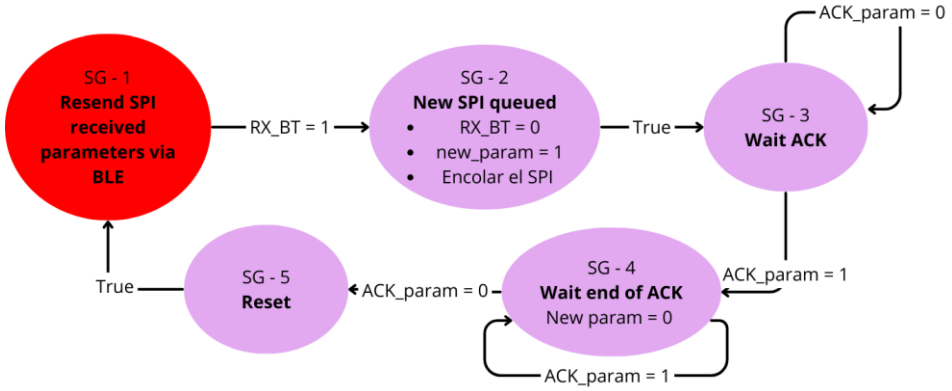

Figure 28 FSM for ESP32.

APPLICATION FUNCTIONALITY

To enable samples of reception and parameters updates from the computer, an application was designed to perform both tasks. This application must update stimulation and acquisition parameters related to the INTAN configuration, as detailed below.

General parameters:

- Experiment ID: Assigns a unique name to identify and recognize the experiment.
- ADC Sampling rate: The sampling frequency used during acquisition.
- DSP Cutoff Frequency: The cutoff frequency configured for DSP if enabled.
- DSP enabled: Binary value indicating whether the DSP high-pass filter is active.
- Channels: Maximum number of channels to be sampled simultaneously.
- Initial Channel: Channel where the conversion begins when converting more than one channel using the CONVERT(63) command.
- Fc High Magnitude: Configures the magnitude of the cutoff frequency for the low-pass filter.
- Fc High Unit: Configures the unit of the cutoff frequency for the low-pass filter.
- Fc low A: Configures the cutoff frequency for high-pass filter A.
- Fc low B: Configures the cutoff frequency for high-pass filter B.
- Amplifier cutoff: Selects which of the two filters (A or B) is applied to the output signal.
- C2 Enabled: Indicates whether data is represented in two's complement format.
- Absolute Value Mode: Indicates whether the sampled result is presented as an absolute value mode.

Stimulation Timing parameters:

- Number of stimulations: Specifies the number of stimulation repetitions to perform.
- Resting time: Duration in the REST state before returning to STIM.
- Stimulation time: Duration in the STIM state before returning to REST.
- Stimulation ON time: Duration in the ON state before switching to OFF.
- Stimulation OFF time: Duration in the OFF state before switching to ON.

Stimulation Characterization parameters:

- Bipolar Stimulation: Indicates whether stimulation is bipolar or unipolar.
- Current Step: Defines the step value used for stimulation.

- Positive/Negative Current Magnitude: Multiplier applied to the Current Step to adjust stimulation current.

Example: If Current Step = 500 nA and Current Magnitude = 10, the stimulation current will be 5000 nA.

Additional features

The application must also provide two visualization modes for acquired data: real-time display to monitor correct system operation, and full signal view for complete analysis. Additionally, the application should allow memory clearing to restart data acquisition and enable data export for reconstruction and post-processing analysis.

3.3.5. SIGNAL PROCESSING MODULE

The signal processing module was designed to perform the analysis of electrocardiographic (ECG) signals acquired during the STRIKE project.

The implementation consists of a program developed in MATLAB (V. 2025b), which requires a computer equipped with the appropriate license and the necessary toolboxes for execution. The program is structured as an ordered set of instructions designed to extract parameters that enable the observation of heart rate variability. The source code for performing the analysis is available in GitHub [65] in the folder ECG_recording_analysis_2, specifically in files OOX_ECG_PanHopkings.

Throughout the course of this work, three iterations of the module were designed and implemented; however, this section focuses exclusively on the final version. The discussion begins with the spectral characterization of the ECG signal, followed by a detailed description of the processing steps incorporated into the final design.

PREVIOUS SPECTRAL ANALYSIS

For the correct implementation of ECG processing in mice, it is essential to understand the spectral characteristics of the signal. Therefore, a study of the main spectral components of rodents ECG signal was carried out. Figure 29 shows two 10-second segments of the ECG signal recorded at a sampling frequency of 10 kHz, along with their spectra in the range of 0 to 500Hz (within the Nyquist frequency range: 5 kHz). The representation on the top shows a normal ECG signal, where only the 50 Hz power line interference is observed in the spectrum. The representation on the bottom shows the ECG signal during stimulation, where the spectrum reveals the 50 Hz power line interference (in red) and stimulation artifacts (in this case at 20 Hz) along with their corresponding harmonics (in black).

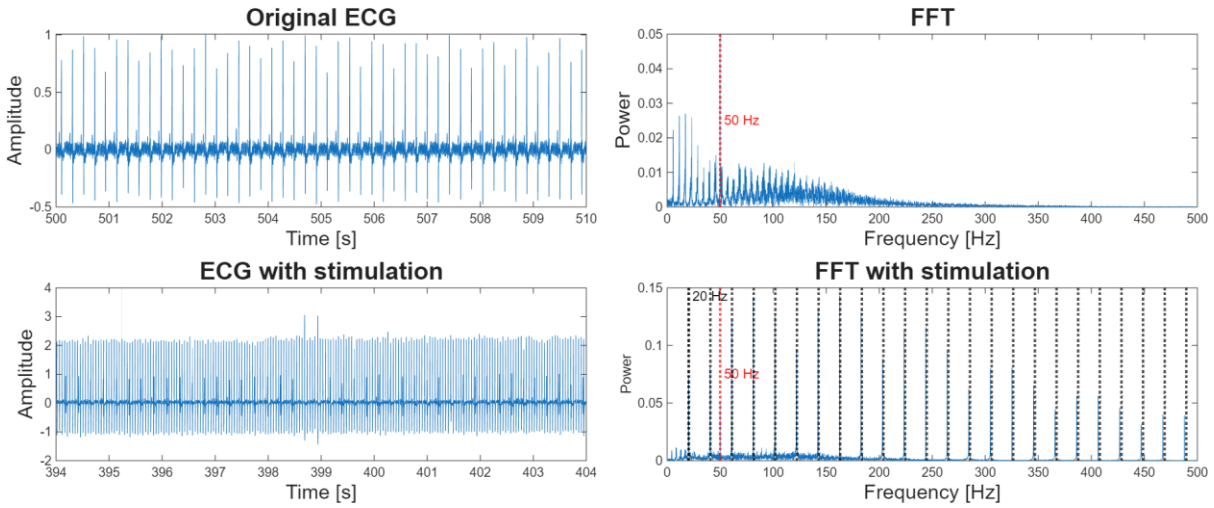

Figure 29 ECG recording during 10 seconds with and without stimulation.

Spectral analysis reveals that the relevant ECG information is concentrated at frequencies below 200 Hz; therefore, the module design will include filtering that preserves this band and discards higher

components that do not provide significant information. Additionally, techniques are incorporated to eliminate interference associated with power line frequency (50 Hz) and artifacts generated by experimental stimulation.

For heart rate estimation, the Pan-Tomkins algorithm [59] was adapted, and its description is presented in later sections.

EVOLUTION OF THE SIGNAL PROCESSING MODULE

The design of the module, represented in the diagram in Figure 30 (explained later), evolved from an initial simplified system. This first analysis algorithm detected R peaks by applying a threshold without prior filtering and calculated heart rate using sliding windows. It also attempted to identify other ECG components (P, QRS and T waves) and analyze their time intervals, resulting in a complex and poorly robust system with frequent errors in R peak detection.

As experiments progressed and results were evaluated, the design was redefined: signal filtering was incorporated, the Pan-Tomkins algorithm was adapted to improve detection, and continuous temporal analysis was implemented, replacing the sliding window approach.

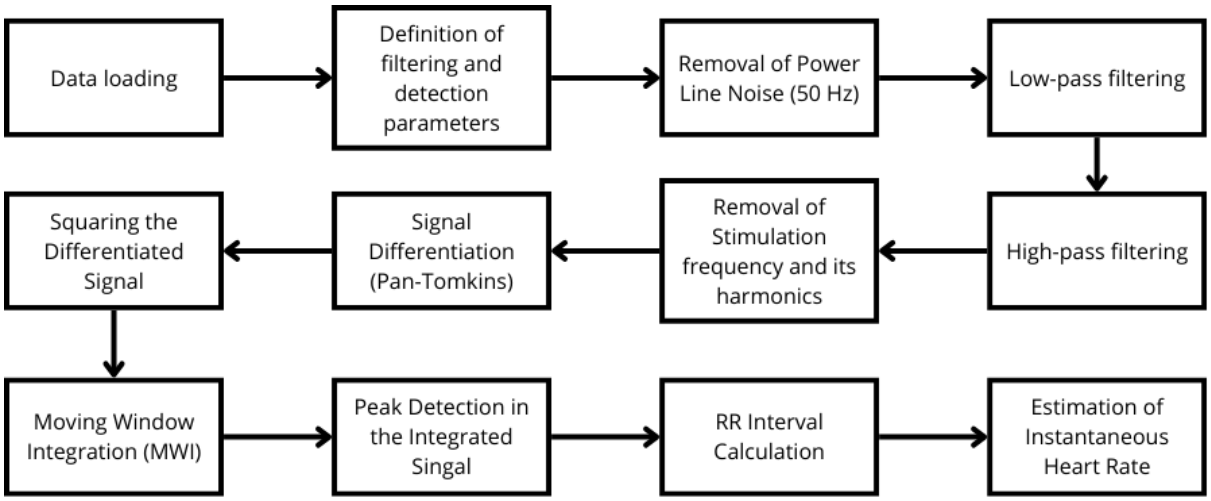

Figure 30 Signal processing module flow chart.

PROCESSING STEPS

The algorithm designed for the signal processing module is composed of 12 steps. Those steps, represented in Figure 30 are explained below.

- Data loading: experimental records containing the raw electrocardiographic signal, the stimulation signal, and the sampling frequency used during acquisition will be loaded. The program used for acquiring those signals (Spike2 [66]) generates a .smr file, this type of file is transformed into a MATLAB file type: mat.
- Definition of filtering and detection parameters: Cutoff frequencies, quality factors, time windows, and thresholds required for filtering, moving integration, and heartbeat detection will be established.
- Removal of power line noise: an IIR notch filter centered at 50 Hz will be applied to suppress electrical interference without significantly affecting ECG morphology.
- Low-pass filtering: a low-pass filter will be used to remove non-physiological high-frequency components and reduce electromyographic noise.
- High-pass filtering: a Butterworth high-pass filter will be applied to eliminate baseline drift and very low-frequency components.
- Removal of stimulation frequency and its harmonics: successive notch filters will be applied at the stimulation frequency and its harmonics to suppress periodic interference induced during the experiments.

- Signal differentiation: the filtered signal will be differentiated to highlight rapid changes associated with the QRS complex.
- Squaring the differentiated signal: the differentiated signal will be squared to emphasize steep peaks and make all values positive.
- Moving Window Integration (MWI): a moving integration using a rectangular window will be applied to obtain a signal representing the energy of the QRS complex over time.
- Peak detection in the integrated signal: local maxima in the integrated signal that exceeds a threshold and respects a minimum distance will be identified and associated with possible heartbeats.
- RR interval calculation: RR intervals will be calculated from the time differences between consecutive detected peaks.
- Estimation of instantaneous heart rate: beat-to-beat heart rate will be obtained, expressed in beats per minute (bpm), from the RR intervals.

This chapter has defined the hardware and software architecture of the prototype, specifying the functional modules and their interactions. The next chapter addresses the implementation of the closed-loop system, detailing how the designed components were integrated and deployed in practice.

4. CLOSED-LOOP IMPLEMENTATION

This chapter presents the implementation of the device carried out during the present work. Based on the design presented in the previous chapter, both the hardware part of the prototype and the software part of the device are implemented. Both implementations are presented below.

4.1. HARDWARE IMPLEMENTATION OF THE PROTOTYPE

The hardware implementation makes use of the devices described in section 3.2. Together, these components enable the implementation of the system proposed in chapter 3. The interconnection between these devices and an image that represents them is shown in Figure 31. For a better view of the components interconnection, a closer picture is presented in Figure 32 but only showing the components is presented.

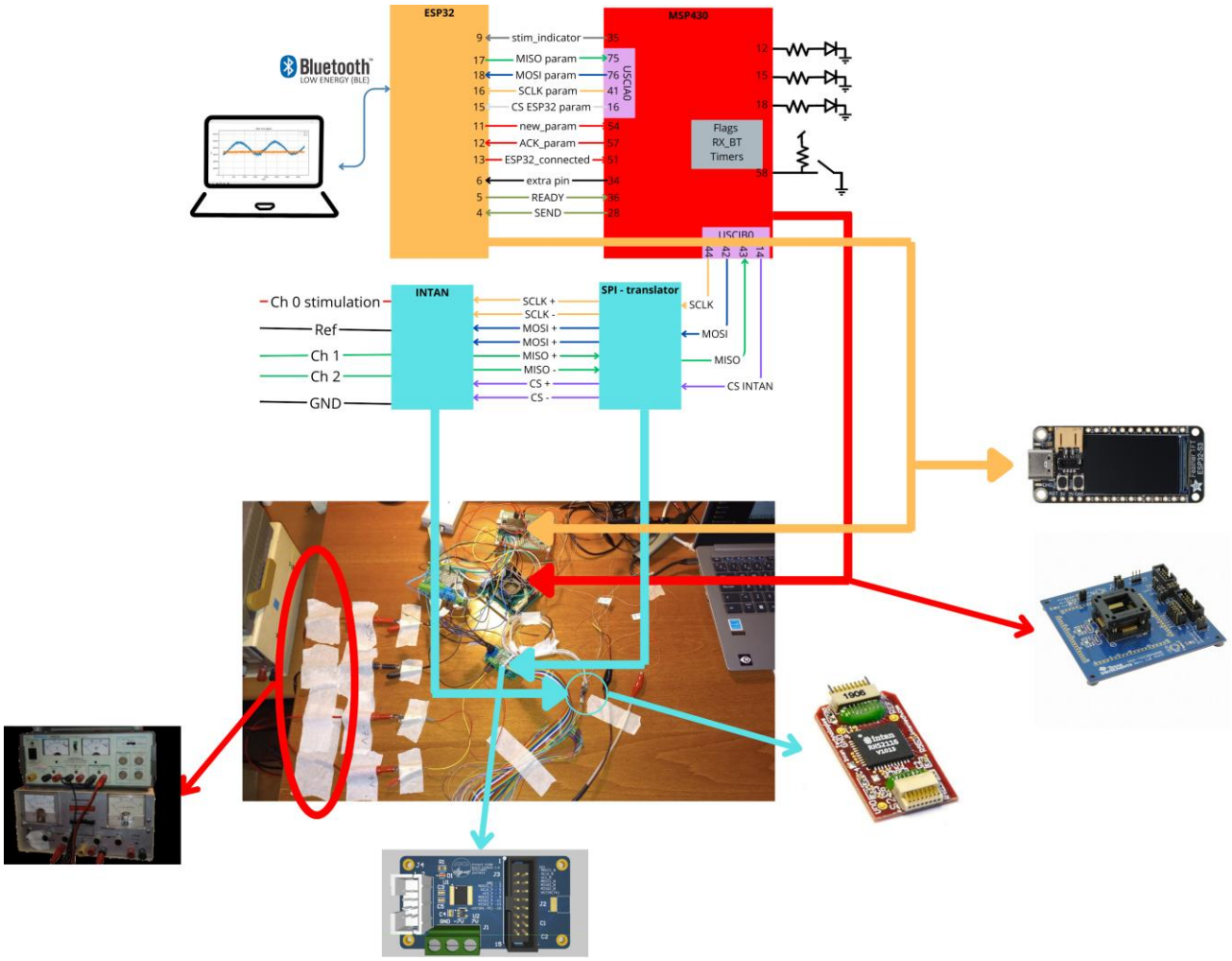

Figure 31 Connection map and components of the designed hardware.

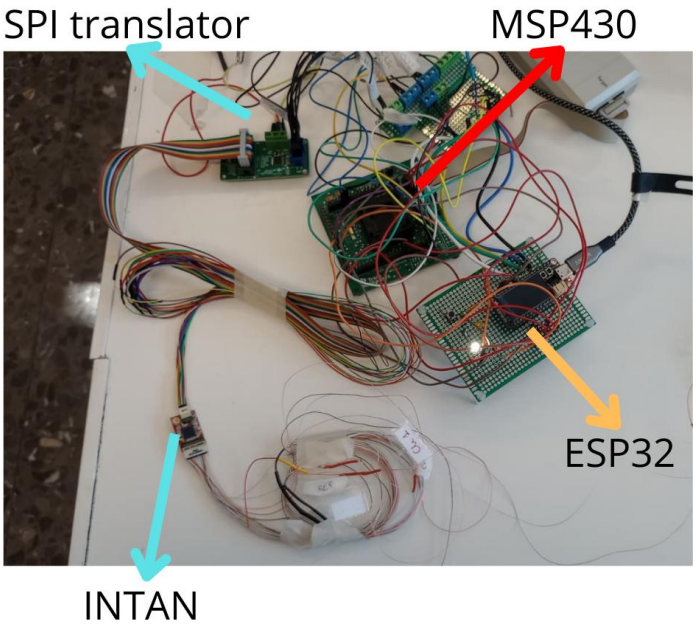

Figure 32 Hardware interconnection.

4.2. SOFTWARE IMPLEMENTATION

To carry out the programming of the MSP430FG479 microcontroller, it was necessary to develop a Hardware Abstraction Layer (HAL). For this purpose, the design of this layer is based on the use of data structures, which help to keep the code well organized by eliminating global variables and grouping related parameters.

The following sections describe the structures used in the software implementation associated with the MSP430, which was programmed using Code Composer Studio (CCS). The HAL of this microcontroller can be found in GitHub, inside folder "0 new common-port/port/MSP430FG479" [67].

In addition, with the aim of achieving a modular and easily adaptable system, in which the different devices that compose it can be replaced without affecting the overall logic, a common-port architecture was adopted for code organization. This structure clearly separates hardware-dependent files specific to the MSP430 from hardware-independent files, including both the MSP430 HAL and the configuration functions for the INTAN device, which were also developed in this work. The code developed can be found in GitHub, inside folder "0 new common-port" [67].

This section also describes the development of the code used to program the ESP32, implemented using the Arduino IDE, which acts as an intermediate system between the MSP430 and the user device (computer), managing communication and parameter exchange between them. The code developed can be found in GitHub, inside folder "2 ESP32S3" [67].

Finally, the implementation of the electrocardiogram (ECG) signal analysis module is presented. This module processes the signals acquired during the experiments and analyzed using MATLAB, detailing the different processing stages and the criteria used to extract experimental conclusions. The code developed can be found in GitHub [65].

4.2.1. USE OF DATA STRUCTURES

The firmware development follows an architecture based on configuration structures, with the aim of organizing and parameterizing the different system functionalities in a clear and scalable manner. This approach allows essential parameters for each module to be defined, modified and reused without the need to create specific functions, thereby reducing code complexity and facilitating maintenance.

The structures act as containers for parameters that determine the behavior of different peripherals and applications, including master/slave mode, clock polarity and phase, bit transmission order, word length and clock source among others. Thanks to this methodology, the system can be easily adapted to different operating scenarios without compromising code stability or clarity.

Notably, instead of implementing specific configuration functions for each SPI module, the same generic configuration functions are reused by passing a pointer to the corresponding structure as an argument. This approach significantly reduces code complexity and facilitates future maintenance and expansion.

TIMER CONFIGURATION

The *TIMER_config* structure is used to configure the internal timer of the MSP430 which plays a fundamental role in generating system timing events. Specifically, this timer is used to precisely define stimulation and rest cycle timing, as well as the ON/OFF intervals of the stimulation signal when the MSP430 acts as the stimulation master with respect to the INTAN.

Using a dedicated timer structure decouples timing logic from the rest of the system and facilitates modification of temporal parameters without affecting other firmware components.

SPI CONFIGURATION

The MSP430 includes two independent SPI communication modules, named USCI_A0 and USCI_B0. Two separate structures have been defined for their configuration: *SPI_config_struct* and *SPI_B_config_struct*.

These structures allow configuration of parameters such as master/slave mode, clock polarity and phase, bit transmission order, word length, and clock source. Having two independent instances is essential to enable simultaneous communication between the MSP430 and two different external devices: the ESP32 and the INTAN, while avoiding interference or bus contention.

As with other modules, generic configuration functions are reused by passing pointers to the corresponding structures, reducing code complexity and improving maintenance.

SD16A CONFIGURATION

The *SD16A_config* structure groups with the parameters required to configure the sigma-delta analog-to-digital converter (SD16), integrated into the MSP430. These parameters include the analog input channel, reference voltage, clock frequency and divider, conversion mode (continuous or single), oversampling ratio (OSR), programmable gain and readout method (interrupts or polling).

INTAN CONFIGURATION

The *INTAN_config* structure consolidates all parameters required to configure the INTAN integrated circuit, which is responsible for both bioelectrical signal acquisition and electrical stimulation generation. These parameters include the internal ADC sampling rate, DSP filtering characteristics, amplifier bandwidth settings, stimulation parameters (current, polarity, activation and rest times), and advanced options such as bipolar stimulation and charge recovery.

The variables contained in this structure directly correspond to the parameters described in section 3.3.4 Application functionality, which details the configurable options available through the graphical user interface developed for the system. As such, the *INTAN_config* structure acts as a bridge between the embedded software layer and the high-level user configuration.

4.2.2. COMMON-PORT SOFTWARE DESIGN

A key feature of this work is modularity, which allows system components to be easily replaced without compromising overall functionality. To achieve this, a common-port architecture has been adopted, whose main objective is to facilitate the replacement of the MSP430 microcontroller with another device without modifying the common system logic.

This structure is organized into two main folders:

- Common folder: contains microcontroller-independent files and functions that implement the common system logic.
- Port folder: includes microcontroller-specific functions, such as the SPI implementation, which are invoked from the common logic.

The directory tree used in this work is shown in Figure 33. The files contained within the main folders structure: common and port, are presented below.

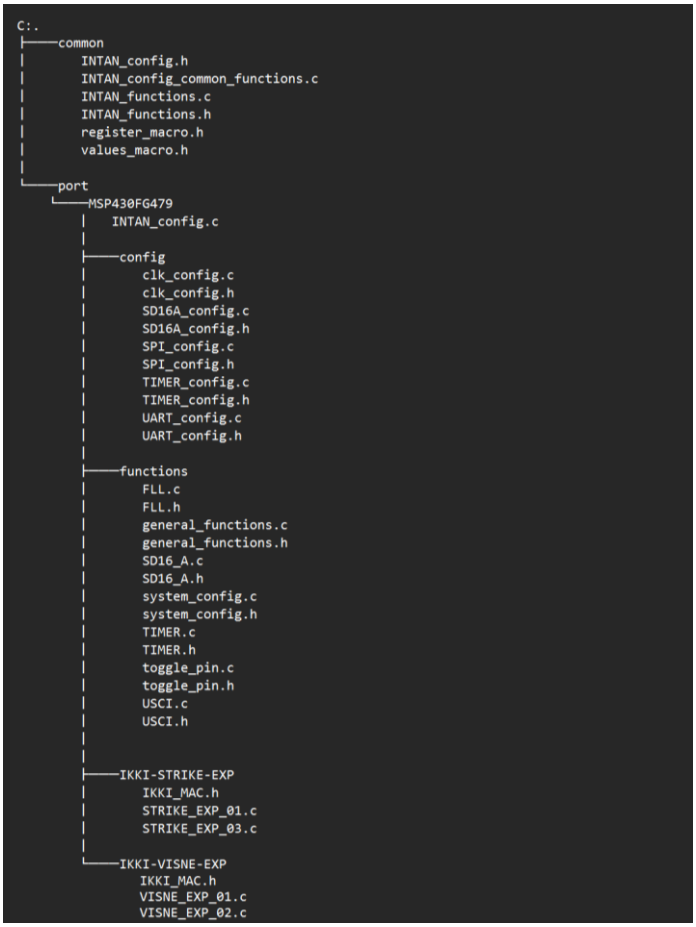

Figure 33 Common-port folder structure.

COMMON FOLDER

Inside the common folder are included the microcontroller-independent files and functions.

INTAN_config (.c and .h)

Defines the *INTAN_config* structure and the functions required to configure the INTAN device, including stimulation parameters, high-pass and low-pass filters.

These functions send commands to read from and write to the internal registers of the INTAN, whose functionality is described in the manufacturer's datasheet [56]. Additionally, a verification mechanism based on the INTAN SPI response is implemented to confirm correct register writing, enabling robust system behavior in critical applications.

INTAN_functions (.h)

Declares functions that encapsulate configuration and testing procedures, such as:

- *Call_configuration_functions*
- *Call_sense_configuration_functions*
- *Call_initialization_procedure_example*
- *INTAN_function_update*

These functions serve as an interface between the common logic and the project-specific configurations.

Register_macro (.h)

Contains macro definitions for all INTAN registers, allowing them to be accessed using descriptive names instead of numeric addresses. Examples include:

- Basic actions: *WRITE_ACTION, READ_ACTION, CONVERT_ACTION*
- Configuration registers: *REGISTER_1, IMPEDANCE_CHECK_CONTROL*
- Stimulation registers: *STIM_ENABLE_A_reg, STIM_STEP_SIZE, CHx_POS_CURR_MAG*

This abstraction improves readability and reduces register-handling errors.

Values_macro (.h)

Defines macros for the possible values that registers can take according to the desired configuration, including cutoff frequencies, stimulation parameters, charge recovery control among others.

This file complements the **register_macro.h** file providing flexible hardware configuration values.

INTAN_config_common_functinos (.c)

Implements functions common to all microcontrollers, delegating hardware-specific operations (such as SPI transmission) to functions defined in the port folder. For example:

- *Send_values*: sends data via SPI using the microcontroller-specific implementation.
- Configuration functions that rely on *send_values* to maintain hardware independence.

PORT FOLDER

The port folder contains all hardware-specific files. In this work, since the MSP430FG479 microcontroller is used, its corresponding folder is organized into four main subfolders:

- Config: contains function and structure definitions required to configure MSP430 modules, such as the system clock, SD16A ADCs, SPI interface, timers and UART (not used in this work).
- Functions: Includes the implementation of functions that configure and initialize the modules.
- IKKI – STRIKE / VISNE – EXP: contains the main code used to execute Type A (STRIKE) and Type B (VISNE) Experiments. The structure and logic of these codes are based on the design presented in section 4.2.3 INTAN configuration functions, where the governing state machines are described.

It is important to note that all configuration functions, also referred to as the Hardware Abstraction Layer (HAL), are responsible for initializing and configuring the registers associated with each microcontroller functionality.

4.2.3. INTAN CONFIGURATION FUNCTIONS

To develop the INTAN configurations, each of the available features was thoroughly studied. Annex C: INTAN configuration functions presents a summary of the functions implemented in this work for each feature, together with the characteristics of the *INTAN_config* structure used during execution, the input parameters or assigned values, and the function type (common or port). In addition to function development, each available configuration was individually tested.

The complete list of configured features is provided below, however, only those considered relevant for this work are discussed in detail after:

- Absolute value.
- AC amplifier bandwidth.
- Analog-to-digital converter.
- Auxiliary digital output.
- Charge recovery switch.
- Command words.
- Constant current stimulator.
- Current-limited charge recovery.
- Compliance monitor.
- Digital Signal Processing.
- Electrode impedance test.
- Fault current detection.

- General configuration.
- Power dissipation.

AC AMPLIFIER BANDWIDTH

The INTAN device includes low-noise AC amplifiers with configurable analog filters that allow the passband to be defined between two cutoff frequencies.

The upper cutoff frequency is set using a third-order Butterworth filter, configured through the *fh_magnitude* and *fh_unit* parameters.

The lower cutoff frequency is defined by a first-order high-pass filter, configurable via the *fc_low_A/B* and *amplifier_cutoff* parameters. Two different filters (A and B) can be configured and switched between them to allow stimulation issues deletion.

COMMAND WORDS

Functions are implemented to transmit all command types supported by INTAN: WRITE, CONVERT, READ, and CLEAN. Initialization routines were also defined, assigning default values to the *INTAN_config* structure while prioritizing configurations that minimize power dissipation, as described below. Additional functions were implemented to enable and disable flags associated with each operation.

Within the Command words class, extra functions were developed to send empty or confirmation commands. This functionality is required to the response latency of the INTAN, which needs the transmission of dummy commands to ensure correct data reception. Verification is subsequently performed using the *check_received_command* function, which confirms the validity of the received response.

CONSTANT CURRENT STIMULATOR

Each stimulator/amplifier block of the INTAN device incorporates a constant current generator capable of delivering positive or negative pulses in a range from 10 nA to 2.55 mA.

The generator is configured by assigning a specific channel and adjusting the *step_DAC*, *positive/negative_current_magnitude*, *positive_negative_current_trim* and *stim_polarity* parameters.

The values of *step_DAC* and *X_current_magnitude* determine the applied current. For example, if *step_DAC* = 500 nA and *X_current_magnitude* = 10, the resulting current is:

$$500\,nA \cdot 10 = 5\,mA$$

The *stim_polarity* parameter defines the signal polarity (unipolar or bipolar) allowing the waveform to be adapted to different experimental protocols.

Two groups of functions were developed for this module:

- Configuration functions, which set the parameter values.
- Stimulation control functions (ON/OFF), with two variants:
    - *ON_INTAN / OFF_INTAN*: prioritize stimulation reliability at the cost of higher latency (≈ 1ms)
    - *ON_INTAN_FASTER(_FASTER) / OFF_INTAN_FASTER*: optimize transmission speed, reducing the minimum inter-stimulus interval to 500 µs, although without 100% execution guarantee.

This design provides flexibility to balance accuracy and speed depending on experimental requirements.

ANALOG-TO-DIGITAL CONVERTER

The INTAN device integrates a 16-bit ADC together with an analog multiplexer, allowing the sampling of both high-gain AC amplifier signals and low-gain DC signals.

Configuration of this functionality is limited to setting the sampling frequency through the *ADC_sampling_rate* parameter, adjusted via the *ADC_sampling_rate_config* function.

It is essential for the user to be aware of the effective sampling rate. In this design, the MSP430 controls the timing and SPI command transmission. Once the rate at which data packets are requested is determined, it must be communicated to the INTAN through the *ADC_sampling_rate_config* parameter.

The acquisition process is completed when the MSP430 sends CONVERT commands to the INTAN to request channel readings. The final sampling rate depends on the time interval between consecutive commands, allowing dynamic adjustment of the acquisition rate.

DSP HIGH-PASS FILTER FOR OFFSET REMOVAL

The INTAN device includes a DSP module that applies single-pole digital high-pass filters to each channel in order to remove residual offsets and improve signal quality.

The cutoff frequency is adjusted as a function of the ADC sampling rate (*ADC_sampling_rate*) and configured using the *DSP_cutoff_freq* and *number_channels_to_convert* parameters. Digital filtering is enabled or disabled using the *DSP_en* parameter, managed through the *enable/disable_digital_signal_processing_HPF* functions.

POWER DISSIPATION

Since the INTAN device is designed for low-power operation, specific register configurations were implemented to minimize power dissipation. During system initialization, the MSP430 executes a function that places the INTAN in its minimum power consumption mode (*minimum_power_disipation*). Subsequently, only the registers required to enable specific functionalities (such as stimulation and signal acquisition) are modified, ensuring an optimal balance between energy efficiency and functionality.

4.2.4. ESP32 – CODE DESCRIPTION

The programming of the ESP32 (ESP32-S3 Feather TFT) was carried out using the Arduino IDE (version 2.3.6). For this purpose, an SPI control library for the ESP32 available online was employed [68].

In addition, configuration functions were developed for each of the pins connected to the MSP430, and the state machine logic defined in section 3.3 was implemented.

The ESP32-S3 software integrates two main communication interfaces: Bluetooth Low Energy (BLE), used to receive configuration parameters from an external device, and SPI in slave mode, used to transmit these parameters to the MSP430. The program is structured around the state machine presented in section 3.3.4, which governs data flow and synchronization between both devices.

The reception of new parameters is performed via BLE through a written characteristic. When the ESP32 receives a valid data packet, the parameters are parsed and stored in internal variables, and the RX_BT flag is asserted to indicate the availability of a new configuration. These parameters include all configuration values defined in section 3.3.

Once the reception flag is activated, the system transitions to the SPI transmission state. In this state, the received values are converted and placed into an SPI transmission buffer with a predefined order. To notify the MSP430 of the availability of new parameters, the NEW_PARAM_PIN is asserted prior to initializing the SPI transfer.

After completing the transmission, the ESP32 enters the confirmation wait state, in which it monitors the ACK pin from the MSP430. This mechanism ensures that the receiving microcontroller has correctly received and processed the new parameters before proceeding.

Once acknowledgment is completed, the notification signal is deasserted and the system returns to its initial state, remaining idle while waiting for new BLE data.

Additionally, the firmware implements supervision of the stimulation state through a dedicated pin, sending BLE notifications whenever transitions between active and inactive stimulation states are detected. This feature allows the remote device to be continuously informed of the system functional status in real time.

4.2.5. USER PC INTERFACE

To enable interaction between the user and the experimental system, a desktop application developed in Python (V 3.14.0) was implemented. This application provides a graphical user interface (GUI), shown in Figure 34, which allows the user to interact with the embedded hardware in a simple and intuitive way.

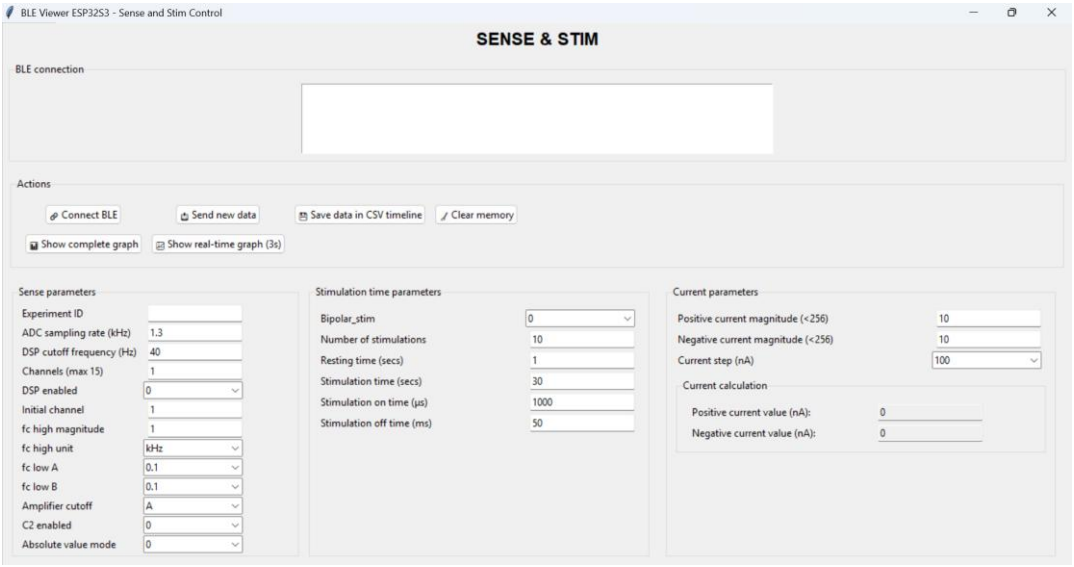

Figure 34 Graphical User Interface made in Python for stimulation and acquisition control.

Through this interface, the user can establish a Bluetooth Low Energy (BLE) connection with the ESP32-S3 device, which acts as the communication bridge between the PC and the MSP430 microcontroller. Once connected, the application receives data acquired by the INTAN ADC, processed by the MSP430 and transmitted by the ESP32-S3. This data can be visualized both in real time and as complete recorded signals after acquisition.

The interface also allows the user to configure sensing and stimulation parameters. New parameter values can be entered through dedicated input fields and sent wirelessly to the ESP32-S3, which updates the configuration of the MSP430 accordingly. Additionally, stimulation events are detected, time-stamped, and synchronized with the acquired signals, enabling clear identification of stimulation intervals during visualization and data export.

The application includes options to display real-time plots, visualize full datasets, clear internal buffers, and export all acquired data and stimulation events to CSV (Comma Separated Values) files for offline analysis.

From a software perspective, the application combines asynchronous BLE communication, a graphical user interface, real-time data processing, and signal visualization. The Python libraries used are *asyncio* and threading for asynchronous execution, ***bleak*** for BLE communication, *tkinter* for the graphical interface, *matplotlib* for signal plotting (including real-time animations), and standard libraries such as *csv*, *datetime* and *time* for handling and storage.

Figure 35 presents an example of the interface during operation, where a test signal generated by a function generator is displayed in real time.

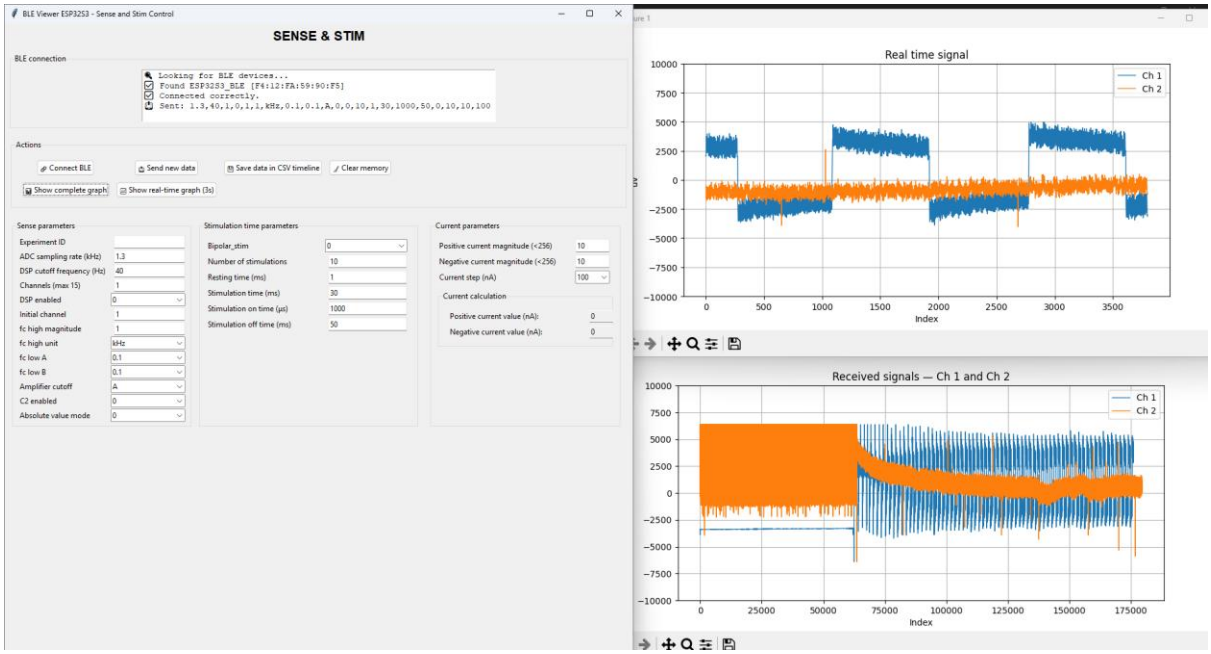

Figure 35 Graphical User Interface and received signals in channels 1 and 2.

4.2.6. SIGNAL PROCESSING MODULE

In section 3.3.5 Signal processing module, the design of the signal processing module used for the analysis of electrocardiographic (ECG) signals during VNS experiments was described. This section details the practical implementation of this module, illustrating each processing stage through the analysis of a real experimental recording obtained in the CTB. The following subsections provide a detailed description of each processing step and the results obtained.

RAW DATA EXTRACTION: DATA LOADING

The processing begins with transforming the Spike2 file format into MATLAB format. Afterwards, the experimental data stored on disk in MATLAB (.mat) format is loaded. Each file contains the recorded ECG signal, the stimulation signal applied during the experiment, and the sampling frequency used during acquisition (10 kHz).

From the loaded file, the ECG channel is extracted, and the corresponding temporal vector is constructed based on the sampling frequency and the total number of recorded samples.

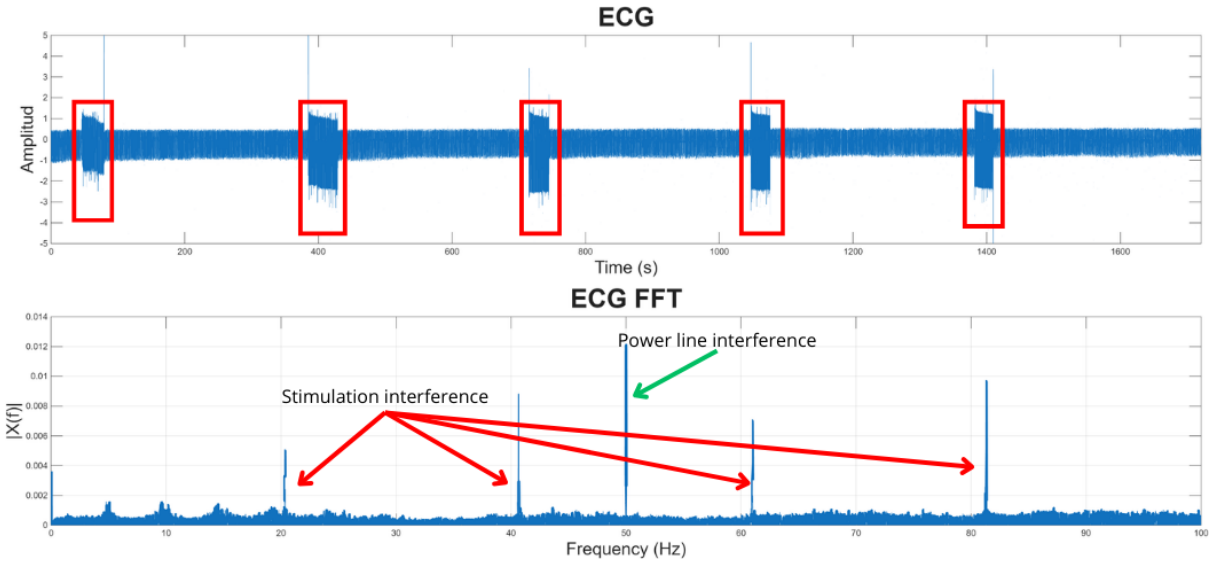

Figure 36 Raw ECG signal and its spectrum.

Figure 36 shows, on the top, the complete ECG signal corresponding to an experiment of approximately 30 minutes. In this temporal representation, segments where the stimulation signal introduces large-amplitude artifacts are clearly visible and highlighted with a red box. The lower panel represents the signal spectrum, where two main sources of interference can be identified: the 50 Hz component associated with the power line and the experimental stimulation frequency (around 20 Hz), along with its harmonics.

POWER LINE INTERFERENCE REMOVAL (50 HZ FILTERING)

To suppress interference produced by the electrical grid, a 50 Hz IIR (Infinite Impulse Response) notch filter is implemented. The filter is designed with a high-quality factor (Q = 200), providing a narrow rejection band and minimizing distortion of the ECG morphology.

Filtering is applied using a zero-phase bidirectional approach (filtfilt), thus eliminating the phase shift introduced by the filter. Figure 37 shows the frequency response of the notch filter, both in magnitude and phase, clearly illustrating the sharp and localized attenuation around 50 Hz and the minimum phase shift on the phase.

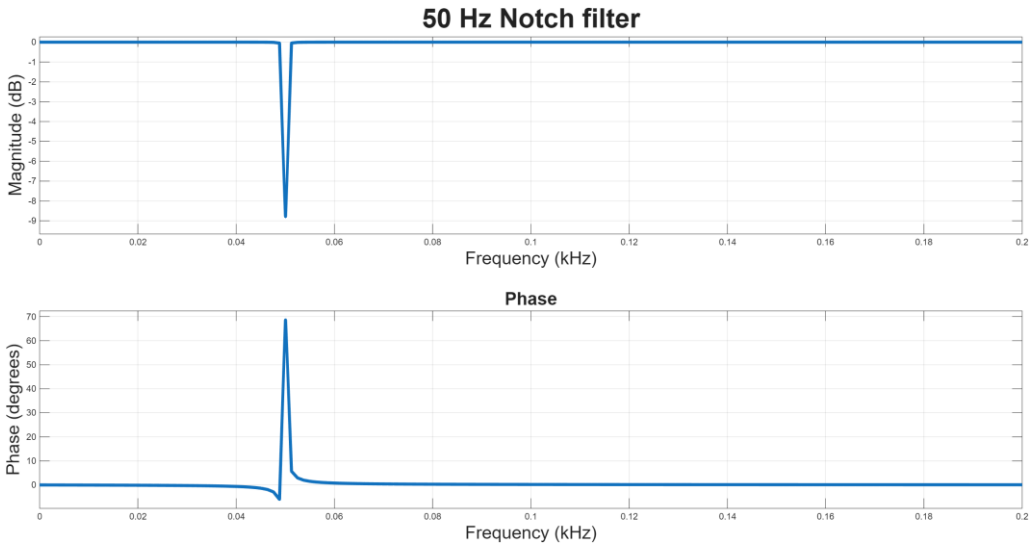

Figure 37 50 Hz notch filter frequency response.

The result of applying this filter to the ECG signal is shown in Figure 38. In the temporal domain, the signal maintains its original morphology, while in the spectral domain, the 50 Hz component is effectively removed, with stimulation-related artifacts still present.

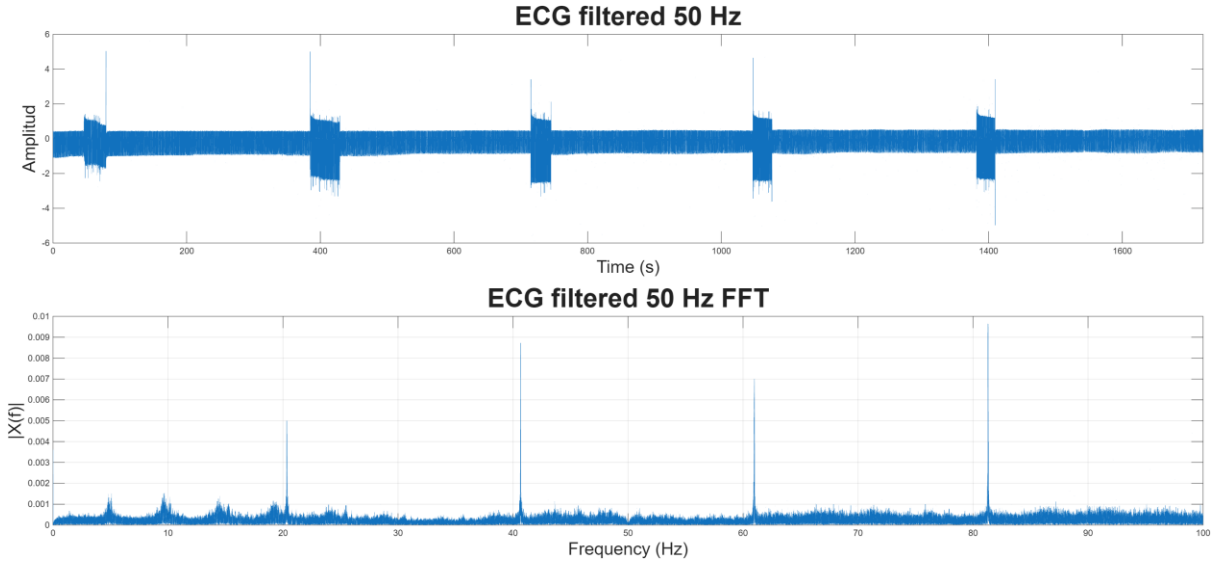

Figure 38 ECG with 50 Hz filtered.

BAND-PASS FILTERING

Once the power line interference has been removed, a band-pass filter is applied to preserve only the relevant spectral content of the ECG. This filtering is implemented in two stages:

1. Low-pass filtering with a cutoff frequency of 250 Hz, using a high-order IIR filter, which removes non-physiological high-frequency components and electromyographic noise.
2. High-pass filtering using a fourth-order Butterworth filter with a cutoff frequency of 1 Hz, to remove the DC component and slow baseline variations

Figure 39 and Figure 40 show the frequency responses of the two low-pass and high-pass filters, respectively. Figure 41 presents on the lower part the ECG signal after band-pass filtering along with its spectrum. Comparing this signal with the signal filtered only at 50 Hz (on the top part of the figure) shows no visible differences in the temporal domain, confirming that band-pass filtering primarily removes out-of-band noise without affecting relevant physiological information.

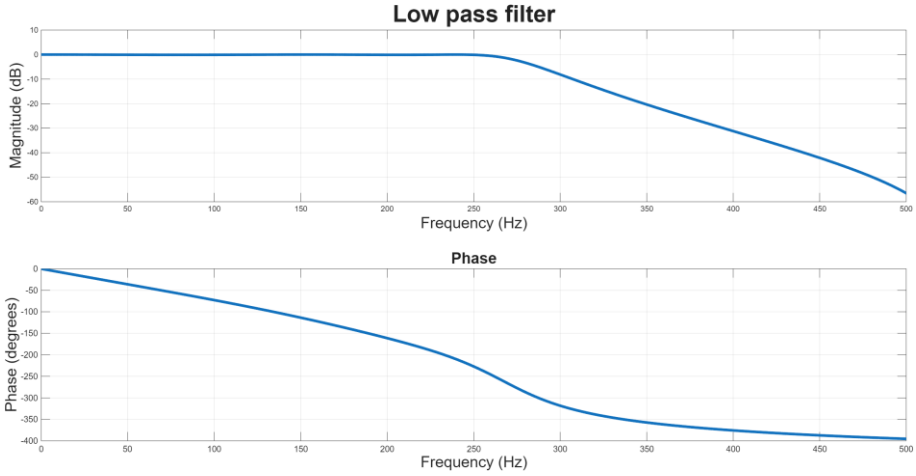

Figure 39 Low-pass filter frequency response.

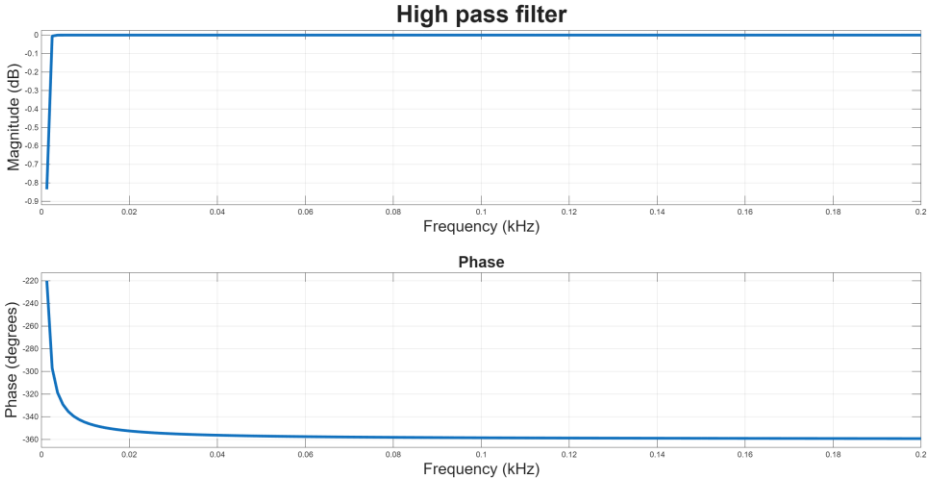

Figure 40 High-pass filter frequency response.

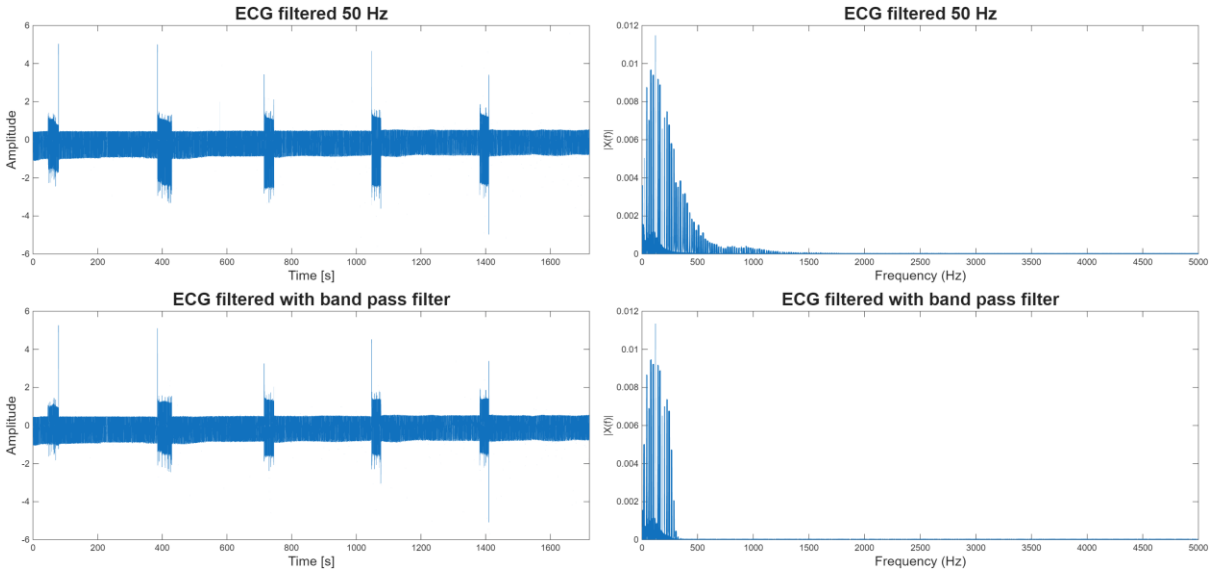

Figure 41 ECG before and after band-pass filtering.

STIMULATION INTERFERENCE REMOVAL

During experimental stimulation periods, the ECG signal is affected by periodic interference at the stimulation frequency (around 20 Hz) and its harmonic multiples. To remove these components, a series of notch filters is implemented, centered on the fundamental stimulation frequency and each of its harmonics up to 500 Hz.

Each notch filter is designed with the same quality factor as the filter used for mains interference, ensuring selective suppression of interference without degrading the ECG signal. Filtering is applied sequentially using bidirectional filtering.

Figure 42 shows the frequency responses of the notch filters corresponding to the stimulation frequency and its harmonics. Figure 43 compares the ECG signals before and after stimulation artifact removal, both in the temporal and spectral domains. After filtering, the visible stimulation artifacts and their spectral content are removed, leaving only the intrinsic ECG components.

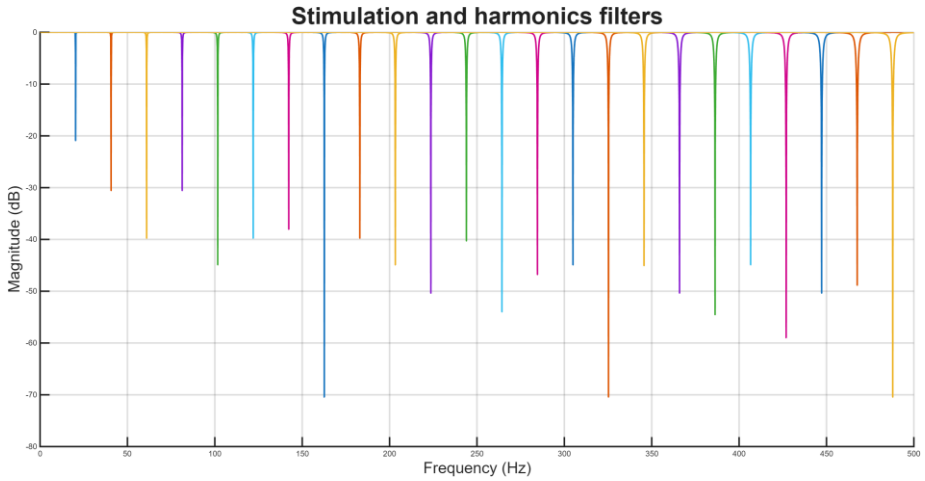

Figure 42 Stimulation and harmonics filtering.

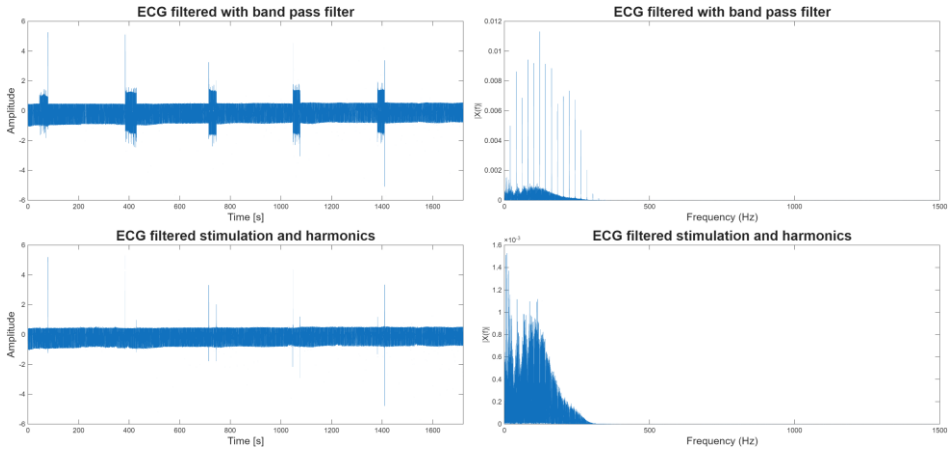

Figure 43 ECG before and after stimulation removal.

APPLICATION OF THE PAN-TOMPKINS ALGORITHM

On the filtered ECG signal, an adaptation of the Pan-Tompkins algorithm is applied for QRS complex detection. This is considered an adaptation because the parameters used in the different stages have been adjusted to the characteristics of the signal, which originates from a mouse rather than a human.

First, a five-point FIR (Finite Impulse Response) derivative filter is applied to emphasize the steep slopes associated with the QRS complex. This filtering is implemented using filtfilt to avoid filter-induced delays.

Next, the derivative signal is squared, enhancing large-amplitude variations and making all samples positive. Subsequently, a moving window integration with a 15 ms rectangular window is applied, producing a signal representative of the QRS energy over time.

Figure 44 shows the result of these stages applied to a 1.5 second segment: filtered ECG, derivative signal, squared signal, and integrated signal. Peak detection is then performed on the integrated signal using a fixed threshold and a minimum peak distance, identifying the instants corresponding to the R-peaks.

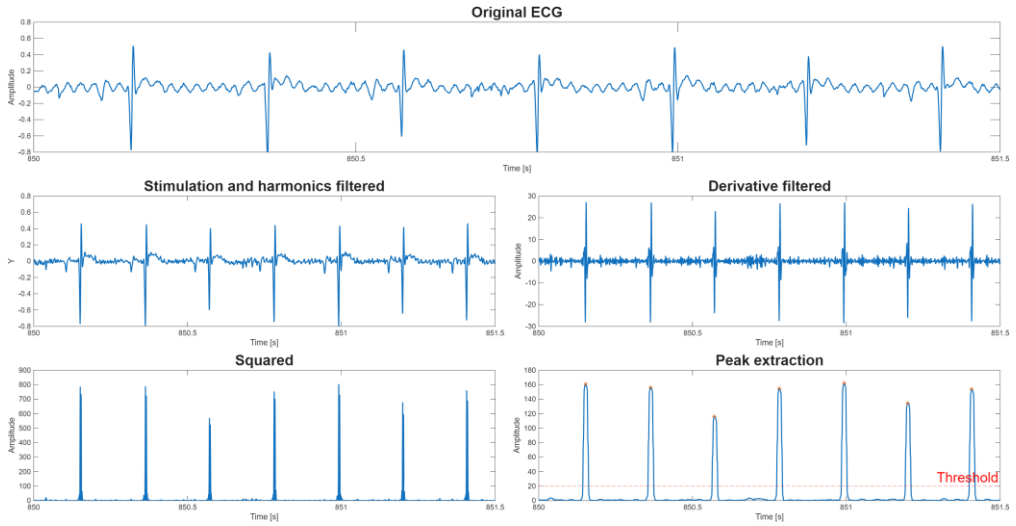

Figure 44 ECG steps when applying Pan-Tomkins algorithm.

BPM CALCULATION

Once the R-peaks are identified, RR intervals are calculated as the temporal differences between consecutive peaks. From these intervals, the instantaneous heart rate is estimated, expressed in beats per minute (BPM), using the inverse relationship between the RR interval and time.

Figure 45 presents the complete analysis of an experiment: the ECG signal over the entire experimental session is shown in blue, while the beat-to-beat heart rate evolution is shown in orange. This representation allows continuous analysis of heart rate variations throughout the experiment.

CONCLUSIONS

The primary objective of this signal processing module is to identify variations in heart rate associated with periods of stimulation. Figure 45 clearly shows that during the intervals in which stimulation is applied, a significant reduction in heart rate occurs, followed by a gradual recovery once the stimulation ceases.

These results confirm the validity of the implemented processing module and its suitability for integration into a closed-loop system.

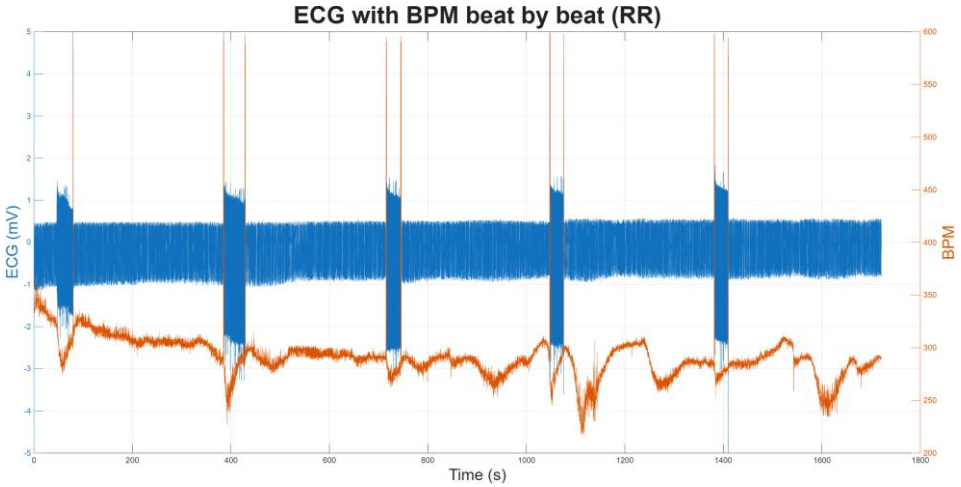

Figure 45 Beats Per Minute analysis.

The following chapter presents the results of the verification of the operation of the prototype designed and implemented during the development of this work.

5. PROTOTYPE VERIFICATION

This chapter presents the experimental verification of the developed prototype, focusing on its operation under real acquisition and stimulation conditions. The objective of these tests is to verify the correct interaction between the different system components as well as to assess the robustness and timing performance of the proposed communication protocol.

Through a set of controlled experiments, the behavior of the system is analyzed at both the signal acquisition and stimulation levels, providing quantitative evidence of correct data transfer, synchronization and functional reliability prior to its use in more complex experimental scenarios.

5.1. ACQUISITION: TESTS WITH MSP430 + INTAN + ESP32-S3

This section presents the operation of the communication protocol defined among the three devices that compose the prototype (MSP430, ESP32 and INTAN). Each device fulfills a different role during acquisition mode:

- MSP430: acts as the master device with respect to both the ESP32 and the INTAN. It is responsible for requesting data from the INTAN and forwarding the acquired samples to the ESP32.
- INTAN: acquires data from its ADCs and updates stimulation whenever requested by the MSP430 and transmits the samples through the SPI_A interface.
- ESP32: receives data from the MSP430 in a transparent manner and forwards it to a personal computer via BLE.

The ordered exchange of information is achieved using the protocol described in chapter 3, which is based on the use of SEND and READY signals. Figure 46 shows a capture obtained with the logic analyzer SP209 from Ikalogic, connected as follows (the INTAN SCLK signal was not connected due to channel limitations, however, this is not considered critical given that the CS, MOSI and MISO signals are available):

- CH1 (brown): MOSI – ESP32
- CH2 (red): MISO – ESP32
- CH3 (orange): SCLK – ESP32
- CH4 (yellow): CS – ESP32
- CH5 (green): MOSI – INTAN
- CH6 (blue): MISO – INTAN
- CH7 (pink): CS – INTAN
- CH8 (gray): SEND
- CH9 (white): READY

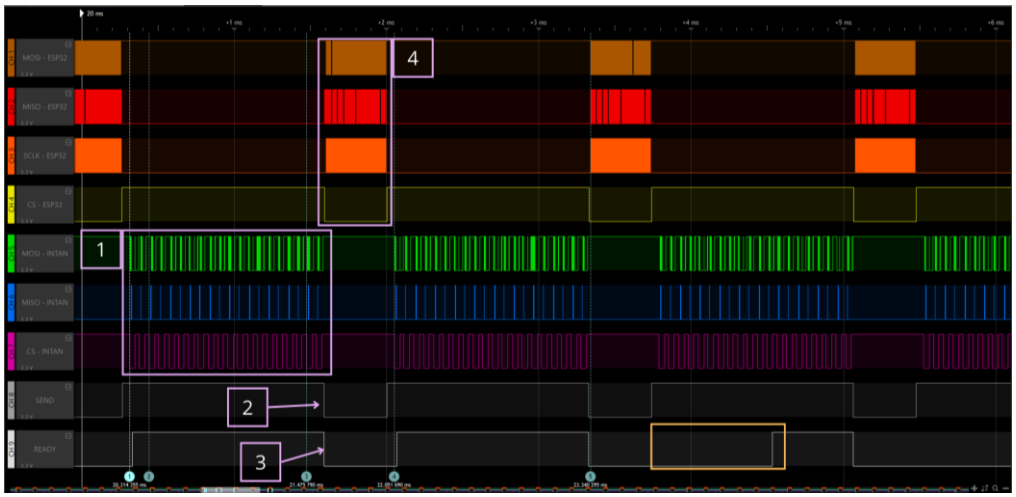

Figure 46 Logic analyzer capture when testing MSP430 + ESP32 + INTAN working algorithm.

The capture illustrates the protocol described in chapter 3:

1. The MSP430 requests data from the INTAN (10 samples per channel) and
2. sets the SEND signal to level 0 when READY is at level 1. In Figure 47 the waiting until READY has level 1 is shown.
3. The ESP32 sets READY to level 1 when it has completed the rest of tasks and sets READY to level 0 when it detects that SEND has been set to 0.
4. When the MSP430 detects that READY has transitioned to level 0, it starts transmitting the data via SPI.

Figure 46 also shows situations (such as the one highlighted by the yellow box) in which the ESP32 is still busy performing other tasks, such as transmitting data over BLE or servicing interrupts. This behavior highlights the relevance of the SEND-READY protocol design. During this time, the MSP430 continues requesting data from the INTAN, meaning that it is not idle. If the number of samples requested from the INTAN were reduced from 10 to fewer samples per channel, the MSP430 would spend more time waiting for READY to be high, thus reducing the effective sampling frequency.

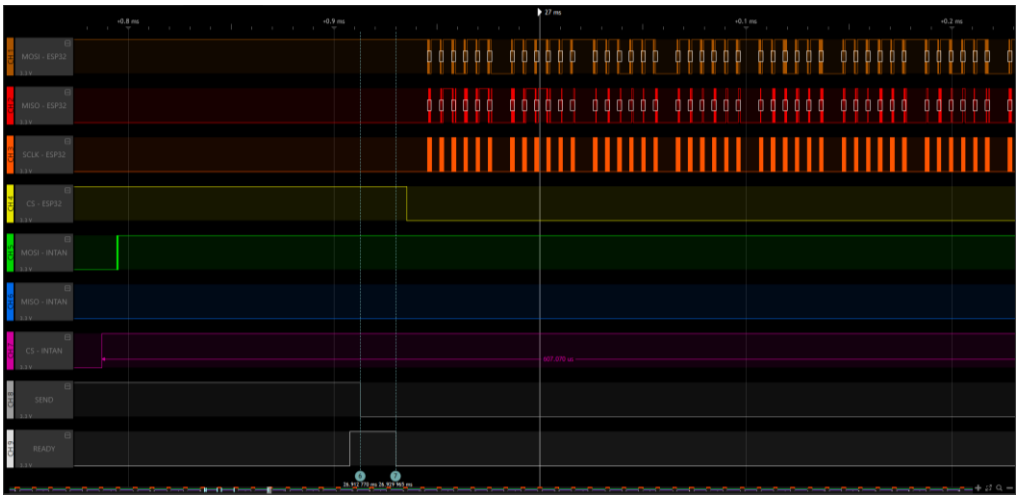

Figure 47 Logic analyzer capture: SEND waits until READY has logic value 0.

5.1.1. SEND-READY PROTOCOL AND SAMPLING FREQUENCY ESTIMATION

From Figure 46, an approximate estimation of the system sampling frequency can be obtained. In each transmission, 5 samples per channel are acquired. The time between two consecutive samples is:

$$20.4433\ ms - 20.314355\ ms = 128.945\ \mu s$$

That is equivalent to a sampling frequency of $f_s = \frac{1}{128.945 \mu s} = 7.755\ kHz$ between consecutive samples.

The time between two samples of the same channel after being transmitted to the ESP32 is:

$$22.051690\ ms - 21.47579\ ms = 575.9\ \mu s$$

That is equivalent to a frequency of $f_s = \frac{1}{575.9\ \mu s} = 1.7364\ kHz$ between sample packets.

Finally, considering the time between the first sample of one packet and the first sample of the following packet:

$$22.05169\ ms - 20.314355\ ms = 1.737335\ ms$$

Considering that 5 samples are transmitted per packet, the effective sampling frequency is:

$$f_s = \frac{5}{1.737335\ ms} = 2.8779\ kHz$$

The effective sampling frequency is high enough to meet the specifications defined for the work in relation to the sampling rate.

5.2. ACQUISITION: TESTS WITH MSP430 + INTAN + ESP32-S3 + LAPTOP

To validate the complete acquisition system (MSP430 + ESP32 + INTAN + personal computer), the setup shown in Figure 48 was assembled. This figure presents both a connection diagram and the real experimental setup used for testing. In this configuration, only one channel (CH 1) was connected to the signal generator, while the second channel (CH 2) was connected to ground.

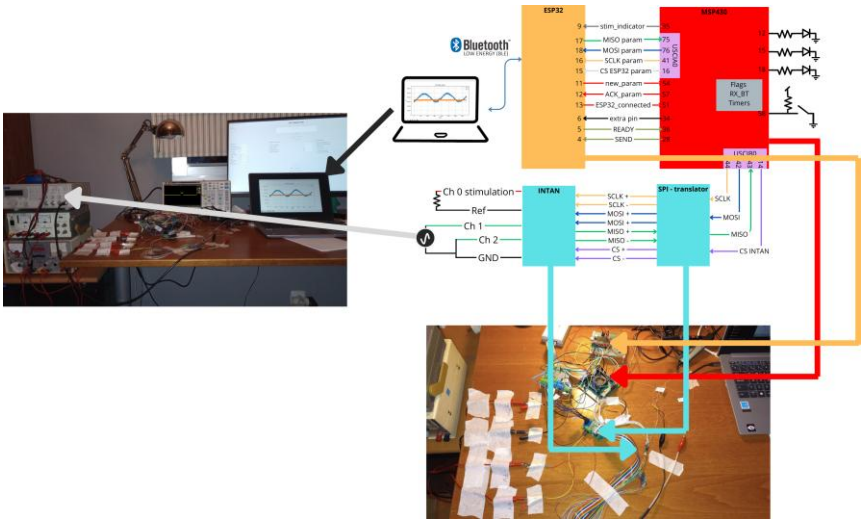

Figure 48 Acquisition test with laptop and function generator setup.

For the tests, the function generator was configured to produce two different waveforms: a sinusoidal signal and a pulse waveform. Given that the maximum AC input amplitude of the INTAN ADC is 10 mVpp, the signal amplitude was set below this limit, specifically to 5 mVpp. The operating frequency for both waveforms was fixed at 3 Hz.

In Figure 49 two different amplitude signals captured with an oscilloscope are presented: both are squared signals of 3 Hz, but one has 5mVpp (left figure) and the other one is 20 dB greater, with 50 mVpp. Two different captures are presented as the left one is used to ensure the amplitude wanted, and the right one to ensure the 3 Hz frequency of the signal.

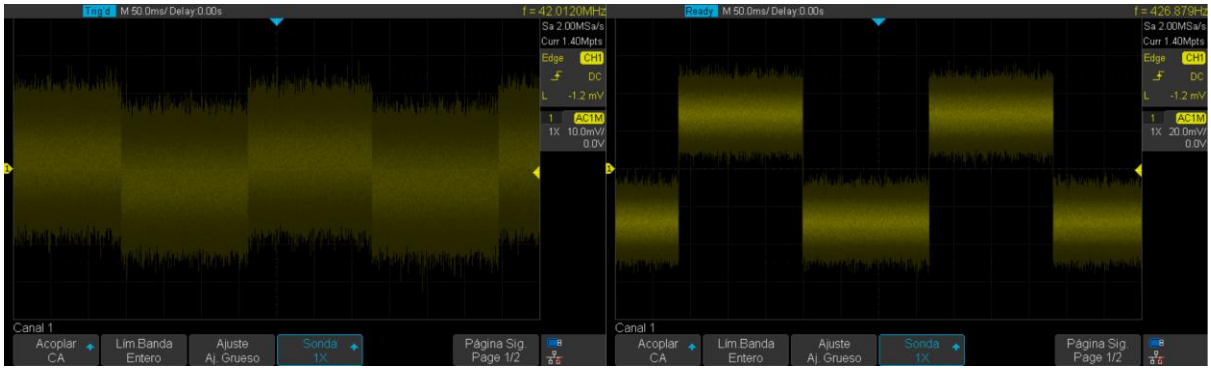

Figure 49 Input square signal of 3 Hz and 5mVpp.

In Figure 50 the results obtained in the computer application for a squared waveform and a sinusoidal is presented.

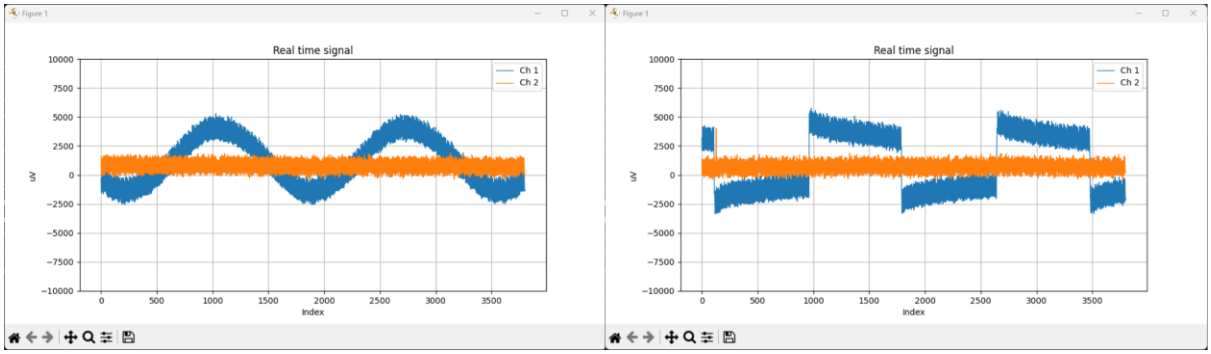

Figure 50 Sinusoidal and squared signals obtained with the real time viewer of the GUI.

Also, after the *Save data in CSV timeline* button is pressed, the data can be recomposed and viewed. In Figure 51 the recomposed information for channel 1 is shown.

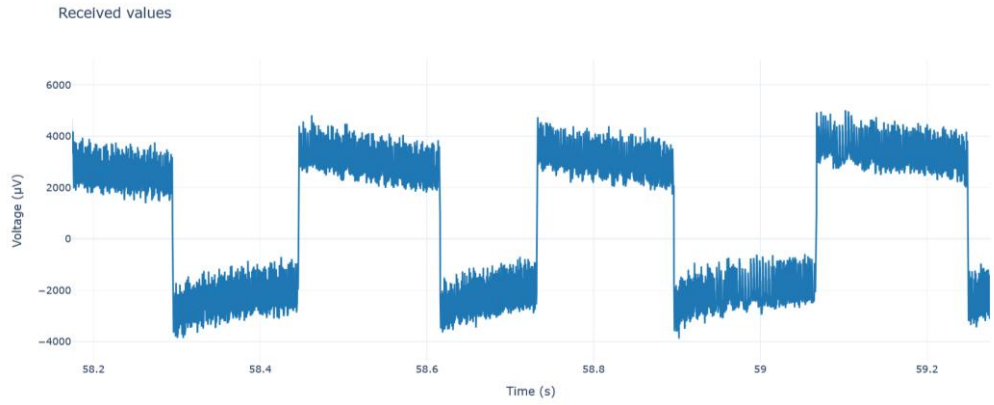

Figure 51 Recomposed data and viewed afterwards.

5.3. STIMULATION: ESP32 + INTAN + MSP430 + LAPTOP

To verify the correct operation of the stimulation functionality, the prototype was connected as shown in Figure 52. In this setup, the system operates simultaneously in stimulation and acquisition modes; however, only the stimulation-related results are discussed in this section. Channel 0 was used as the stimulation channel.

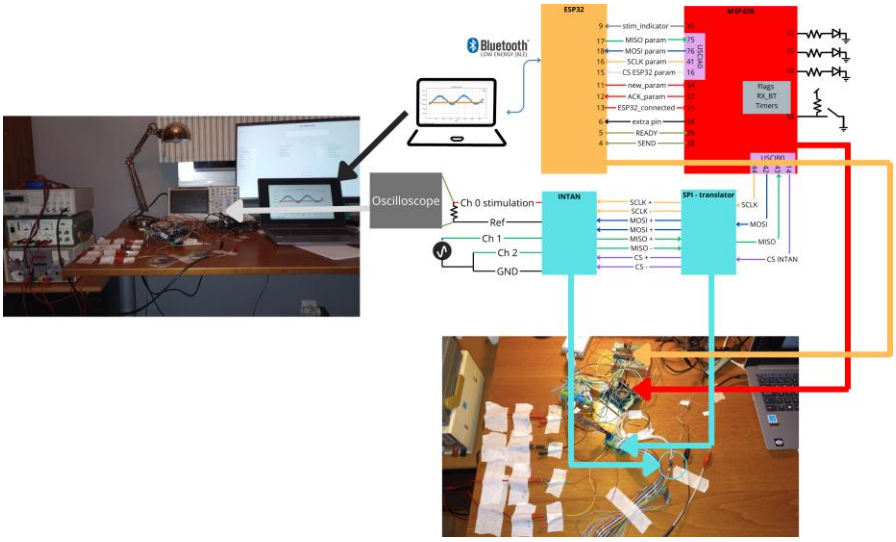

Figure 52 Stimulation test with laptop and function generator setup.

The performed test allows the verification of two main aspects:

- That the configured stimulation current corresponds to the current delivered during the stimulation intervals.
- That the minimum timing requirements of 500 µs are satisfied.

Figure 53 shows the result of generating a pulse with a duration of 500 µs and an amplitude of 1 V across an 800 Ω resistor, after configuring a stimulation amplitude of 1.25 mV. Additional stimulation configurations and timing parameters are presented later in the experiments section.

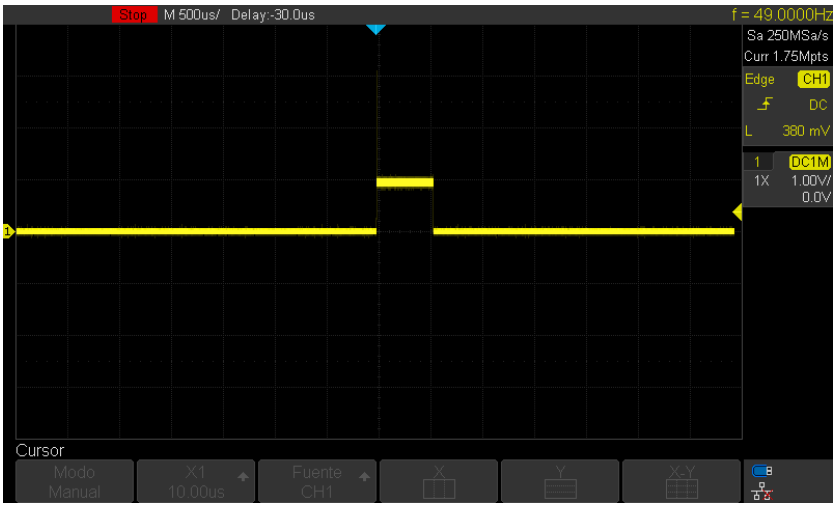

Figure 53 Stimulation pulse of 500 µs.

In Figure 54 the behavior of STIM_ENABLE output pin is illustrated. In this figure, channel 1 (yellow) represents the stimulation signal, while channel 2 (pink) corresponds to the STIM_ENABLE signal, which is active at a low level. The value of this pin allows for coordination and configuration of other types of stimulation, such as visual stimulation using an external triggered module.

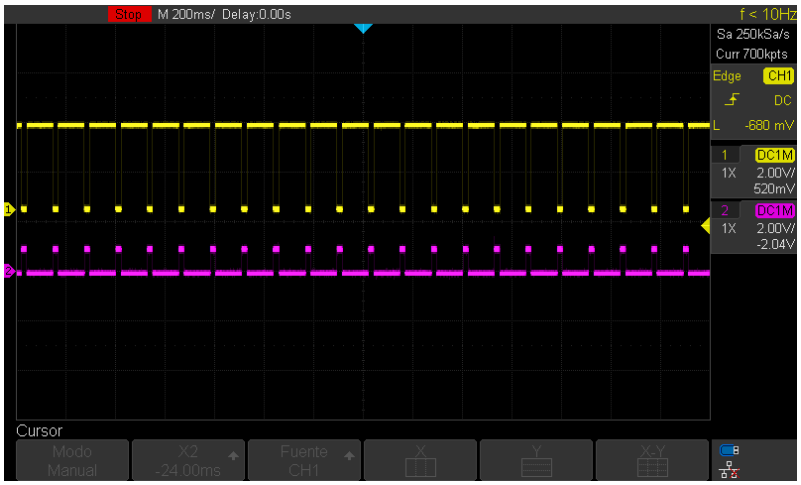

Figure 54 STIM_ENABLE behavior depending on stimulation value.

5.4. CONCLUSION OF THE VERIFICATION

The results of the presented tests confirm that the device has been successfully verified, as it meets the specifications defined in the project objectives and its operation behaves as expected.

In the following chapter, the experiments designed to carry out the validation of the prototype are presented.

6. EXPERIMENTS DESIGN

This chapter presents the experiments designed and conducted throughout the development of this work. The main objective of these experiments is to assess whether the system performs the functions for which it was designed, as well as to identify potential issues or improvements to be considered in future versions of the device.

The experiments presented in this chapter are grouped into two categories:

- Experiments associated with the STRIKE project, in which the ECG analysis module is used to evaluate vagus nerve stimulation.
- Experiments aimed at the verification and validation of the developed device, including both stimulation functionality and signal acquisition functionality.

All experimental procedures were carried out at the CTB, with the assistance of Flor Negrete, who was responsible for animal handling in accordance with the corresponding Ethical Committee guidelines and approvals. Further details regarding the Ethical Committee can be found in Annex A: Ethical, economic, social and environmental aspects.

6.1. EXPERIMENTS RELATED TO STRIKE PROJECT

During the development of the work, two types of experiments have been carried out within the STRIKE project. The first type consists of electrical stimulation of the auricular branch of the vagus nerve (aVNS) with the aim of verifying the effect of such non-invasive stimulation during stroke recovery. The electrodes used in these experiments are those presented in Figure 55-A.

The second type of experiment involves electrical stimulation of the cervical branch of the vagus nerve (cVNS). This type of experiment is carried out in two ways: by using non-invasive electrodes such as those presented in Figure 55-B, or by using invasive, hook-shaped electrodes (or a similar adaptation using thinner needles) such as those presented in Figure 55-C. The purpose of this type of experiment is to verify that when stimulating the vagus nerve, the heart rate is modified, allowing this indicator to be used as a verification system that stimulation is taking place in the nerve.

Figure 55 Electrodes used in STRIKE experiments. (A) Acupuncture electrodes used for ECG recording and aVN stimulation. (B) cBVN electrodes for superficial stimulation [69]. (C) cBVN hook electrodes for invasive stimulation [70].

In both cases, the systems that have been used for the stimulation and acquisition of the electrocardiogram are those already present in the laboratory of the Center for Biomedical Technology (CTB) that are explained below.

6.1.1. ECG MEASUREMENT EQUIPMENT

The electrocardiographic acquisition system used in the STRIKE project experiments is composed of four elements, shown in Figure 55 and Figure 56: electrodes, an instrumentation amplifier, an amplification and filtering stage, and an analog-to-digital converter (ADC) connected to a computer for data recording and analysis.

- Electrodes: Three needle-type electrodes are used, arranged as shown in Figure 57. Two electrodes are placed on the anterior limbs and the third on the posterior limb, following a standard configuration to obtain leads comparable to Lead II.

- Instrumentation amplifier: The first element in the ECG acquisition system is the AMC3330EVM [71], with a fixed gain of 2 (Figure 56 - A). This device provides galvanic isolation and initial signal amplification, ensuring electrical safety and reducing noise from the experimental environment.
- Amplification and filtering stage: The signal is then processed using a DAM 80 differential amplifier from World Precision Instruments (WPI) [72] (Figure 56 - B). This equipment allows adjustment of gain and configuration of band-pass filters with different cutoff frequencies, optimizing the quality of the electrocardiographic signal.
- Digital conversion and acquisition: Finally, the amplified signal is digitized using a 12-bit ADC manufactured by Cambridge Electronic Design (CED) [73] (Figure 56 - C). This converter is connected to a computer where the Spike2 software is used for data acquisition, visualization, and storage for subsequent analysis.

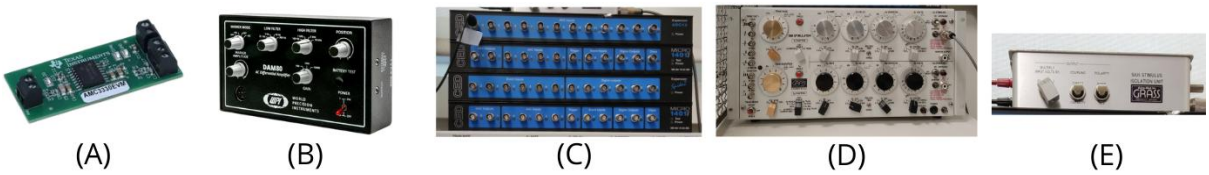

Figure 56 ECG measurement and stimulation equipment used in CTB. (A) Instrumentation amplifier [71]. (B) Amplification and filtering stage [72]. (C) Digital conversion and acquisition [73]. (D) Pulse generator. (E) Isolation unit.

Figure 57 shows the complete system setup including the individual devices and the connection scheme between them.

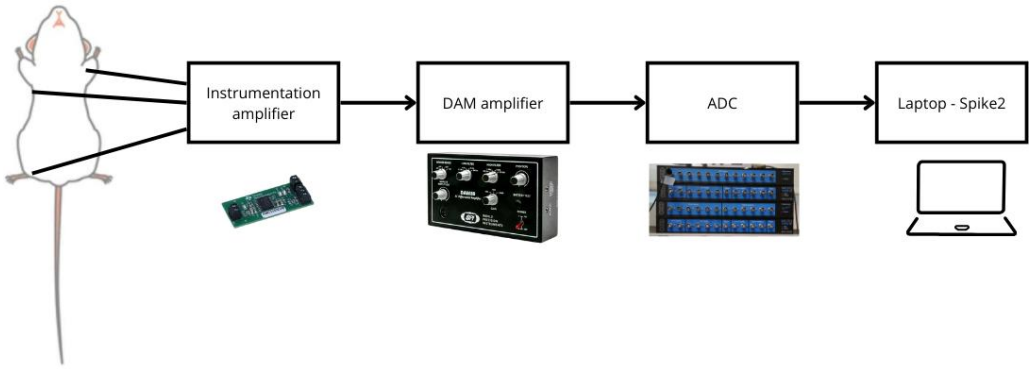

Figure 57 ECG acquisition system configuration.

6.1.2. STIMULATION EQUIPMENT

The stimulation equipment used in the initial experiments is shown in Figure 56. This system consists of a pulse generator (Figure 56-D), whose output is connected to an isolation unit (Figure 56-E) and finally to the stimulation electrodes (Figure 55), as illustrated in Figure 58.

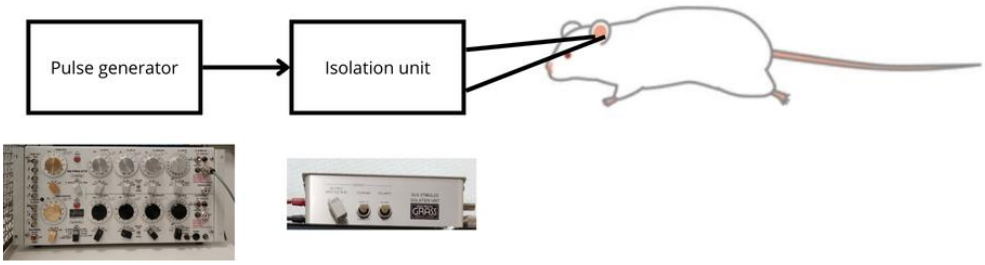

Figure 58 Stimulation configuration.

It is worth noting that the equipment used has a considerable size and limited portability, which hinders its use in dynamic experimental environments. This limitation constitutes one of the main motivations for the development of a more compact, versatile, and easily transportable stimulation system.

6.1.3. OBJECTIVE AND SETUP OF THE STRIKE EXPERIMENTS

In this section, both the objectives and the setup of cervical and auricular stimulation are presented.

CERVICAL STIMULATION

Cervical vagus nerve stimulation (cVNS) is performed using either an invasive or a non-invasive procedure. The invasive method is the one described here, as it proved to be the most effective. The main objective is to verify correct activation of the vagus nerve by evaluating variations in heart rate during the stimulation period. These experiments arise from the need to confirm the effectiveness of auricular stimulation.

For this purpose, hook-shaped electrodes specifically adapted for placement on the cervical branch of the vagus nerve are used. Figure 59 shows the electrodes built for this experiment, based on the purchased electrodes of Figure 55–C. The placement scheme and the connection to the ECG acquisition system are shown also in Figure 59. The purple line represents the cervical vagus nerve, while the red and blue lines represent the hook-shaped electrodes.

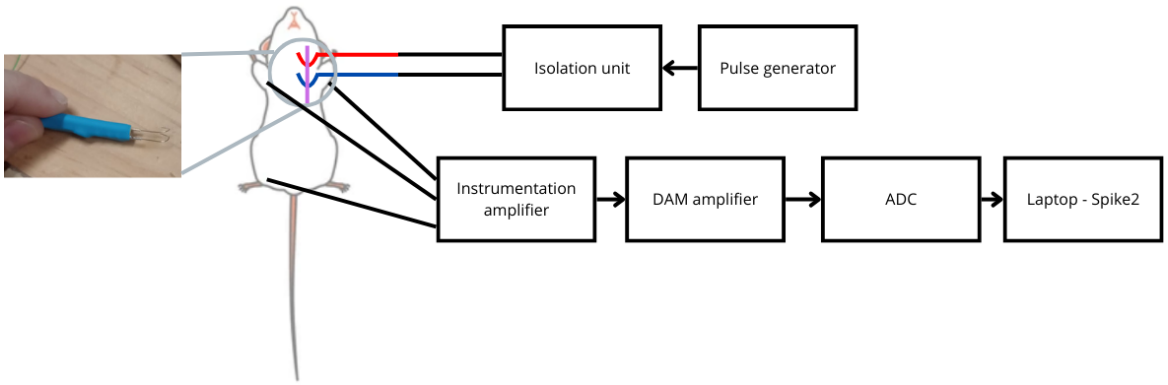

Figure 59 cVNS invasive with adapted hook electrodes.

AURICULAR STIMULATION

Auricular stimulation is performed non-invasively on the auricular branch of vagus nerve, located in the cymba conchae region, as explained in section 2.2.3. The objective is to analyze the effect of stimulation on the ECG signal as an indirect indicator of vagal activation in the context of post-stroke recovery.

For this purpose, needle-type electrodes of 0.5 mm are used, separated by a distance of 2.5 mm [74], and adapted for this type of experiment. Figure 60 shows the placement scheme, and connection to the ECG acquisition system.

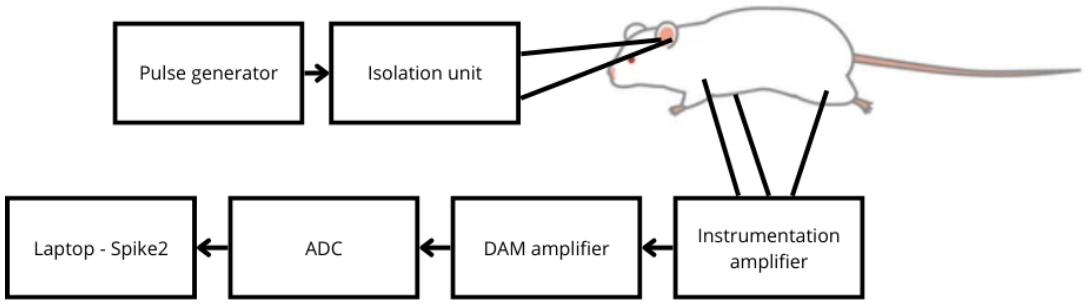

Figure 60 aBVN stimulation and ECG acquisition system.

6.1.4. SUMMARY OF THE EXPERIMENTS

During the development of this work, a total of 10 different experiments were conducted within the STRIKE project. Table 1 presents a summary including the experiment number, the number of mice used in each experiment, and relevant comments explaining the diversity and quantity of experiments performed.

Of all the rodents that have been used in the experiments, some of them have been discarded when carrying out the analysis of the experiments, since they were used to control how anesthesia affects the rodents (being very variable depending on the subject) or it was detected that the stimulation was not being carried out correctly during the performance of the experiment. The results of these experiments are presented in section 7.1.1.

Number of experiment	Total of rodents	Number of control rodents	Description of the experiment differences
002	5	2	aVNS initial experiments for learning where to place electrodes on the concha.
003	4	0	aVNS changing anesthesia due to very big changes on heart rate variation, looking if are caused due to anesthesia effects.
004	6	2	aVNS
005	5	3	aVNS changing the stimulation – resting times to see if differences are seen, as no knowledge about what kind of variations we were looking for.
006	4	2	aVNS multiple stimulations on the same rodent
007	1	0	aVNS multiple stimulations on the same rodent in the right ear.
008	4	0	aVNS using a Doppler machine to record blood flow.
009	7	0	cVNS using the purchased surface electrodes for the development of non-invasive cervical experiments.
010	5	0	cVNS using the hook electrodes purchased for the development of invasive cervical experiments.
011	4	0	cVNS using hook-shaped needle electrodes for the development of invasive cervical experiments.

Table 1 Experiments summary.

6.1.5. RESULTS DEFINITION: FAVORABLE OR UNFAVORABLE

To evaluate the experiments conducted within the STRIKE project, the signal processing algorithm developed in this work, focused on electrocardiographic analysis, has been applied. The obtained results are classified as favorable or unfavorable.

DEFINITION OF RESULTS: FAVORABLE

Favorable results indicate that the applied stimulation (auricular or cervical) produced a significant variation in the animal's heart rate, thus confirming activation of the vagus nerve. Figure 61 shows an example of a favorable result. The stimulation periods are shown in red, the ECG signal in blue, and the heart rate in beats per minute (BPM) in black. In the figure, it can be seen that at the times when stimulation is taking place, the value of the pulses per minute decreases. As time goes by, this value is gradually recovered until it returns to its normal value or behavior of the heart.

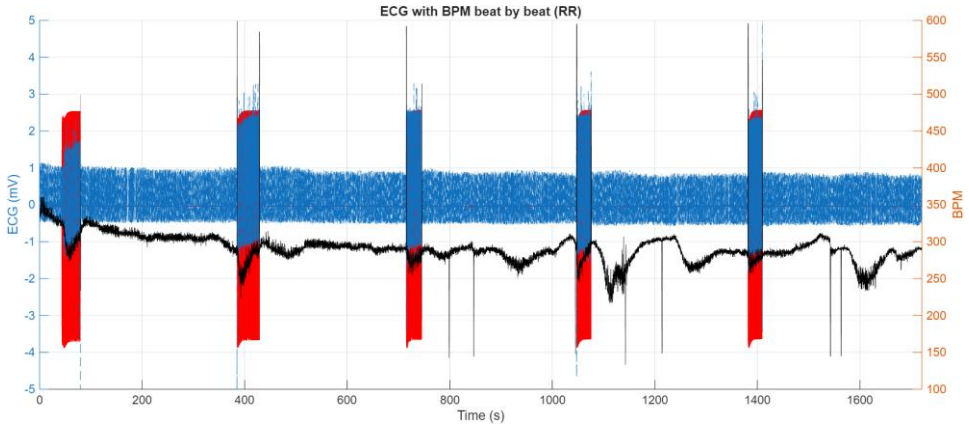

Figure 61 Favorable ECG analysis of an experiment for STRIKE project.

DEFINITION OF RESULTS: UNFAVORABLE

Unfavorable results indicate that no clear variation in heart rate was observed, and therefore vagus nerve activation cannot be ensured. It is important to note that an unfavorable result does not imply a complete absence of stimulation, but rather insufficient evidence to confirm it. For this reason, these experiments are retained in the global analysis of the STRIKE project. Figure 62 shows an example of an unfavorable result. The stimulation periods are shown in red, the ECG signal in blue, and the heart rate in beats per minute (BPM) in black. It can be observed that no stimulation-related variations in BPM occur during the stimulation intervals.

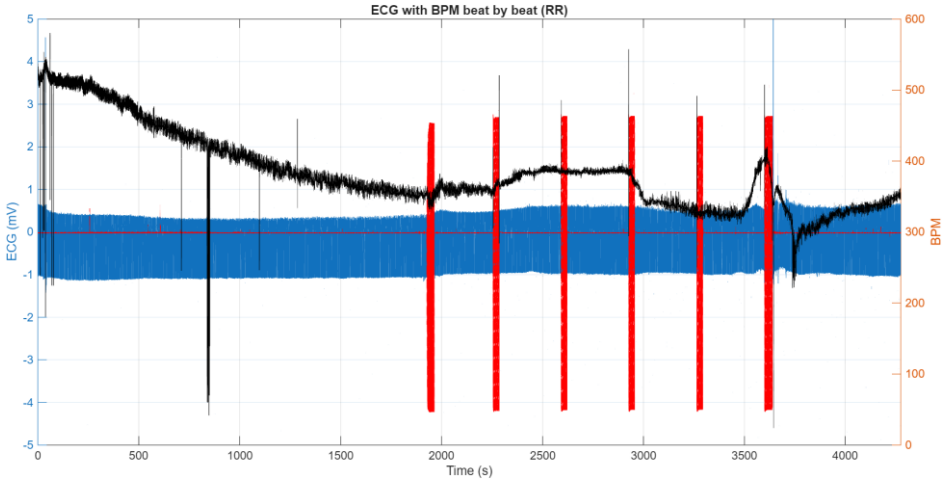

Figure 62 Unfavorable result of VNS.

6.2. EXPERIMENTS USED FOR DEVICE VALIDATION

In order to validate the prototype developed in this work, two types of experiments were designed, previously defined in section 2.4: Experiments Type A and Type B. The methodology, stimulation parameter configuration, and obtained results for each case are described below.

6.2.1. TYPE A EXPERIMENTS

This set of tests consists of stimulating the auricular branch of vagus nerve using the device designed in this work and evaluating heart rate variations during stimulation.

The experimental setup, parameter configuration tables, an example of the stimulation signal captured with an oscilloscope, and the results obtained after applying the signal processing module are presented below.

SETUP

Figure 63 shows the experimental setup. The device developed in this work is represented in purple, while the CTB acquisition system used as the acquisition module is shown in gray.

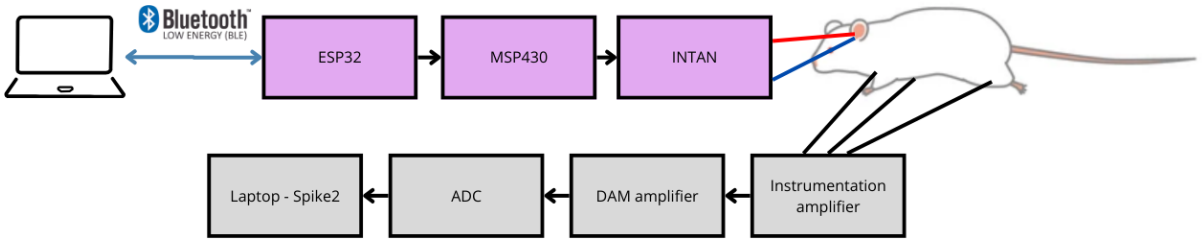

Figure 63 Prototype test type A experiments setup.

EXPERIMENTAL DESCRIPTION

The CTB experiments are characterized by the following parameters:

- Unipolar signals.
- Frequency: 20 Hz.
- Amplitude: 0.5 mA.
- Pulse duration: 0.5 ms.

The experiments designed to validate the device replicate these conditions and introduce variations to assess the flexibility and robustness of the system. The defined protocols are summarized below:

- 01: Exact replication of the CTB protocol.
- 02: Same as 01, with amplitude increased to 1 mA.
- 03: Same as 01, but with bipolar polarity.
- 04: Same as 01, with 1 mA amplitude and bipolar polarity.
- 05: Same as 01, with frequency reduced to 10 Hz.
- 06: Same as 01, with frequency increased to 40 Hz.
- 07: Same as 01, with pulse width increased to 1 ms.

Table 2 summarizes the parameters used in each protocol, including polarity, number of stimulations, rest and stimulation times, frequency, ON/OFF duration, amplitude, and current configuration. Some parameters are common for all the protocols, such as:

- Number of stimulations: 5.
- Resting time: 5 minutes.
- Stimulation time: 30 seconds.
- Current step: 5000 (nA).

Protocol number	01	02	03	04	05	06	07
Polarity	Monopolar	Monopolar	Bipolar	Bipolar	Monopolar	Monopolar	Monopolar
Frequency	20 Hz	20 Hz	20 Hz	20 Hz	10 Hz	40 Hz	20 Hz
On time	0.5 ms	0.5 ms	0.5 ms	0.5 ms	0.5 ms	0.5 ms	1 ms
Off time	49.5 ms	49.5 ms	49.5 ms	49.5 ms	99.5 ms	24.5 ms	49 ms
Current amplitude	0,5 mA	1 mA	0.5 mA	1 mA	0.5 mA	0.5 mA	0.5 mA
+ current amplitude	100	200	100	200	100	100	100
- current amplitude	-	-	100	200	-	-	-

Table 2 Parameters configuration for Type A Experiments execution.

CONFIGURATION EXAMPLE

Figure 64 shows an example of the signal generated as stimulation corresponding to Protocol 01. The oscilloscope captures show:

- Pulse on time (T_ON): ~500 µs.
- Pulse off time (T_OFF): ~49 ms.
- Total stimulation duration: ~30 s.
- Rest time between cycles: 5 minutes (≈300 s).
- Positive-only stimulation.

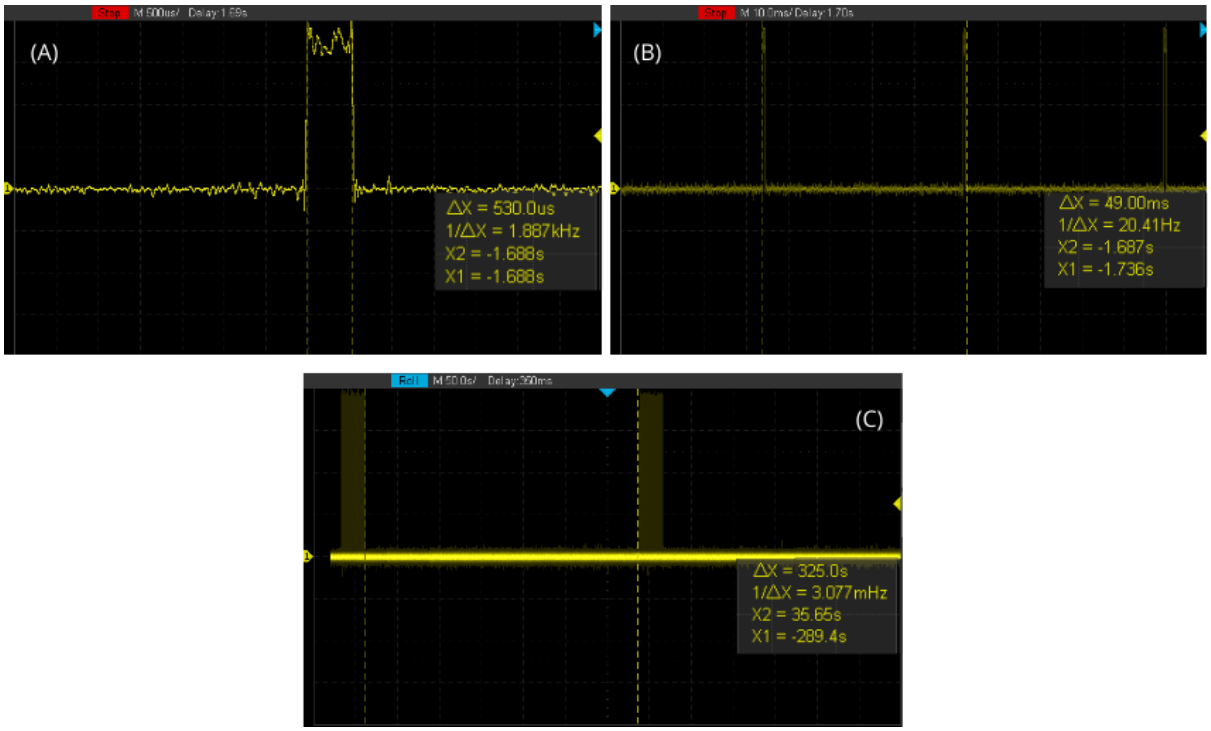

Figure 64 Experiments Type A example of signal generated. A: represents one stimulation pulse. B: represents the time between two stimulation pulses in milliseconds. C: represents the resting time between two stimulation train pulses.

6.2.1. TYPE B EXPERIMENTS

This set of tests aims to evaluate neuronal responses in the visual cortex to two types of stimulation: electrical and visual, using the device developed in this work.

The experimental setup, parameter configuration tables, an example of stimulation signal captured with an oscilloscope, and the results obtained after applying the signal processing module are presented below.

SETUP

Two stimulation modalities are used in these experiments.

Electrical stimulation

Figure 65 shows the connection diagram of the designed system, integrating the acquisition module and the electrical stimulation module. Five electrodes are implanted: two stimulation electrodes (red) in the thalamic region and three recording electrodes located in both visual cortices (black) and one reference electrode (blue).

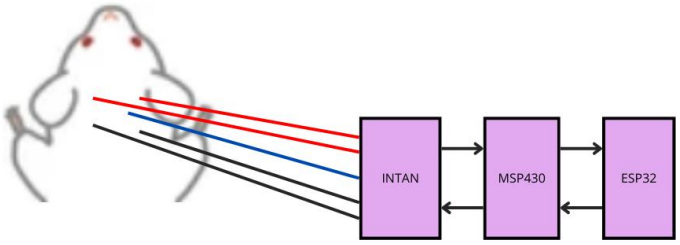

Figure 65 Type B experiments setup with electrical stimulation.

Visual stimulation

Figure 66 shows the connection scheme for visual stimulation. Neuronal recording is performed using the acquisition module of the designed system, whole visual stimulation is generated by a second ESP32 based device controlling the light stimulus.

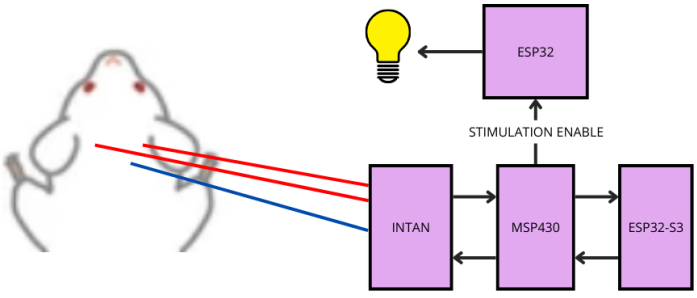

Figure 66 Type B experiments setup with visual stimulation.

The new ESP32 and MSP430 (the prototype system and the visual module) communicate via the STIM_ENABLE pin, ensuring synchronization between stimulation and recording. Three electrodes are implanted: one reference electrode (blue) and two recording electrodes (red).

EXPERIMENTAL DESCRIPTION

The CTB experiments are characterized by the following parameters:

- Unipolar signals.
- Frequency: 1 Hz.
- Amplitude: 0.5 mA.
- Pulse duration: 0.5 ms.

As the purpose of this device is to provide lower amplitudes to the experiments, in Table 3 there it is proposed a summary of parameters used in each protocol, including stimulation type (electrical or visual), polarity, number of stimulations, rest and stimulation times, frequency, ON/OFF duration, and current configuration.

Protocol number	01	02	03	01 box	02 box	03 box
Type of stimulation	Electrical	Electrical	Electrical	Visual	Visual	Visual
Waveform shape	One shot	Pulse train	Pulse train	One shot	Pulse train	Pulse train
Number of stimulations	(during 60 seconds of recording)	5	5	(during 60 seconds of recording)	5	5
Resting time	0 ms	900 ms	975 ms	0 ms	900 ms	975 ms
Stimulation time	1000 ms	20 ms	25 ms	1 s	20 ms	25 ms
ON time	500 µs	500 µs	500 µs	1000 µs	1000 µs	1000 µs
OFF time	999 ms	19 ms	4 ms	999 ms	19 ms	4 ms
Current amplitude	40 nA	40 nA	40 nA	-	-	-
+ current magnitude	2	2	2	-	-	-
Current step	20 (nA)	20 (nA)	20 (nA)	-	-	-

Table 3 Parameters configuration for Type B Experiments execution.

CONFIGURATION EXAMPLE

Figure 67 shows an example corresponding to protocol 01. The oscilloscope capture shows:

- Pulse ON time (T_ON): ~500 µs.
- Pulse OFF time (T_OFF): 1s.
- Total stimulation duration: ~500 µs per pulse.
- Rest time between cycles: 1 s.
- Positive only stimulation.

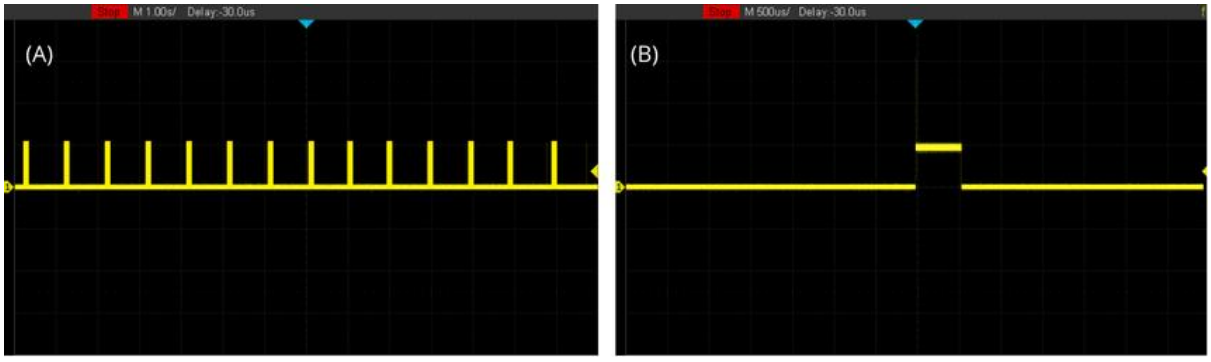

Figure 67 Experiments Type B example of signal generated. A: represents one stimulation every one second. B: represents one stimulation width.

Figure 68 illustrates the outcome of the visual stimulation test performed using the system presented in Figure 66. The image shows the prototype assembled during the development of this work, integrated with the ESP32-WROOM32 microcontroller employed in Type B visual stimulation experiments. The ESP32 is connected via the I2C protocol to the HT16K33 LED Backpack matrix, which serves as the visual stimulus generator.

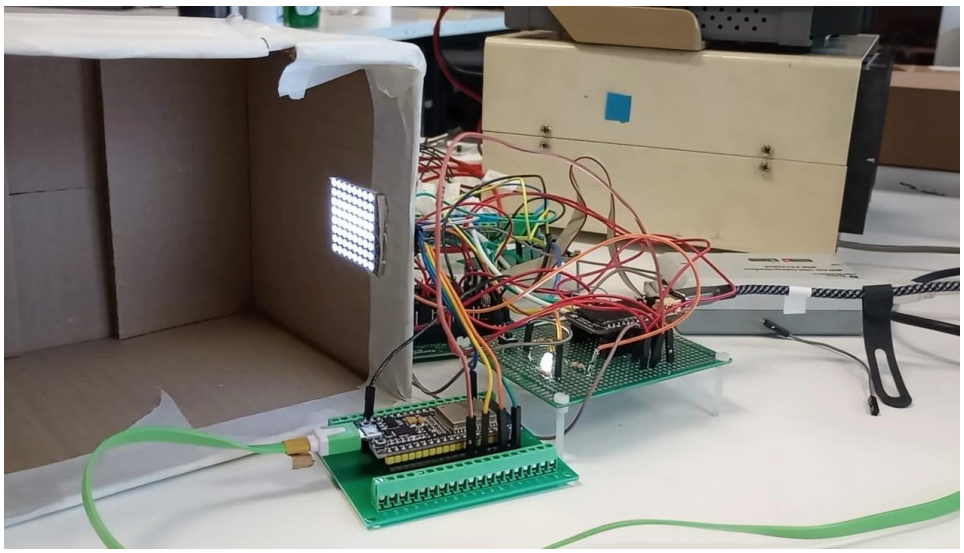

Figure 68 Visual stimulation protocol in the laboratory.

6.3. CONCLUSION OF THE EXPERIMENT DESIGN

This chapter has outlined the experimental designs developed for both the STRIKE project and the validation of the prototype. Together, these experiments provide the methodological basis needed to assess the system's performance under realistic stimulation and acquisition conditions.

The following chapter presents the results obtained from carrying out these experiments and evaluates the effectiveness and reliability of the proposed system.

7. EXPERIMENTS RESULTS

In this chapter, the results of the experiments that have been carried out within the development of this work are presented, both those related to the STRIKE project and those carried out for the validation of the prototype designed and implemented.

7.1.1. STRIKE RELATED EXPERIMENTS RESULTS

In Annex C: INTAN configuration functions, the result of each of the experiments that have been carried out during the development of this work within the STRIKE project is presented. Here, only the summary of the results observed after the analysis of each of the cases is presented in Table 4. This table also presents the reasons why some of the experiments are discarded.

Number of experiment	Total of rodents analyzed	Number of favorable results	Number of rodents discarded	Reasons to discard the rodents
002	3	2	-	-
003	4	2	-	-
004	4	0	-	-
005	2	0	-	-
006	2	0	1	The second rodent's file was corrupted when trying to open it.
007	1	0	-	-
008	4	1	-	-
009	7	0	-	-
010	5	-	5	The person conducting the experiments (Flor) noticed that, when manipulating the nerves, she had to force them a lot because the electrodes used were too large compared to the mouse.
011	4	3	-	-

Table 4 Experiments results for STRIKE project ECG analysis.

7.1.2. DEVICE VALIDATION EXPERIMENTS RESULTS

This section presents the results obtained during the validation of the designed and developed device through the execution of the Type A and Type B experiments previously defined in chapter 6.

TYPE A EXPERIMENTS

For the purpose of validating the device under conditions comparable to those used in the STRIKE project, the number of experiments conducted was reduced with respect to those initially planned in Table 2. Although four variations were originally intended, one of the mice exhibited a strong adverse response to anesthesia, which required reducing the final number of experiments to three.

The experiments performed correspond to protocols 01, 03 and 04 from Table 2. All the stimulations were done in aVNS format as it easier to setup, even though the percentage of favorable is lower than the cVNS. The following subsections present the ECG recordings obtained during these experiments, together with the corresponding analysis results.

Figure 69 shows the experimental setup used for system validation within the STRIKE project. The image depicts the mouse undergoing the stimulation and acquisition protocol, as well as the acquisition and stimulation systems, both connected to the computer and interfaced with the animal.

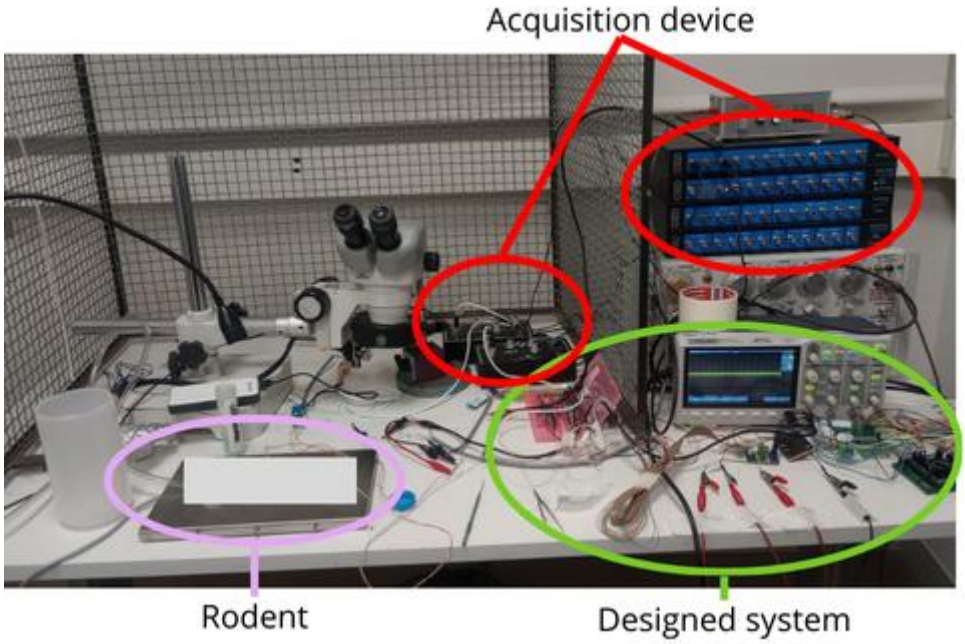

Figure 69 CTB experimental setup for Type A experiments: STRIKE.

RODENT 1: PROTOCOL 01

The first validation experiment employed the same stimulation protocol previously used at CTB. The stimulation parameters were as follows:

- Current amplitude: 0.5 mA.
- Polarity: Unipolar.
- Stimulation frequency: 20 Hz.
- Stimulation duration: 30 seconds.
- Resting interval: 5 minutes.
- Number of cycles: 5.

Figure 70 – A shows an oscilloscope capture acquired during stimulation. To enable accurate current monitoring, a 1 kΩ resistor was connected in series with the stimulation path, allowing the current to be computed from the voltage drop measured across it.

The figure highlights four stimulation pulses (in red). Although system noise makes visualization difficult, the expected stimulation pattern is clearly identifiable. A total of five stimulation periods were configured, although only four are visible in the oscilloscope frame. The pulses correspond to the programmed 5 cycles with unipolar stimulation pattern (negative only), with 30 second stimulation periods and 5-minute rest intervals. The measured voltage of 500 mV across the 1 kΩ resistor confirms a stimulation current of 0.5 mA.

Figure 70 – B presents the ECG analysis performed using the signal processing module developed in this work. Stimulation periods are indicated in red.

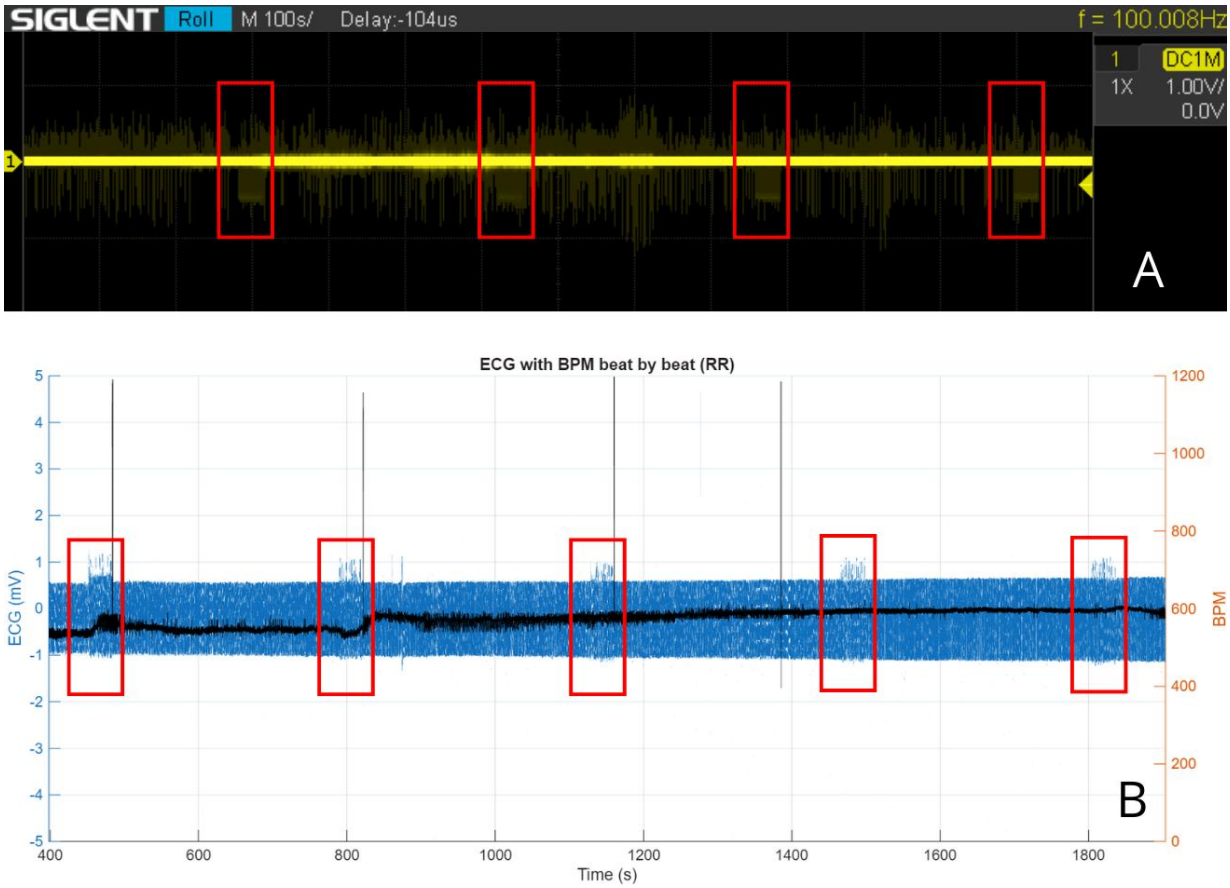

Figure 70 A: Stimulation recording on Rodent 1. B: ECG analysis for Experiment Type A validation on Rodent 1.

RODENT 2: PROTOCOL 03

The second experiment (protocol 03) consisted of modifying stimulation polarity while maintaining the remaining parameters unchanged, implementing a bipolar stimulation mode. Figure 71 - A shows the oscilloscope capture obtained during stimulation, using the same 1 kΩ series resistor. The measured voltage drop again corresponds to a stimulation current of 0.5 mA, now applied in bipolar mode. Figure 71 – B displays a longer duration capture, showing the complete structure of the stimulation cycles: 30 seconds of stimulation followed by 5-minute intervals of rest.

Figure 71 – C presents the ECG response to the bipolar stimulation, analyzed using the signal processing module developed in this work. As in the previous case, stimulation periods are marked in red.

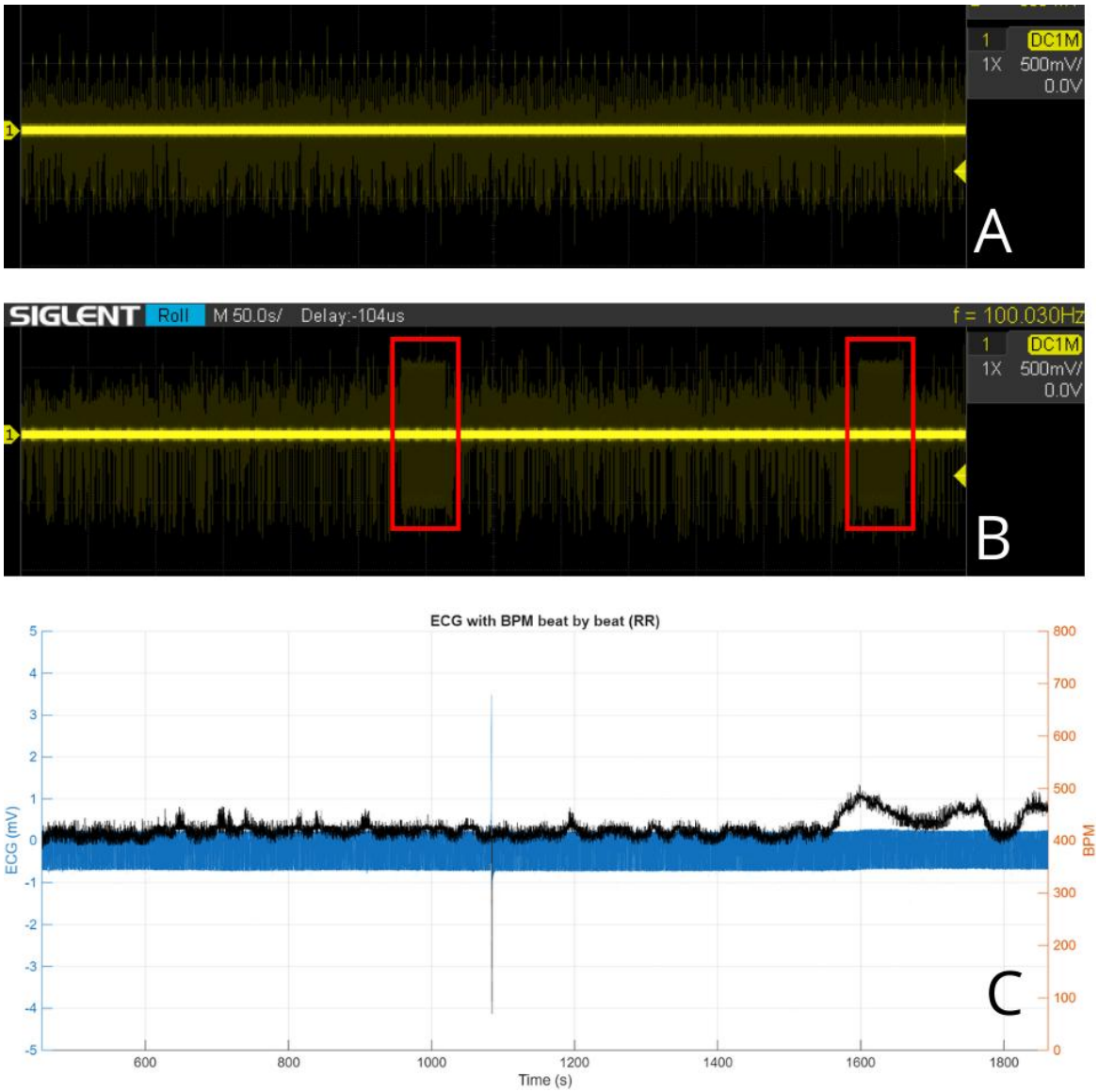

Figure 71 A: Stimulation recording on Rodent 2 during one stimulation period. B: Stimulation recording on Rodent 2. C: ECG analysis for Experiment Type A validation on Rodent 2.

RODENT 3: PROTOCOL 04

The third experiment (protocol 04) combined a change in stimulation polarity with an increase in the stimulation current to 1mA, while maintaining all other parameters constant. Figure 72 – A shows the oscilloscope capture obtained during stimulation though the same 1 kΩ resistor. The recorded voltage drop of 1 V confirms the delivery of a 1 mA bipolar stimulation current.

A second capture (Figure 72 - B) displays several stimulation cycles, each consisting of 5 cycles with 30 seconds of stimulation followed by 5 minutes of rest.

Figure 72 – C presents the ECG analysis corresponding to this protocol, again highlighting in red the periods during which stimulation was applied.

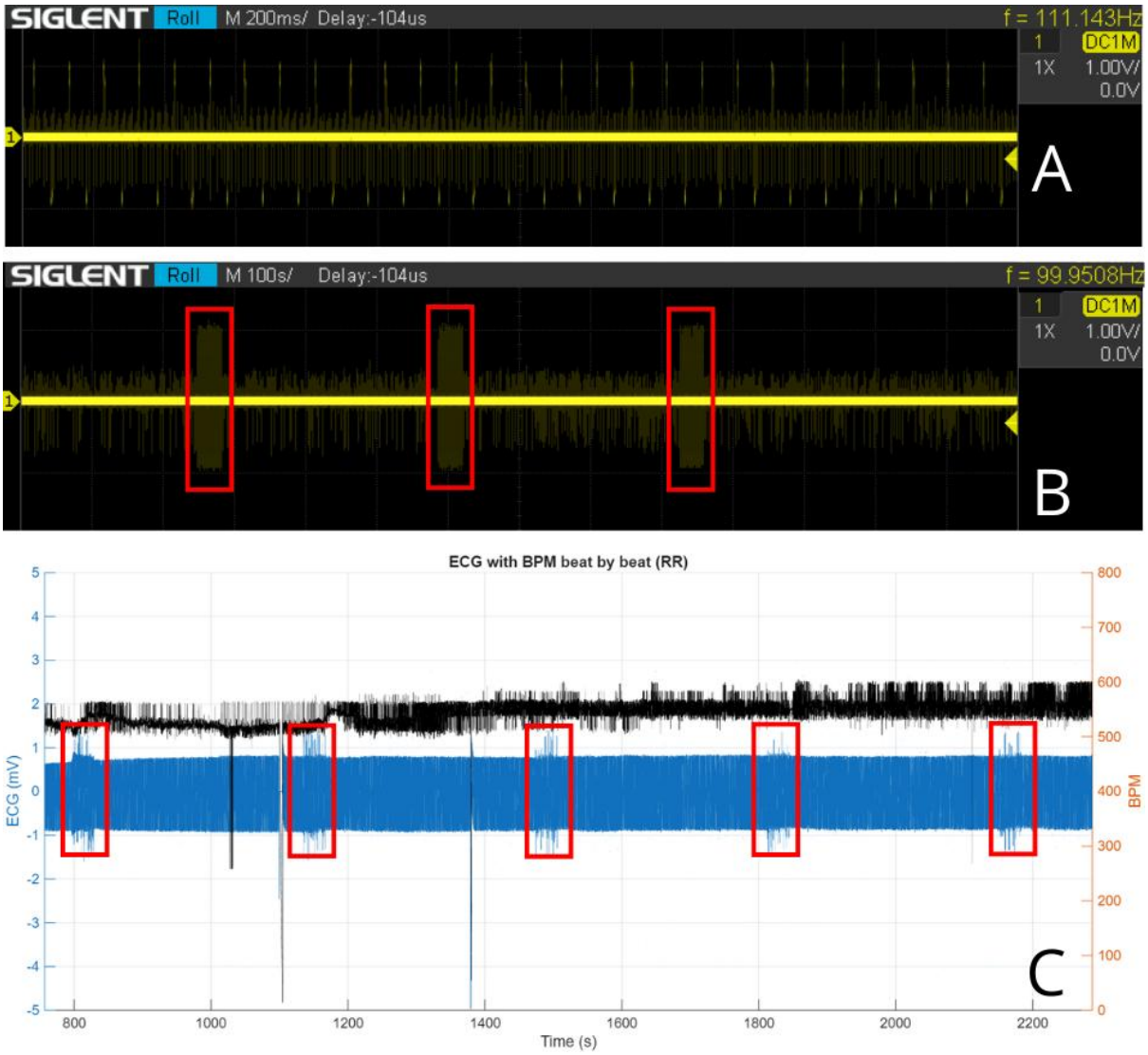

Figure 72 : Stimulation recording on Rodent 3 during one stimulation period. B: Stimulation recording on Rodent 3. C: ECG analysis for Experiment Type A validation on Rodent 3.

TYPE B EXPERIMENTS

In this type of experiment, the objective is to validate the designed prototype in both the acquisition and stimulation processes, whether electrical or visual. The following section first presents the results obtained during acquisition and electrical stimulation, followed by the results obtained during acquisition and visual stimulation.

To validate the acquisition system, the reference used responds to the average of 60 samples over 3 repetitions, as this is the type of data currently obtained with the acquisition system in use at the CTB (MATRIX acquisition system and ENERGY integrated stimulator from micromed [75]). In Figure 73

a picture of the available stimulation and acquisition devices currently used in the CTB for this kind of experiment is presented.

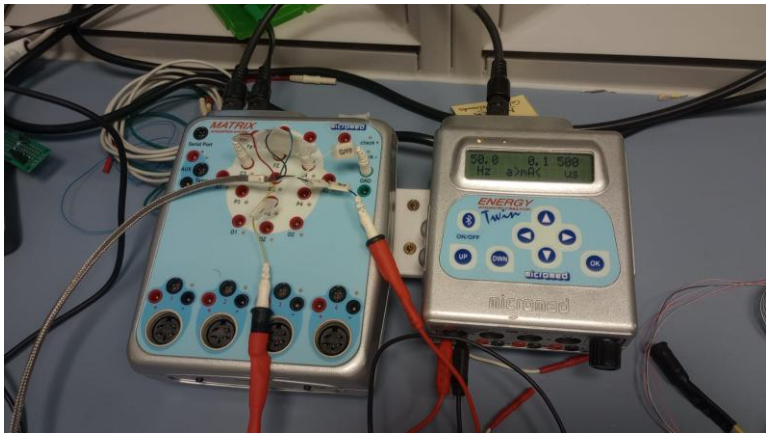

Figure 73 Available stimulation and acquisition devices for type B experiments [75].

Figure 74 shows the result of the acquisition for both channels during electrical stimulation. Figure 75 shows the result of the acquisition for both channels during visual stimulation. These measurements were carried out on the same mouse used for the device validation.

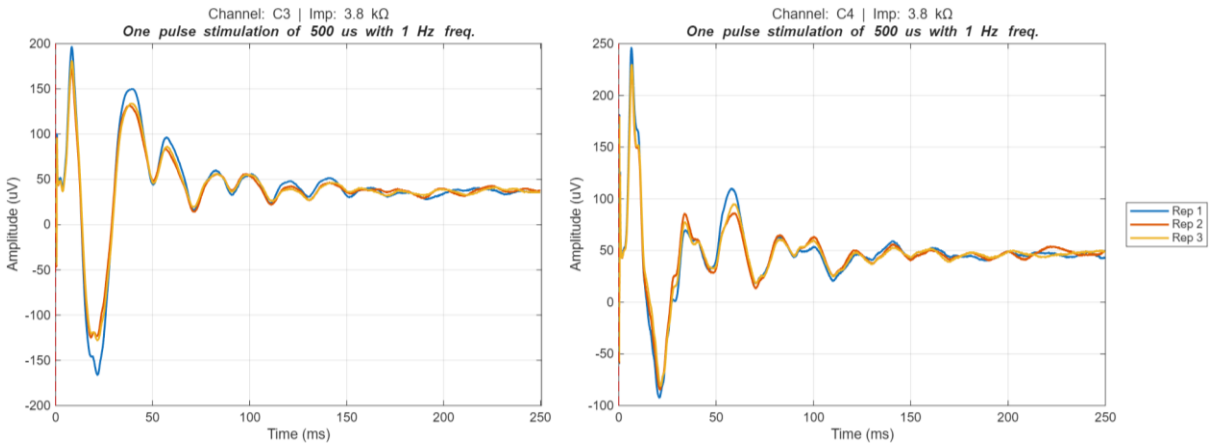

Figure 74 Acquisition results obtained with the CTB current acquisition system, electrical stimulation protocol.

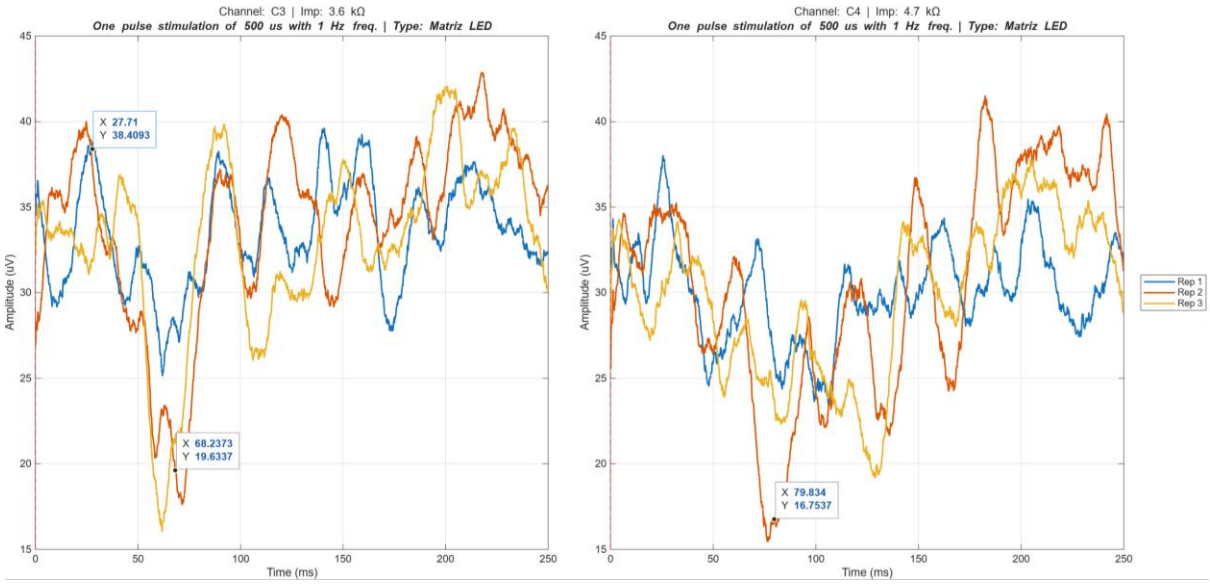

Figure 75 Acquisition results obtained with the CTB current acquisition system, visual stimulation protocol.

ELECTRICAL STIMULATION

The setup used for electrical stimulation and described in Figure 65 is shown in Figure 76.

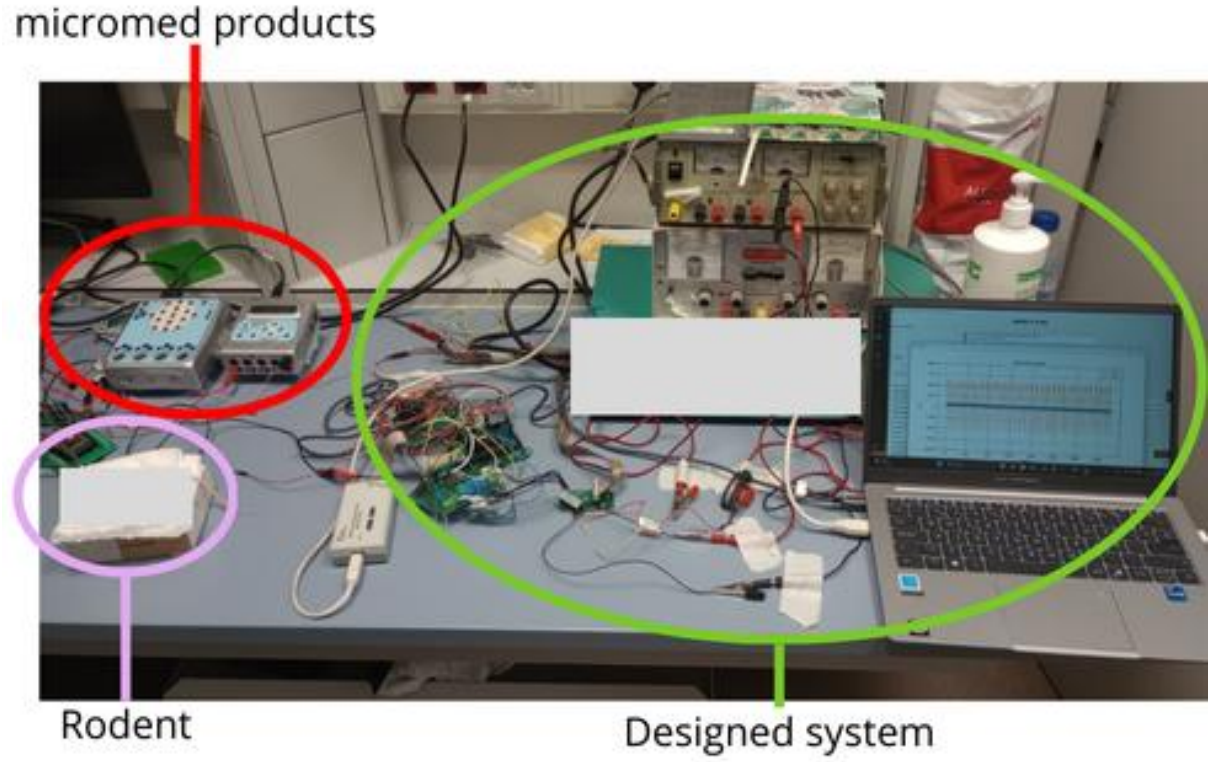

Figure 76 Setup for validation of the device with electrical stimulation.

To validate the electrical stimulation capability, the same experiment presented in Figure 74 was conducted, but using lower currents, since one of the goals of the device is to enable the use of significantly smaller currents than those currently employed at the CTB. In this section only the result for one experiment is presented, the complete set of results for the experiments is presented in Annex E: Results of the experiments conducted for the stimulation and acquisition validation.

Figure 77 presents the result of stimulating and recording data from both channels during a stimulation period of approximately 10 seconds. As shown, the obtained signal exhibits a high level of noise, due to the INTAN filters being configured to provide the maximum bandwidth in order to allow post-processing of the data.

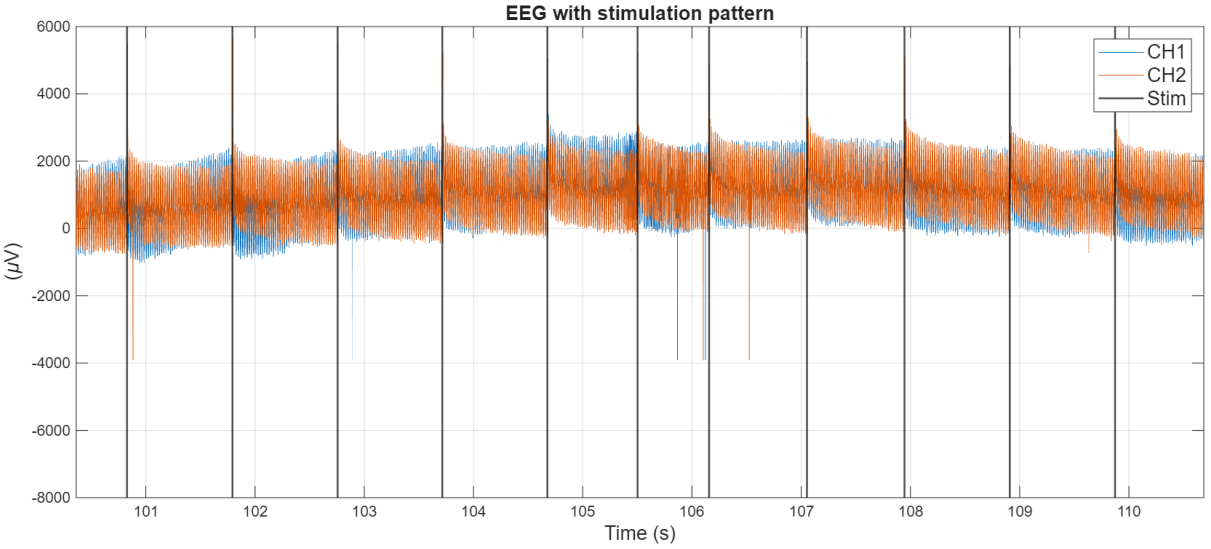

Figure 77 Original signals recorded and stimulation times indicated.

To determine the appropriate filtering required, the spectrum of the recorded signal (shown in Figure 78) was analyzed. The analysis reveals that the highest power content lies between 40 and 100 Hz, as well as a power peak at 50 Hz caused by the power line. Consequently, the signal was processed using two filters: a 50 Hz notch filter and a band pass filter between 40 and 100 Hz.

The resulting filtered signal is shown in Figure 79, where the outcome for a single stimulation is displayed for each channel.

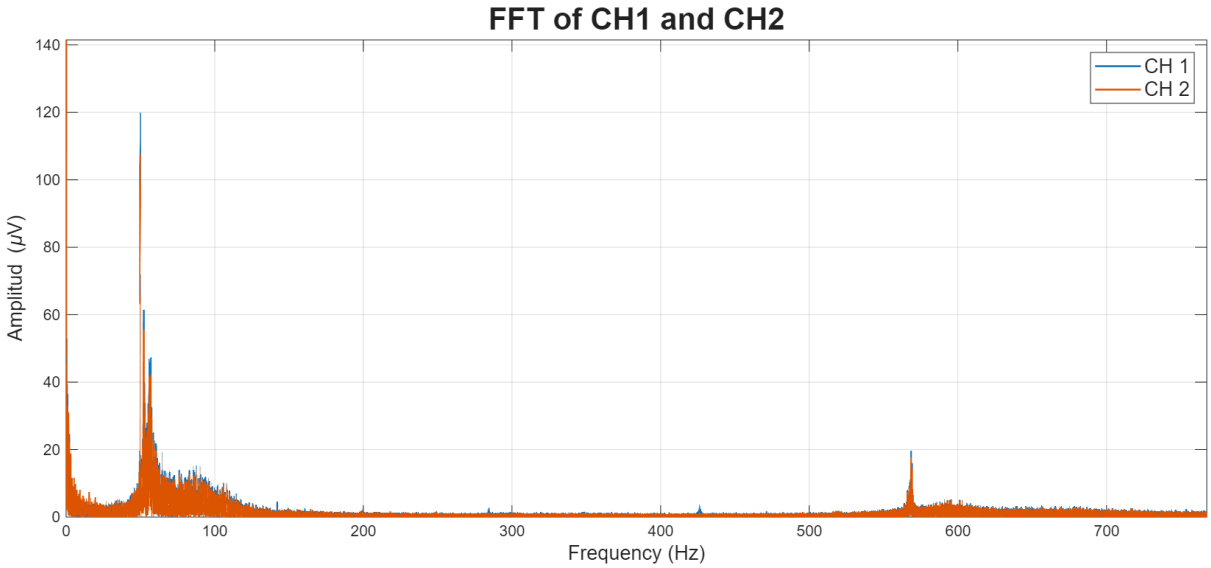

Figure 78 FFT of the recorded signals for validation of the prototype.

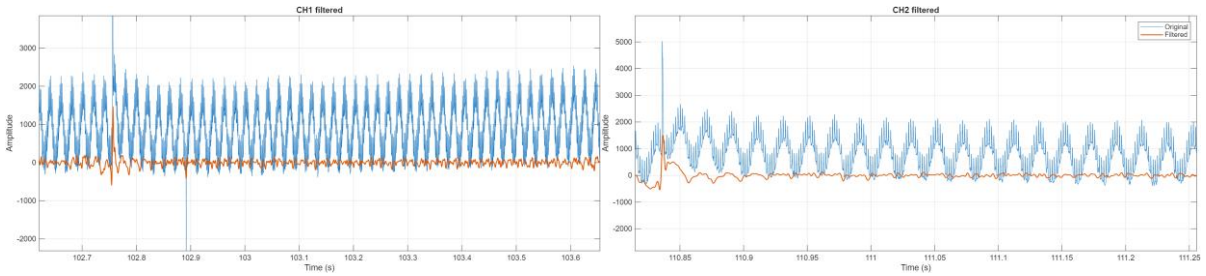

Figure 79 Signal results of filtering.

Following the filtering stage, and with the aim of representing the data in a manner comparable to the original experiments performed at the CTB, an additional plot was generated. This plot includes the average of several stimulation events (represented by a thick black line) together with the superimposed individual stimulations. The resulting representation shown in Figure 80, demonstrates a high degree of similarity to the results previously presented in Figure 74.

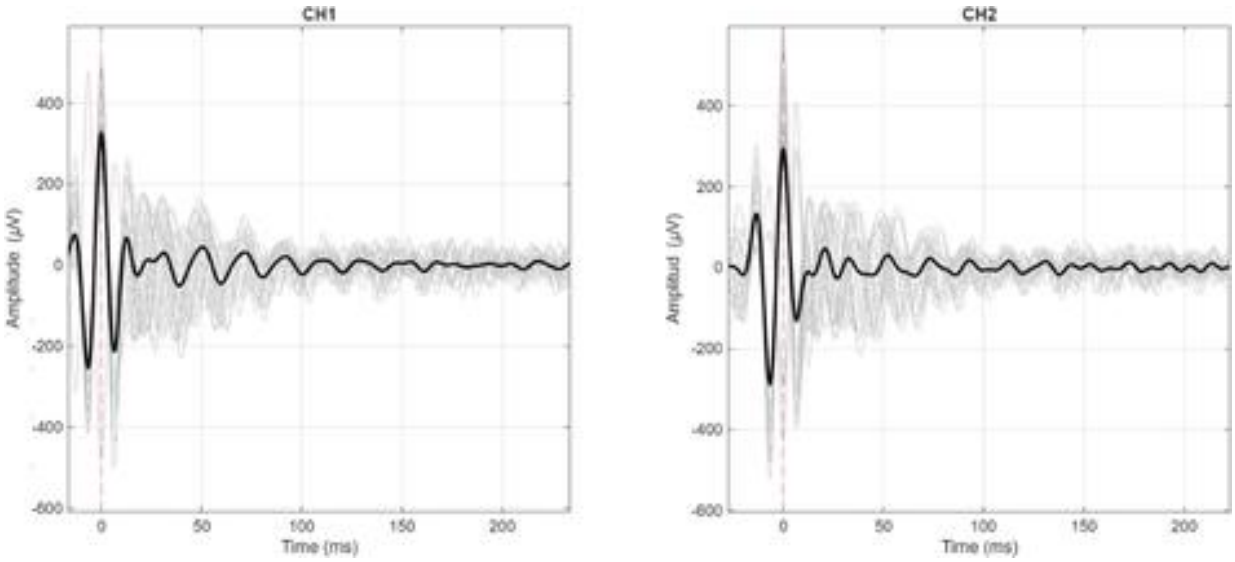

Figure 80 Result of electrical stimulation and acquisition validation.

VISUAL STIMULATION

The setup used for visual stimulation and described in Figure 66 is shown in Figure 81. In the picture it can be seen that the rodent is inside the box presented in Figure 68, as only the visual stimulation is intended to be seen by the rodent.

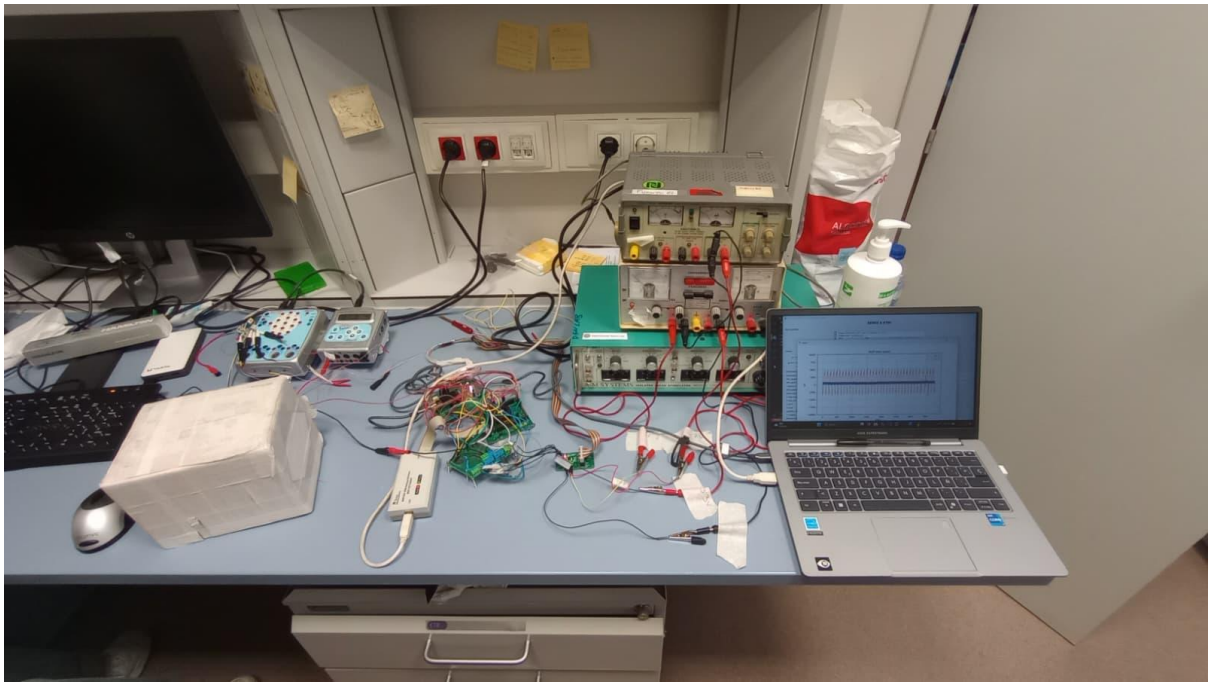

Figure 81 Setup for validation of the device with visual stimulation.

The result of applying visual stimulation to a mouse and acquiring the signals present in the visual cortex is shown in Figure 82. In this figure, two channels are displayed. The right channel (CH2) should be disregarded, as the recorded values were incorrect due to improper electrode placement. In contrast, the left channel (CH1) shows that, after approximately 50 ms, a change occurs in the recorded electrical signal. This change is also observed in the reference experiment conducted using the existing devices at the CBT.

The reference result is presented in Figure 75. In this figure, variability can be observed at the time at which this change occurs, since it corresponds to a physiological response, which does not always take place at the same instant.

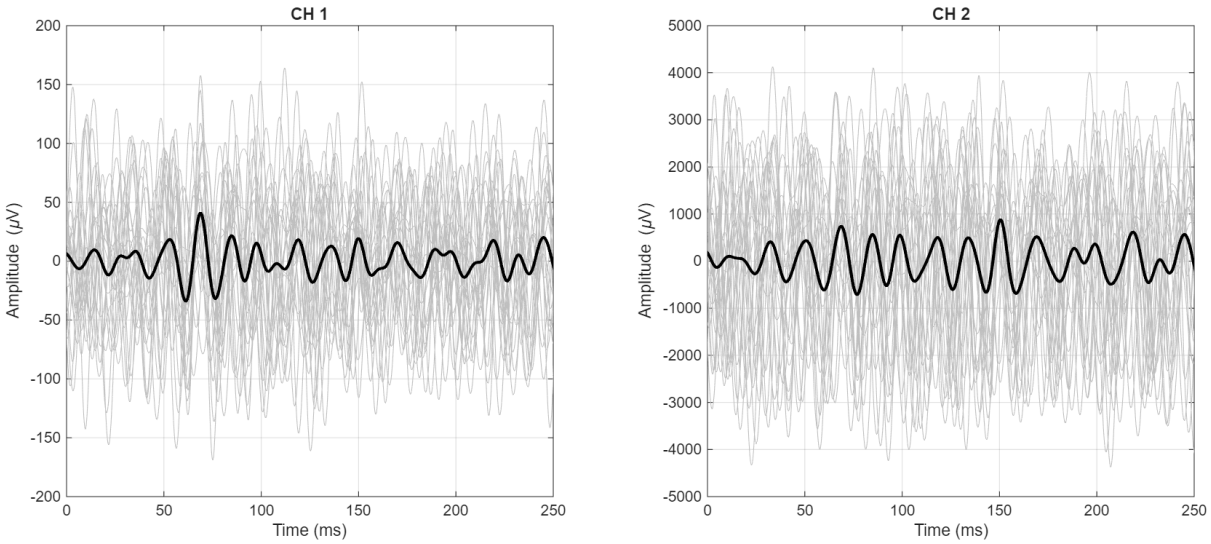

Figure 82 Result of visual stimulation and acquisition validation.

EXPERIMENTAL CONCLUSION

Based on the experiments presented and the results obtained, it is confirmed that the prototype designed and developed in this work has been successfully validated.

8. CONCLUSIONS AND NEXT STEPS

This chapter presents the conclusions obtained from the development of this work and the future lines that open as a continuation of it.

8.1. CONCLUSIONS

The results obtained in this work directly address the general and specific objectives defined in section 1.2, which included the definition of the system requirements, the design of a modular closed-loop architecture, the development of configurable hardware and software modules, and their validation within the STRIKE project framework.

The work carried out in this project has resulted in the successful design and implementation of a modular system for biological signal acquisition and stimulation, aligned with the objectives of the STRIKE project. An extensive analysis of the requirements for stimulation and acquisition systems was conducted, serving as the foundation for the development process. The configuration and operation of the INTAN device were thoroughly studied, and the necessary functions were implemented and validated. Likewise, configuration functions for the MSP430 microcontroller were developed at the Hardware Abstraction Level, including the complete implementation of the timing module.

The architecture of the closed-loop system was defined, specifying its functional characteristics, state machines, and hardware interconnections, which enabled the integration of stimulation and acquisition modules. This design was implemented at both hardware and software levels, resulting in a functional prototype whose performance was verified through characterization and experimental validation. The experiments designed and carried out confirmed the correct operation of the stimulation and acquisition modules, both individually and jointly, demonstrating the feasibility of simultaneous operation within the proposed architecture.

Finally, the analysis of experimental data using the developed signal processing tools yielded favorable results, reinforcing the robustness and applicability of the system in research and clinical contexts.

8.2. NEXT STEPS

Following the verification and validation of the closed-loop system designed and implemented in this work, the following future research directions are proposed:

- Verify the correct implementation of the software in common-port format by integrating the system with a different microcontroller to replace the MSP430.
- Characterize and optimize the stimulation module to achieve pulse durations below 500 µs.
- Improve the sampling frequency of the acquisition system by replacing the MSP430 with a microcontroller operating at a higher clock frequency.
- Characterize the overall power consumption of the system depending on its operating mode.
- Remove the wiring from the prototype and integrate all components into a single PCB.
- Better analyze and understand experimental data obtained from stimulation of the thalamic region.

9. BIBLIOGRAPHY

[1] Ministerio de Ciencia e Innovación, «Plan Estatal de Investigación Científica, Técnica y de Innovación 2021-2023,» Ministerio de Ciencia e Innovación, Madrid, 2021.

[2] I. N. d. Estadística, «Defunciones según la Causa de Muerte,» 2021.

[3] A. P. Menéndez, «El 90% de los casos de ictus se podrían evitar con una adecuada prevención de los factores de,» Sociedad Española de Neurología, 2017.

[4] E. Candelario-Jalil, «Injury and repair mechanisms in ischemic stroke: considerations for the development of novel neurotherapeutics,» *Current opinion in investigational drugs,* vol. 10, nº 7, pp. 644-654, 2009.

[5] P. M George y G. K Steinberg, «Novel Stroke Therapeutics: Unraveling Stroke Pathophysiology and Its Impact on Clinical Treatments,» *Neuron,* vol. 87, nº 2, pp. 297-309, 2015.

[6] M. Gutiérrez, J. Joaquín Merino, M. Alonso de Leciñana y E. Díez-Tejedor, «Cerebral protection, brain repair, plasticity and cell therapy in ischemic stroke,» *Cerebrovascular Diseases,* vol. 27, pp. 177-186, 2009.

[7] I. R Violante, K. Alania, A. M Cassarà , E. Neufeld, E. Acerbo, R. Carron, A. Williamson, D. L Kurtin, E. Rhodes, A. Hampshire, N. Kuster, E. S Boyden, A. Pascual-Leone y N. Grossman, «Non-invasive temporal interference electrical stimulation of the human hippocampus,» *Nature Neuroscience,* vol. 26, nº 11, pp. 1994-2004, 2023.

[8] Z. Zheng Gang y M. Chopp, «Neurorestorative therapies for stroke: underlying mechanisms and translation to the clinic,» *Lancet Neurology,* vol. 8, nº 5, pp. 491-500, 2009.

[9] D. C Hess, L. R Wechsler, W. M Clark, S. I Savitz, G. A Ford, D. Chiu, D. R Yavagal, K. Uchino, D. S Liebeskind, A. P Auchus, S. Sen, C. S Sila, J. D Vest y R. W Mays, «Safety and efficacy of multipotent adult progenitor cells in acute ischaemic stroke (MASTERS): a randomised, double-blind, placebo-controlled, phase 2 trial,» *Lancet Neurology,* vol. 16, nº 5, pp. 360-368, 2017.

[10] A. Jaillard, M. Hommel, A. Moisan, T. A Zeffiro, I. M Favre-Wiki, M. Barbieux-Guillot, W. Vadot, S. Marcel, L. Lamalle, S. Grand y O. Detante, «Autologous Mesenchymal Stem Cells Improve Motor Recovery in Subacute Ischemic Stroke: a Randomized Clinical Trial,» *Transl Stroke Res,* vol. 11, nº 5, pp. 910-923, 2020.

[11] E. Kaniusas, S. Kampusch, M. Tittgemeyer, F. Panetsos, R. Fernandez Gines, M. Papa, A. Kiss, B. Podesser, A. Mario Cassara, E. Tanghe, A. Mohammed Samoudi, T. Tarnaud, W. Joseph, V. Marozas, A. Lukosevicius, N. Ištuk, A. Šarolić, S. Lechner, W. Klonowski, G. Varoneckas y J. Constantin Széles, «Current Directions in the Auricular Vagus Nerve Stimulation I – A Physiological Perspective,» *Front Neuroscience,* vol. 13, 2019.

[12] S. A Hays, A. Ruiz, T. Bethea, N. Khodaparast, J. B Carmel, R. L Rennaker 2nd y M. P Kilgard, «Vagus nerve stimulation during rehabilitative training enhances recovery of forelimb function after ischemic stroke in aged rats,» *Neurobiol Aging,* vol. 43, pp. 111-118, 2016.

[13] N. D Engineer , T. J Kimberley, C. N Prudente, J. Dawson, W. Brent Traver y S. A Hays, «Targeted Vagus Nerve Stimulation for Rehabilitation After Stroke,» *Frontiers in Neuroscience,* vol. 13, 2019.

[14] J. Ma, L. Zhang, G. He, X. Tan, X. Jin y C. Li, «Transcutaneous auricular vagus nerve

stimulation regulates expression of growth differentiation factor 11 and activin-like kinase 5 in cerebral ischemia/reperfusion rats,» *Jouran of the Neurological Sciences,* vol. 369, pp. 27-35, 2016.

[15] D. González-Nieto, L. Fernández-García, J. Pérez-Rigueiro, G. V Guinea y F. Panetsos, «Hydrogels-Assisted Cell Engraftment for Repairing the Stroke-Damaged Brain: Chimera or Reality,» *Polymers,* vol. 10, nº 2, p. 184, 2018.

[16] S. Mora-Lee, M. Salomé Sierol-Piquer, M. Gutiérrez-Pérez, U. Gomez-Pinedo, V. D Roobrouck, T. López, M. Casado-Nieto, G. Abizanda, M. Teresa Rabena, C. Verfaille, F. Prósper y J. M. García-Verdugo, «Therapeutic effects of hMAPC and hMSC transplantation after stroke in mice,» *PloS One,* vol. 7, nº 8, 2012.

[17] M. Gutiérrez-Fernández, B. Rodríguez-Frutos, J. Ramos-Cejudo, L. Otero-Ortega, B. Fuentes y E. Díez-Tejedor, «Stem cells for brain repair and recovery after stroke,» *Expert opinion on biological therapy,* vol. 13, nº 11, pp. 1479-1483, 2013.

[18] L. Fernández-García, J. Pérez-Rigueiro, R. Martínez-Murillo, F. Panetsos, M. Ramos, G. V Guinea y D. González Nieto, «Cortical Reshaping and Functional Recovery Induced by Silk Fibroin Hydrogels-Encapsulated Stem Cells Implanted in Stroke Animals,» *Frontiers in cellular neuroscience,* vol. 12, 2018.

[19] L. Fernández-García, N. Marí-Buyé, J. A Barios, R. Madurga, M. Elices, J. Pérez-Rigueiro, M. Ramos, G. V Guinea y D. González-Nieto, «Safety and tolerability of silk fibroin hydrogels implanted into the mouse brain,» *Acta Biomaterialia,* vol. 45, pp. 262-275, 2016.

[20] C. PErucca Orfei, G. Talò, M. Viganò, S. Perteghella, G. Lugano, F. Fabro Fontana, E. Ragni, A. Colombini, P. De Luca, M. Moretti, M. Luisa Torre y L. de Girolamo, «Silk/Fibroin Microcarriers for Mesenchymal Stem Cell Delivery: Optimization of Cell Seeding by the Design of Experiment,» *Pharmaceutics,* vol. 10, nº 4, 2018.

[21] «Transcranial magnetic stimulation (TMS) in stroke: Ready for clinical practice?,» *Journal of clinical neuroscience,* vol. 31, pp. 10-14, 2016.

[22] A. Arboix, J. Díaz, A. Pérez-Sempere y J. Á. Sabin, «ICTUS: TIPOS ETIOLÓGICOS Y CRITERIOS DIAGNÓSTICOS,» de *Guía para el diagnóstico y tratamiento del ictus*, Barcelona, Prous Science, 2006, pp. 10-32.

[23] World Health Organization, «The top 10 causes of death,» World Health Organization, 17 August 2024. [En línea]. Available: https://www.who.int/news-room/fact-sheets/detail/the-top-10-causes-of-death. [Último acceso: 11 November 2025].

[24] Ministerio de Sanidad de España, «Estrategia del Ictus del Sistema Nacional de Salud. Actualización 2024,» 2024.

[25] B. Fernández Martínez, «Diagnóstico Y Tratamiento Del Ictus,» *NPunto,* vol. 5, nº 51, 2022.

[26] A. Fernández, A. Renú Jornet, X. Urra Nuin y Á. Chamorro Sanchez, «Portal Clínic - Tratamiento del Ictus,» Clínic Barcelona, 27 12 2022. [En línea]. Available: https://www.clinicbarcelona.org/asistencia/enfermedades/ictus/tratamiento#tratamiento-del-ictus-hemorragico. [Último acceso: 24 04 2025].

[27] L. A. Serna Corredor, A. Ricaurte-Fajardo, N. Useche y H. Bayona, «Trombólisis intravenosa y terapias de reperfusión por encima de las 4,5 h en ataque cerebrovascular isquémico agudo: «Expandiendo la ventana»,» *Neurología Argentina,* vol. 14, nº 3, pp. 171-182, 2022.

[28] E. Bravo-Esteban y E. López-Larraz, «Potenciación del reaprendizaje motor y la recuperación funcional en pacientes con ictus: estrategias no invasivas de modulación del sistema nervioso

central,» *Rev Neurol,* vol. 62, nº 6, pp. 273-281, 2016.

[29] M. Bayón, «Estimulación magnética transcraneal en la rehabilitación del ictus,» *Rehabilitación,* vol. 45, nº 3, pp. 261-267, 2011.

[30] F. Alda, «B.log.ia 2.0,» 03 06 2016. [En línea]. Available: https://b-log-ia20.blogspot.com/2016/06/sistema-nervioso-i-aspectos-generales.html. [Último acceso: 24 04 2025].

[31] S. Andalib, A. A. Divani, C. Ayata, S. Baig, E. M. Arsava, M. A. Topcuoglu, E. L. Cáceres, V. Parikh, M. J. Desai, A. Majid, S. Girolami y M. D. Napoli, «Vagus Nerve Stimulation in Ischemic Stroke,» *Current Neurology and Neuroscience Reports,* vol. 23, nº 12, pp. 947-962, 11 2023.

[32] R. H. Howland, «Vagus nerve stimulation,» *Current Behavioral Neuroscience Reports,* vol. 1, nº 2, pp. 64-73, 2014.

[33] J. Zabara, «Inhibition of experimental seizures in canines by repetitive vagal stimulation,» *Epilepsia,* vol. 33, nº 6, pp. 1005-1012, 1992.

[34] G. L Morris, D. Gloss, J. Buchhalter, K. J Mack, K. Nickels, Harden y Cyntia, «Evidence-based guideline update: vagus nerve stimulation for the treatment of epilepsy: report of the Guideline Development Subcommittee of the American Academy of Neurology,» *Neurology,* vol. 81, nº 16, pp. 1453-1459, 2013.

[35] R. H Howland, L. S Shutt, S. R Berman, C. R Spotts y T. Denko, «The emerging use of technology for the treatment of depression and other neuropsychiatric disorders,» *Ann Clin Psychiatry,* vol. 23, nº 1, pp. 48-62, 2011.

[36] S. E Krahl, «Vagus nerve stimulation for epilepsy: A review of the peripheral mechanisms,» *Surg Neurol Int.,* vol. 3, nº 2, pp. 47-52, 2012.

[37] G. M De Ferrari y P. J Schwartz, «Vagus nerve stimulation: from pre-clinical to clinical application: challenges and future directions,» *Heart Fail Rev.,* vol. 16, nº 2, pp. 195-203, 2011.

[38] R. S. Terry, W. B. Tarver y J. Zabara, «The implantable neurocybernetic prosthesis system,» *Pacing Clin Electrophysiology,* vol. 14, nº 1, pp. 86-93, 1991.

[39] electroCore, «GammaCore,» 2025. [En línea]. Available: https://www.gammacore.com/. [Último acceso: 29 04 2025].

[40] D. P. A. Ballesteros, «Anatomía del corazón,» de *Libro de la salud cardiovascular del Hospital Clínico San Carlos y de la Fundación BBVA*, Bilbao, Editorial Nerea, S. A., 2009, pp. 35-40.

[41] D. L. Azcona, «El electrocardiograma,» de *Libro de la salud cardiovascular del Hospital Clínico San Carlos y la Fundación BBVA*, Bilbao, Editorial Nerea, S. A., 2009, pp. 49-56.

[42] M. Ufnal y P. Konopelski, «Electrocardiography in Rats: a Comparison to Human,» *Physiological research / Academia Scientiarum Bohemoslovaca,* vol. 65, nº 10.33549/physiolres.933270, pp. 717-725, 2016.

[43] P. Driscoll, «The normal rat electrocardiogram,» de *The Rat Electrocardiogram in Pharmacology and Toxicology*, New York, Pergamon Press, 1981, pp. 1-14.

[44] M. Hadjem y F. Nait-Abdesselam, «An ECG T-wave Anomalies Detection Using a Lightweight Classification Model for Wireless Body Sensors,» . *IEEE ICC 2015 - Workshop on ICT-enabled services and technologies for eHealth and Ambient Assisted Living,* pp. 278-283, June 2015.

[45] M. a. J. W. a. S. A. a. E. O. A. Safa, «Hardware Architecture for Adaptive Dual Threshold Filter and Discrete Wavelet Transform based ECG Signal Denoising,» *International Journal of Advanced Computer Science and Applications,* nº 10.14569/IJACSA.2021.0121106, 2021.

[46] R. Hill, A. Howard y G. Gresham, «The electrocardiographic appearances of myocardial infarction in the rat,» *British Journal of Experimental Pathology,* vol. 41, nº 6, p. 633, 1960.

[47] A. Sgoifo, S. F. De Boer, B. Buwalda, G. Korte-Bouws, J. Tuma, B. Bohus, J. Zaagsma y J. M. Koolhas, «Vulnerability to arrhythmias during social stress in rats with different sympathovagal balanc,» *American Journal of Physiology-Heart and Circulatory Physiology,* vol. 275, nº 2, pp. H460-H466, 1998.

[48] P. P Pereira - Junior, M. Marocolo, F. P Rodrigues, E. Medei y J. H M Nascimento, «Noninvasive method for electrocardiogram recording in conscious rats: feasibility for heart rate variability analysis,» *Anais da Academia Brasileira de Ciências,* vol. 82, pp. 431-437, 2010.

[49] H. Mongue-Din, A. Salmon, M. Fiszman y Y. Fromes, «Non-invasive restrained ECG recording in conscious small rodents: a new tool for cardiac electrical activity investigation,» *Pflügers Archiv-European Journal of Physiology,* vol. 454, pp. 165-171, 2007.

[50] «emka technologies ecgTUNNEL,» emka Technologies, 2016. [En línea]. Available: https://emka.scireq.com/ecgtunnel. [Último acceso: 28 07 2025].

[51] J. D. Falcone, «A novel microwire interface for small diameter peripheral nerves in a chronic, awake murine model,» *Journal of Neural Engineering,* vol. 17, nº 4, 2020.

[52] N. Xue, I. Delgado Martinez, J. Sun, Y. Cheng y C. Liu, «Flexible multichannel vagus nerve electrode for stimulation and recording for heart failure treatment,» *Biosensors and Bioelectronics,* vol. 112, pp. 114-119, 2018.

[53] C. Keling, Z. Wang, J. Bai, J. Xiong, J. Chen y J. Ni, «Research advances in the application of vagus nerve electrical stimulation in ischemic stroke,» *Frontiers,* vol. 16, 2022.

[54] P. S. Ortiz, *Experiments realization for VISNE project.,* Madrid, 2025.

[55] Intan Technologies, «Intan Tech - RHS Stim/Amplifier Chips,» Intan Technilogies, 2025. [En línea]. Available: https://intantech.com/products_RHS2000.html. [Último acceso: 26 12 2025].

[56] INTAN technologies, «INTAN RHS2116 datasheet,» 2010-2025. [En línea]. Available: https://intantech.com/files/Intan_RHS2116_datasheet.pdf. [Último acceso: 30 12 2025].

[57] Texas Instruments Incorporated, «MSP430FG479,» [En línea]. Available: https://www.ti.com/product/es-mx/MSP430FG479. [Último acceso: 21 05 20205].

[58] Texas Instruments, «Texas Instruments - SN65LVDT41PWR,» Texas Instruments, [En línea]. Available: https://www.ti.com/product/SN65LVDT41/part-details/SN65LVDT41PWR?utm_source=google&utm_medium=cpc&utm_campaign=asc-null-null-asc_opn_en-cpc-storeic-google-ww_en_pur&utm_content=Device&ds_k=SN65LVDT41PWR&DCM=yes&gclsrc=aw.ds&gad_source=1&gad_campaignid=817. [Último acceso: 30 12 2025].

[59] C. Eunmi, K. Taekyung, S. Hing, K. Taewoo, K. Minhee, S. Young-Min y P. Eunkyong, «Transcutaneous Auricular Vagus Nerve Stimulation Can Alter Autonomic Function and Induce an Antiepileptic Effect in Pentylenetetrazol- Induced Seizures in Rats,» *IEEE Access,* vol. PP, pp. 1-1, 2024.

[60] P. Jiapu y W. J. Tompkins, «A Real-Time QRS Detection Algorithm,» *IEEE Transactions on*

Biomedical Engineering, Vols. %1 de %2BME-32, nº 3, pp. 230-236, 1985.

[61] Texas Instruments, «Texas Instruments MSP-TS430PN80,» 2025. [En línea]. Available: https://www.ti.com/tool/es-mx/MSP-TS430PN80USB. [Último acceso: 05 08 2025].

[62] Adafruit, «Adafruit ESP32-S3 TFT Feather,» Adafruit, 03 01 2023. [En línea]. Available: https://learn.adafruit.com/adafruit-esp32-s3-tft-feather/overview. [Último acceso: 02 01 2026].

[63] Espressif, «ESP32-S3 Series Datasheet V2.1,» 2021.

[64] A. C. Moreno, *Máster Universitario en Ingeniería de Sistemas Electrónicos: Trabajo final de Máster. Diseño e implementación de un dispositivo para la captura de señales biológicas aplicado en el tratamiento del ictus isquémico.,* Madrid: ETSIT - UPM, 2025.

[65] A. Calatrava Moreno, «Github - ECG analysis,» 2025. [En línea]. Available: https://github.com/alimudena/ECG_recording_analysis.git.

[66] Cambridge Electronic Design Limited, «Data acquisition & analysis: Spike 2 software,» [En línea]. Available: https://ced.co.uk/es/products/spike2. [Último acceso: 16 01 2026].

[67] A. Calatrava Moreno, «GitHub - MSP430-INTAN,» 2025. [En línea]. Available: https://github.com/alimudena/INTAN-RHS2116.git.

[68] noshpineapple28, «Arduino Nano ESP32 - Can't get SPI slave to work,» 1 july 2024. [En línea]. Available: https://forum.arduino.cc/t/arduino-nano-esp32-cant-get-spi-slave-to-work/1285250?utm_source=chatgpt.com. [Último acceso: 02 01 2026].

[69] Brainbox, «Sintered Ag/AgCl Electrode,» [En línea]. Available: https://www.brainbox.shop/products/silver-silverchloride-electrode/19386520000041674 67?variant=19386520000041674 61. [Último acceso: 02 01 2026].

[70] TerniMed, «Bipolar stimulation probe,» [En línea]. Available: https://www.ternimed.de/en/p/bipolar-stimulation-probe-two-90-hook-tips. [Último acceso: 02 01 2026].

[71] Texas Instruments, «AMC3330EVM,» [En línea]. Available: https://www.ti.com/product/AMC3330EVM/part-details/AMC3330EVM?utm_source=google&utm_medium=cpc&utm_campaign=asc-null-null-asc_opn_en-cpc-storeevm-google-ww_en_pur&utm_content=Device&ds_k=AMC3330EVM&DCM=yes&gclsrc=aw.ds&gad_source=1&gad_campaignid=81783967. [Último acceso: 02 01 2026].

[72] World Precision Instruments, «DAM80,» [En línea]. Available: https://www.wpi-europe.com/products/amplifiers/extracellular/dam80.aspx. [Último acceso: 02 01 2026].

[73] Cambridge Electronic Design Limited, «Micro1410,» [En línea]. Available: https://ced.co.uk/es/products/mic4eu. [Último acceso: 02 01 2026].

[74] A. Vázquez-Oliver, C. Brambilla-Pisoni, M. Domingo-Gainza, R. Maldonado, A. Ivorra y A. Ozaita, «Auricular transcutaneous vagus nerve stimulation improves memory persistence in naïve mice and in an intellectual disability mouse model,» *Frontiers,* vol. 13, nº 2, pp. 494-498, 2020.

[75] micromed, «micromed: solutions for neurophysiology,» [En línea]. Available: https://arcmednet.ro/image/data/Micromed/EMG.pdf. [Último acceso: 01 02 2026].

ANNEX A: ETHICAL, ECONOMIC, SOCIAL AND ENVIRONMENTAL ASPECTS

A.1 INTRODUCTION

This Master's Thesis is developed within the framework of the STRIKE project, a multidisciplinary initiative aimed at improving the treatment of ischemic stroke through the integration of three techniques: transcranial magnetic stimulation, the implantation of mesenchymal stem cells encapsulated in silk fibroin, and electrical stimulation of the auricular branch of the vagus nerve. The system designed and developed seeks to meet, through a closed-loop approach, the stimulation, acquisition, and biological signal processing requirements of the experiments conducted within the STRIKE project.

This project addresses an urgent medical need, given the significant impact of strike on public health, as it is one of the leading causes of death and disability in Spain. From a social perspective, the system aims to improve patients' quality of life through more personalized and effective treatments. From an ethical point of view, priority has been given to the use of non-invasive methods, avoiding aggressive interventions. Legally, animal experimentation protocols and biomedical safety regulations have been strictly observed. From an environmental perspective, the system's energy efficiency and its potential to reduce resource consumption in clinical trials have been taken into consideration.

A.2 DESCRIPTION OF RELEVANT IMPACTS RELATED TO THE PROJECT

During the analysis phase, several relevant impacts have been identified:

SOCIAL IMPACT

Ischemic stroke represents one of the leading causes of death and disability worldwide. Currently, available treatments are limited and must be applied at very early stages of the disease. The STRIKE project, within which this work is framed, proposes new therapies based on minimally invasive techniques that could significantly improve neurological recovery and reduce stroke-associated mortality.

If the outcomes of the STRIKE project are favorable, the clinical implementation of these therapies could be accelerated, contributing to a reduction in the healthcare burden on medical centers and an increase in patient survival rates.

Furthermore, the system developed in this work has been designed to be adaptable and portable, facilitating its integration into clinical environments without compromising patient comfort.

ECONOMIC IMPACT

Stroke generates very high healthcare and social cost due to prolonged hospitalization, rehabilitation, and post-care requirements. The implementation of more effective therapies and adaptive monitoring systems could significantly reduce these costs by shortening hospital stays and decreasing the need for long-term care. Moreover, the development of compact and reusable biomedical devices, such as the one proposed in this work, promotes resource optimization and reduces costs associated with bulky and non-portable equipment currently used in experimental settings.

ETHICAL IMPACT

The STRIKE project and the developed system are aligned with ethical principles by pursuing less invasive and safer therapies for patients. Stimulation of the vagus nerve through its auricular branch, for instance, avoids complex surgical procedures, thereby reducing risks and improving quality of life. Additionally, the modular and configurable design of the system allows it to be adapted to different experimental and clinical protocols, ensuring responsible and safe use in both research and medical practice. Section A.3 Detailed analysis of some of the main impacts provides a detailed analysis of the

ethics committee that approved the experiments related to the STRIKE project, as well as the technical report submitted for its evaluation.

STAKEHOLDER GROUPS

The main stakeholder groups of the STRIKE project and the system developed are as follows:

- Biomedical researchers: who require versatile and cost-effective devices for the acquisition of biological signals and neurological stimulation in experimental environments.
- Academic institutions: which may incorporate the device into research projects, teaching activities, or technology transfer initiatives.
- Healthcare professionals: including physicians, neurologists, and clinical staff who could benefit from more precise and accessible tools for treatment monitoring. The device may also be particularly useful in low-resource settings.
- Patients: especially those who have suffered an ischemic stroke, as the objectives of the STRIKE project could contribute to improving their recovery through personalized therapies.

A.3 DETAILED ANALYSIS OF SOME OF THE MAIN IMPACTS

In order to assess the relevance and scope of the project under development, a detailed analysis of its social impact has been conducted, as this has been identified as the most significant among the set of impacts considered. As discussed in previous sections, ischemic stroke represents one of the leading causes of death and disability worldwide, which justifies the need to advance new therapeutic strategies aimed at improving patient prognosis.

The STRIKE project is framed within this context, proposing the development of new therapies based on minimally invasive interventions. Unlike other approaches focused exclusively on in vitro studies, this project incorporates in vivo experimentation using animal models (mice), allowing the validation of treatment efficacy under physiological conditions that are closer to real clinical scenarios.

The importance of this research lies in the fact that, should the results obtained prove favorable, the application of these treatments in real clinical settings could be accelerated. This would not only contribute to improving patient survival rates but also to reducing the healthcare burden on health systems, optimizing resources, and enhancing the quality of life of affected individuals.

It is worth noting that, although in vitro experimental alternatives have been explored, the complexity of the central nervous system makes the use of animal models essential to obtain reliable results. Accordingly, the project has been designed in strict compliance with the ethical and legal principles governing animal experimentation.

In this regard, the project has been submitted for evaluation to the *Comité de Experimentación Animal* of the Universidad Complutense de Madrid, together with the corresponding technical report. Likewise, compliance with the provisions of Rogal Decree 53/2013 of 1 February, which establishes the basic standards for the protection of animals used in experimentation and other scientific purposes, has been ensured. Furthermore, the technical report entitled *"NUEVOS ENFOQUES TERAPÉUTICOS DE ESTIMULACIÓN MÍNIMAMENTE INVASIVA PARA EL TRATAMIENTO DEL ICTUS CEREBRAL ISQUÉMICO"* has been approved under registration code ES 280790002070 and accepted by the *Dirección General de Agricultura Ganadería y Alimentación"* with the verification code 0999597095352455584367. These measures ensure that the research is conducted under ethically responsible and legally regulated conditions.

Overall, the social impact of the STRIKE project is reflected in its potential to transform the clinical management of ischemic stroke, improve therapeutic outcomes, and contribute to the advancement of scientific knowledge in the field of neuroscience.

A.4 CONCLUSIONS

The development of the system within the framework of the STRIKE project has made it possible to address in a comprehensive manner the ethical, economic, social, and environmental impacts associated with biomedical research in the treatment of ischemic stroke. From a social perspective, the transformative potential of the proposed therapies has been demonstrated, as this could significantly improve patient recovery and reduce the healthcare burden on health systems. The device design, focused on adaptability and ease to use, further enhances its applicability in both clinical and experimental environments.

From an economic standpoint, a low-cost approach has been prioritized, fostering the replicability of the device in other academic and clinical contexts, and promoting knowledge transfer and resource optimization. This strategy contributes to strengthening the research community by providing accessible and functional tools.

From an ethical and legal perspective, the project has been developed in strict adherence to the principles of animal experimentation, ensuring compliance with current regulations and evaluation by the relevant committees. This ethical responsibility ensures that scientific advances are achieved within a regulated framework that respects animal welfare.

Finally, environmental impact has been taken into account through the use of low-power electronic components and a design that minimizes the need for additional infrastructure, thereby reducing the device's ecological footprint. Overall, the STRIKE project and the implemented system represent a significant contribution to the advancement of neurosciences, with positive implications across multiple dimensions of the biomedical field.

ANNEX B: ECONOMIC BUDGET

LABOR COST (Direct Costs)		Hours	Cost/hour	Total
	First contract (internship)	240	39	9.360,00 €
	Second contract (full-time)	640	11 €	7.333 €
Total				16.693,33 €

COST OF MATERIAL RESOURCES (Direct Costs)	Purchase price	Usage in months	Amortization (in years)	Total
Personal computer	1.076,00 €	11	8	123,29 €
Jira License	73,80 €	11	1	67,65 €
Development Card (MSP430 + SPI TRANS)	85,40 €	4	3	9,49 €
MATLAB 2025 License	344,74 €	16	2	229,83 €
ESP32-S3	25,00 €	4	4	2,08 €
INTAN RHS2116	247,94 €	4	1	82,65 €
Power Supply 1 (Tektronix CPS250)	355,95 €	4	5	23,73 €
Power Supply 2	355,95 €	4	5	23,73 €
Teledyne test tools T3DSO2502A	1.627,45 €	4	5	108,50 €
Function generator	81,41 €	4	5	5,43 €
Logic analyzer	542,35 €	4	5	36,16 €
TOTAL COST OF MATERIAL RESOURCES				**712,53 €**

OVERHEAD (Indirect Costs)	15%	on DC	**2.610,88 €**
INDUSTRIAL MILL	6%	on DC+IC	**639,40 €**

FUNGIBLE MATERIAL	
Petrol	**25,00 €**
TOTAL FUNGIBLE MATERIAL	**75,00 €**

BUDGET SUBTOTAL		**20.731,14 €**
APPLICABLE VAT	21%	**4.353,54 €**

TOTAL BUDGET	**25.084,69 €**

ANNEX C: INTAN CONFIGURATION FUNCTIONS

During the development of this work, the operation of the INTAN device was analyzed through an in-depth review and interpretation of its datasheet [56]. Each functionality offered by the device was examined in detail, and a set of configuration functions was designed and implemented accordingly. The following sections present these functions, outlining their purpose, parameters and implementation approach.

AC AMPLIFIER BANDWIDTH

Pages 9-11 INTAN datasheet

Function	Description	Parameters needed	Values		Function Type
Fc_high	Configure the upper bandwidth for filtering all ADCs out there. It is a common filter.	**Fh_magnitude**: from the table it takes values highlighted in yellow	750, 500, 300, 250, 200, 150, 100	20, 15, 10, 7.5, 5.0, 3.0, 2.5, 2.0, 1.5, 1.0	Common
		Fh_unit: toma valores k o H	H	k	
Fc_low_A	Selecting the lower frequency of filter A.	**Fc_low_A**: From the table, the values are defined in Hz ranging from 1000.0 to 0.1 respectively.	1000, 500, 300, 250, 200, 150, 100, 75, 50, 30, 25, 20, 15, 10, 7.5, 5.0, 3.0, 2.5, 2.0, 1.5, 1.0, 0.75, 0.5, 0.3, 0.25, 0.1		Common
Fc_low_B	Selecting the lower frequency of filter B.	**Fc_low_B**: From the table, the values are defined in Hz ranging from 1000.0 to 0.1 respectively.			Common
A_or_B_cutoff_frequency	It allows you to change, for each channel individually, which lower cut-off frequency is used as a reference (A or B).	**amplifier_cutoff_frequency_A_B** 16-element array. Each of the elements corresponds to a different channel. Take 'A' or 'B' values.	A, B		Common
		Waiting_trigger: lo pone a true	True, false		
amp_fast_settle	Function that allows the amplifiers to be placed on the baseline to continue sampling. It uses a register that needs a trigger. In addition, since when putting a	**Amplifier_reset**: An array that contains one element per channel. It establishes whether there is a channel that needs to be placed on the baseline.	True, false		Common

	channel to baseline it is necessary to wait a bit, the instruction is set to 1 in the time restriction array. After making the call to this function, amp_fast_settle_reset must be called to reset the record	**Time_restriction**: An array that contains whether the instruction has time constraints. It makes it true. When the shipment is made, it will be taken into account that it has these restrictions, pausing the rest of the shipments for a while.	True, false	
		Waiting_trigger: lo pone a true.	True, false	
amp_fast_settle_reset	Resets the register used in amp_fast_settle returning the ADCs to their normal read state	**Waiting_trigger**: lo pone a true	True, false	Common
Power_up_AC	Configure the ADCs to be powered. When they are not being used, it is recommended that they are without food. This power is removed in the mínimum_power_disipation function.	-	-	Common

CONSTANT-CURRENT STIMULATOR

Pages 12, 13 INTAN datasheet

Function	Description	Parameters needed	Values	Function Type
Step_sel_uni_1	Internal configuration function, for more information get inside the code and see what it does	-	-	Common
Stim_step_DAC_configuration	Configure, from the options of the different step sizes that exist, which one you want for stimulation. Step parameters are common to all channels.	**Step_DAC**: contains the step size you want to have when stimulating (goes in nA)	10, 20, 50, 100, 200, 500, 1000, 2000, 5000, 10000	Common
Stim_pnBIAS_configuration	Set up other registers that are needed to define this stimulation.			
Stim_current_channel_configuration	Configure, for each channel separately, which stimulation values are to be used by choosing the positive and negative stimulation values separately and defining the channel as input. *It is interesting to remember that the times in which the stimulation is working are measured by the external timer.*	**Channel**: channel for which the stimulation is to be configured	0 - 15	Common
		neg_current_trim, pos_current_trim		
		neg_current_mag, pos_current_mag		
		Waiting_trigger = true	True, false	
All_stim_channels_off	The stimulation of all channels is turned off. What is actually changed is the value of the INTAN_config structure (Stimulation_on) and made to be 0. Then a call must be made to Stimulation_on so that this change is made in the INTAN records.	-	.	Common

Stimulation_on	An array defines which channels are going to be used to stimulate. When they have already defined themselves in this array, this function allows them to be able to stimulate. They are registers that need triggers. In addition, an external pin needs to be enabled, otherwise, it cannot stimulate.	**Stimulation_on:** is an array that contains Boolean values, one for each channel. With them, it is defined whether it is going to be stimulated through that channel or not.	Array de true y false	Common
		Waiting_trigger = true	True, false	
Stimulation_polarity	The polarity of each of the channels is defined in an array.	**Stimulation_pol:** is an array that contains boolean values, one for each channel. They define what polarity each channel has.	P or N arrray	Common
		Waiting_trigger = true	True, false	
Stimulation_polarity_faster	Only the polarity of the channel passed to the function is defined as a parameter. This channel could be modified directly in the function.	**Stimulation_pol:** is an array that contains boolean values, one for each channel. They define what polarity each channel has.	P or N arrray	Common
		Waiting_trigger = true	True, false	
		Channel: indicates the channel to which you want to set the polarity.	0-15	
Stimulation_disable	Disabling stimulation. The values of the records corresponding to the authorization are set to zero here.	-	-	Common

Stimulation_enable	Stimulation enablement. The values of the corresponding records are put in the required pattern defined in the datasheet.	-	-	Common
ON_INTAN	Enable and turn on stimulation of the channels that have been enabled for stimulation. To ensure that stimulation is initiated, the same command is sent twice in a row to reduce the number of errors that are caused by errors in SPI communication.			Common
ON_INTAN_FASTER	Enables and turns on channel stimulation that is indicated in the value of the channel passed to the function.	**Channel:** indicates the channel to which you want to enable and start the stimulation.	0-15	Common
ON_INTAN_FASTER_FASTER	Instead of making the calls to the functions, what is done is to make the content of the functions directly to avoid losing clock cycles by not having to enter the functions.	**Channel:** indicates the channel to which you want to enable and start the stimulation.	0-15	Common
OFF_INTAN	The stimulation of all channels is turned off.	-	-	Common
OFF_INTAN_FASTER	Stimulation of all channels is turned off using the fastest SPI command call.	-	-	Common

COMPLIANCE MONITOR

Page 13 INTAN datasheet

Function	Description	Parameters needed	Values	Function Type
Clean_compliance_monitr	Allows you to clean up the log that contains the compliance monitor. This log shows if there is an electrode that has a voltage that is too high or too low (close to vstim+-).	It makes a call to enable and disable the M flag before and after writing to the registry. This allows you to clean up registry values, even if it's only a read log. 't' for read command	-	Common
Check_compliance_monitor	It allows you to check what value the record has that shows if any of the electrodes has a voltage that is too high or low (close to vstim+-). You can act accordingly with some of the advice given on the INTAN website.	'M' for read command	-	Common

CHARGE RECOVERY SWITCH

Page 13 INTAN datasheet

Function	Description	Parameters needed	Values	Function Type
Connect_channel_to_gnd	It allows a specific channel to be connected to gnd, eliminating the problem of redox reactions that occur in the electrodes. There is one electrode common to all that is stim_GND that connects to GND. Calling this function configures the channel that needs to be connected to gnd with stim_GND. Can be used when the voltage value read is too high or in other cases	***Channel***: Specifies the channel you want to connect to stim_gnd.	0-15	Common
Disconnect_channels_from_gnd	It allows all gnd channels to be disconnected, undoing the effect that has been produced by using the connect_channel_to_gnd function.	***Waiting_trigger:*** lo pone a true		Common

CURRENT-LIMITED CHARGE RECOVERY CIRCUIT

Page 14 INTAN datasheet

Function	Description	Parameters needed	Values	Function Type
Charge_recovery_current_configuration	Configuration of the constant current with which a channel is to be carried at a specific voltage.	**current_recovery**: Current defined to carry the defined voltage. Comes in nA	1, 2, 5, 10, 20, 50, 100, 200, 500, 1000	Common
Charge_recovery_voltage_configu[illegible]	Recovery voltage to which the channel is to be taken.			Common
Enable_charge_recovery_sw	Enable the recovery switch for a specific channel. This allows the voltage of a channel to be brought to the level that has been set in charge_recovery_voltage_configuration and charge_recovery_current_configuration	Channel: Specifies the channel for which you want to enable the recovery switch.		Common
Disable_charge_recovery_sw	Disable the recovery switch for all channels.	-		Common

FAULT CURRENT DETECTOR

Page 20 INTAN datasheet

Function	Description	Parameters needed	Values	
Fault_current_detect_ion	It is usually used to check, when nothing is stimulating, if there is a fault current between stim_gnd and sense_gnd.	'f' del read command	-	Common

GENERAL CONFIGURATION

Function	Description	Parameters needed	Values	
Enable_C2	Enables a2 plug-in on ADCs	**C2_enabled**: A parameter in the structure that configures whether or not the A2 add-in has been enabled. It is set to true in the function, you don't need to touch it.	True	Common
Disable_C2	Allows you to disable the a2 plugin in ADCs	**C2_enabled**: A parameter in the structure that configures whether or not the A2 add-in has been enabled. It is set to false in the function, you don't need to touch it.	False	Common
Check_INTAN_SPI_array	Create a generic array to test the INTAN SPI response and see if it is communicating correctly. It is specific to each master's degree, it must be programmed in a dedicated way.	-	-	Port
Write_register_1	Defines and writes to record 1 the values of all items that are configured in that record. It is called within each of the functions that configure something in that register. You don't need to make a call to that function unless you set the value of one of the parameters separately without using a configuration function.	-	-	Common

ANALOG TO DIGITAL CONVERTER

Page 16 INTAN datasheet

Function	Description	Parameters needed	Values	Function Type
ADC_sampling_rate_config	It is responsible for configuring the corresponding records depending on the sampling rate of the ADC to be obtained. It depends on the speed of sending by SPI from the master.	**ADC_sampling_rate**: Sampling rate at which the ADC will operate.	-	Common

AUXILIARY DIGITAL OUTPUTS

Page 20 INTAN datasheet

It has three programmable digital outputs. The logic is explained in the datasheet. There are enable and disable functions. Once enabled, they can be turned on and off with power on-off. The digoutOD allows you to do things with devices that need voltages greater than 3.3V. It does not have associated functions but an element of the structure, look at datasheet to understand how it works. It is configured in register 1 with the write_register_1 function.

Function	Description	Parameters needed	Values	Function Type
Enable_ditigal_output_X	Enable the X digital output pin (1 or 2). If it is disabled, you cannot control anything about them. If enabled, it can be turned on or off with the power_ON or power_OFF function	**digoutXHz** (the structure parameter is set alone, no need to touch it)	True, false	Common
Disable_digital_output_X_	Disable the X digital output pin (1 or 2). If it is disabled, you cannot control anything about them. If enabled, it can be turned on or off with the power_ON or power_OFF function	**digoutXHz** (the structure parameter is set alone, no need to touch it)	True, false	Common
Power_ON_output_X	Turn on the X-output digital pins (1 or 2). If it is disabled, you cannot control anything about them. To enable and disable them, the enable_digital_output_X and disable_digital_output_X functions are used.	**digoutX** (the structure parameter is set alone, you don't have to touch it)	True, false	Common
Power_OFF_output_X	Turn off the X-output digital pins (1 or 2). If it is disabled, you cannot control anything about them. To enable and disable them, the enable_digital_output_X and disable_digital_output_X functions are used.	**digoutX** (the structure parameter is set alone, you don't have to touch it)	True, false	Common

ABSOLUTE VALUE MODE

Page 21 INTAN datasheet

It can be used with the DSP high pass filter enabled, thus eliminating offset and the base level is eliminated by setting the DC to zero. DC low-gain amplifiers are not affected. It is often used in threshold detection applications, so as not to implement positive or negative detection logic.

Function	Description	Parameters needed	Values	
Enable_absolute_value	Enables the use of the absolute value.	**absmode** (the parameter of the structure is set alone, you don't have to touch it)	True, false	Common
Disable_absolute_value	Disables the use of the absolute value.	**absmode** (the parameter of the structure is set alone, you don't have to touch it)	True, false	Common

POWER DISIPATION

Page 21-24 INTAN datasheet

There are a number of settings that can be put in place to minimize consumption

Function	Description	Parameters needed	Values	Function Type
Minimum_power_disipation	Set up your entire device to keep consumption to a minimum. It should be used first. From the call to the function, it will then be necessary to enable and configure the parameters again of everything you want to use.	**current_recovery**: it is set to 1nA (according to datasheet), it is not to be touched, it is put on its own.	-	Common
		step_DAC: Set to 10nA (according to datasheet). You don't have to touch it, it stands on its own.	-	
		fc_low_B: Set to 0.1Hz (according to datasheet). You don't have to touch it, it stands on its own.	-	

DSP HIGH-PASS FILTER FOR OFFSET REMOVAL

Page 21 INTAN datasheet

It has a DSP to remove the continuous value from reading ADCs. The records associated with the filter cut-off frequency are set by taking into account the sample rate at which the channels are sampled and a K-factor. The calculation is made in reverse of the value of the K depending on the cut-off frequency sought.

Function	Description	Parameters needed	Values	Function Type
Enable_digital_signal_processing_HPF	Enables the use of DSP to eliminate continuous.	**DSPen** (the structure parameter is set alone, you don't have to touch it)	True, false	Common
Disable_digital_signal_processing_HPF	Disable the use of DSP to eliminate continuous.	**DSPen** (the structure parameter is set alone, you don't have to touch it)	True, false	Common
Dsp_cutoff_frequency_configuration	Depending on the cut-off frequency that is desired in the DSP (DSP_cutoff_freq), the necessary registers are valued. As this cut-off frequency depends on the sample rate of each channel, it is necessary to know the number of channels to be sampled and the sample rate of the ADC (to obtain the sample rate of each channel)	**ADC_sampling_rate**: frequency at which the ADC samples (depends on the speed of sending the master's SPI)	Type uint16_t	Common
		number_channels_to_convert: Number of channels to sample	1 - 16	
		DSP_cutoff_freq: cut-off frequency at which the DSP filter is desired		
		DSP_cutoff_freq_register (the structure parameter is set alone, you don't have to touch it)	1 – 15	

SPI COMMAND WORDS

Page 31-34 INTAN datasheet

Function	Description	Parameters needed	Values	Function Type
Send_SPI_commands	It is responsible for sending the array of instructions that has been defined within the INTAN_config_struct. There are a series of arrays (array1, array2, array3, array4) that are used to store the instructions. It is a port-type function, so the function must be defined depending on the device that is going to be used as a master. Before sending, add three test data packets to the data array to be able to check all the data sent from the first to the last configuration. To do this, he makes a call to send_confirmation_values. After sending the shipment, it makes a call to check_received_command that allows it to check if INTAN has returned what was needed and acts accordingly (ON_INTAN_LED, OFF_INTAN_LED) these actions can be configured depending on the desired application.	**Max_size**: For each command you want to send, max_size has increased by 1. It is used as a counter to know the number of commands to send. No need to touch it	N	Common
		Time_restriction: There are some commands that require a temporary restriction (such as connecting a channel to the GND). Therefore, it is checked for each send if it is necessary to wait a while before moving on to the next command (which in the example should be disconnect the channel from gnd). It is used as a check, no need to touch it.	True, false	

Send_spi_commands_faster	The commands are sent by SPI as in send_spi_command but in this case the values that have been returned by INTAN are not reviewed. This makes the system less robust but allows for more restrictive stimulation changes over time.	**Max_size**: For each command you want to send, max_size has increased by 1. It is used as a counter to know the number of commands to send. No need to touch it	N	Common
		Time_restriction: There are some commands that require a temporary restriction (such as connecting a channel to the GND). Therefore, it is checked for each send if it is necessary to wait a while before moving on to the next command (which in the example should be disconnect the channel from gnd). It is used as a check, no need to touch it.	True, false	
Check_received_command	It is responsible for verifying that the data obtained from INTAN are what was expected. Compare the value obtained with the expected value, if a specific value was expected. If a specific value was not expected but it is a certain statement (such as checking a series of flags), they are checked one at a time.	**Expected_RX_bool**: to check if a specific answer was expected (for example in the scriptures). In the case of readings, the value obtained is not known, so it makes no sense to check it.	True, false	Common
		Obtained_RX: contains the value obtained through SPI by the slave.	-	
		Expected_RX: value that was expected to be received.	-	
		Instruction: Can take multiple values. Depending on the char it contains, it is activated in one way or another.	M, f, other	
Initialize_INTAN	All elements of the structure are initialized with a specific value. It can be modified to be initialized in another way. Later they can be configured again without the need to call this function.	All	-	Common

Enable_X_flag	Change the structure element associated with the X flag (M, U, H, D) by setting it to true.	**X_flag**: Indicates the flag that is being configured.	True, false	Common
Disable_X_flag	Change the element of the structure associated with the X flag (M, U, H, D) by setting it to false.	**X_flag**: Indicates the flag that is being configured.	True, false	Common
Convert_channel	Sends the conversion command for a channel. The response will be received several commands later. Configure flags according to the elements of the structure. Add the data needed to sample a channel to the send arrays. It is specific to each device	Array1, array2, array3, array4, X_flag	-	
		Channel: Indicates which channel you want to sample.		Port
Convert_N_channels	There is a specific command that allows you to sample several channels in a row, always sending the same data. It is responsible for adding the same command to the SPI command array several times, as many times as number_of_channels_to_convert you want to sample starting with the initial_channel_to_convert	**Number_of_channels_to_convert**: indicates the number of consecutive channels to be sampled.		Port
		Initial_channel_to_convert: If multiple channels are being used, the cyclic conversion of channels from the east is initialized		
		Instruction: Type an O in the expected instruction type.	'O'	
Convert_N_channels_faster	It does the same as the convert_N_channels function but in fewer clock cycles, thus allowing those experiments that are more restrictive in time to be carried out.	**Number_of_channels_to_convert**: indicates the number of consecutive channels to be sampled.		Port

		Initial_channel_to_convert: If multiple channels are being used, the cyclic conversion of channels from the east is initialized		
		Instruction: Type an O in the expected instruction type.	'O'	
Clear_command	Configures the clear command that initializes the ADCs for normal operation for sending. It must be configured after the chip is powered on to maximize the accuracy of the ADC.	**C2_enabled**: depending on whether complement 2 has been enabled or not, one value or another is expected to be received.	True, false	Port
		Instruction: Type an L in the expected instruction type.	'T'	
Write_commmand	Configures the write command that allows you to write a value to a specific record.	**X_flag**: to configure whether flags are sent or not		Port
		Array1… 4, expected_RX, expected_RX_bool		
		Instruction: Writes the value 'W' in the expected instruction type.	'W'	
Read_command	Configures the read command that allows a value to be read from a particular register.	**Instruction: Writes** the value passed by ID to the expected statement type.	id	Port
Send_values	Ships the elements in the arrays by SPI in order. It is specific to each device, it must be configured according to the specifications of the device used as a master.	Array 1… 4 Obtained_RX	-	Port

Send_confirmation_values	It sends the necessary bits by SPI to confirm that the sending and receiving has been carried out correctly through INTAN. The ID is expected to be received but not verified. It is specific to each device, it must be configured according to the specifications of the device used as a master.	Array 1… 4 Expected_RX	-	Port

ELECTRODE IMPEDANCE TEST

Page 17 INTAN datasheet

Function	Description	Parameters needed	Values	Function Type
Impedance_check_control	Sets the impedance measurement of an electrode connected to a specific channel. Configure record 2 with the values of the elements in the structure.	zcheck_select zcheck_DAC_enhable zcheck_load zcheck_scale zcheck_en	Mirar datasheet	Common
Impedance_check_DAC	Defines the voltage at which the chip's DAC operates.	zcheck_DAC_value		Common

ANNEX D: STRIKE EXPERIMENTS RESULTS

This annex presents the results obtained from the ECG analysis of the experiments conducted within the STRIKE project during the development of this work. For this purpose, the signal processing module implemented in this work was employed. In the figures, stimulation signals are shown in red, the ECG waveform in blue, and the instantaneous heart rate in beats per minute (BPM) in black.

EXPERIMENT 002: AVNS INITIAL EXPERIMENTS

In this set of experiments, stimulation was applied to the auricular branch of the vagus nerve using a non-invasive approach, employing the electrodes shown in Figure 55 B. This is the approach wanted to be used when stimulation is applied in future experiments in STRIKE project. After analyzing the three rodents, the first and the last (Rodent 1 and Rodent 3) may seem to change their beats per minute due to the stimulation in some of the stimulations.

Rodent 1:

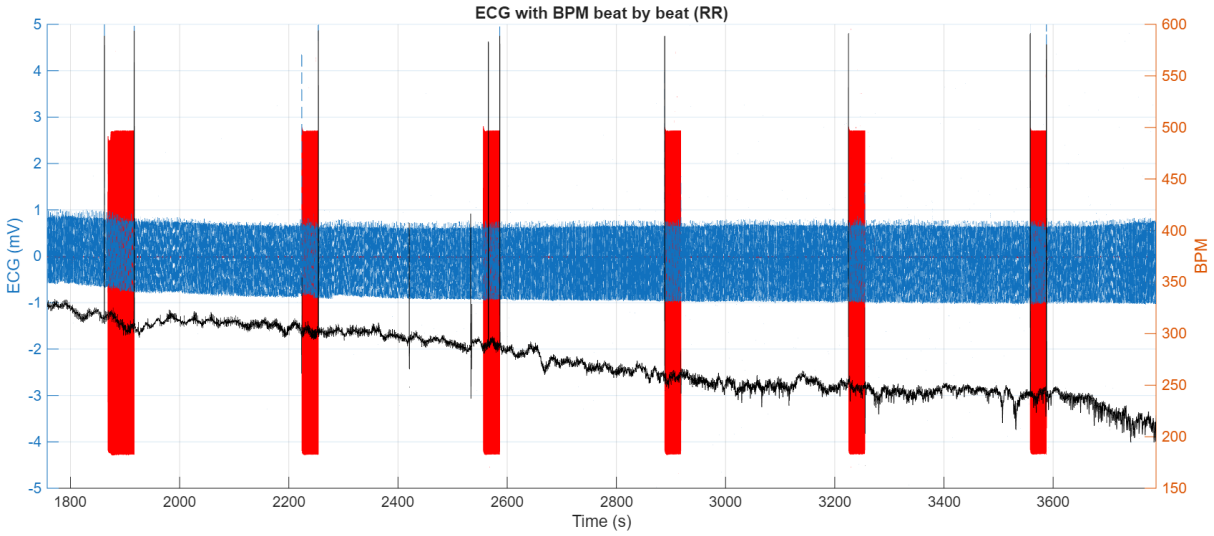

Rodent 2:

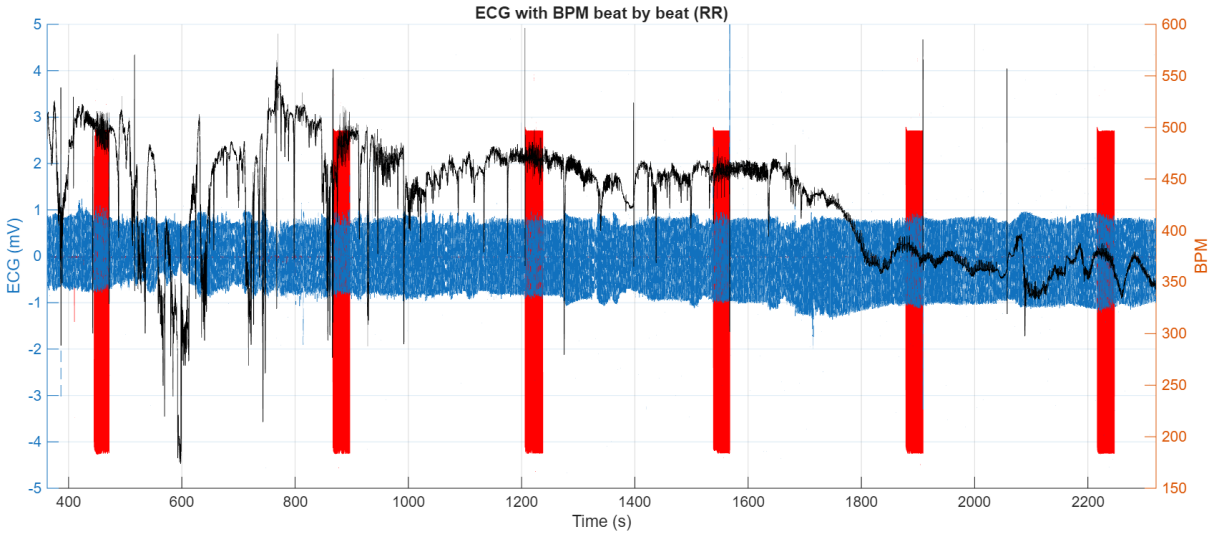

Rodent 3:

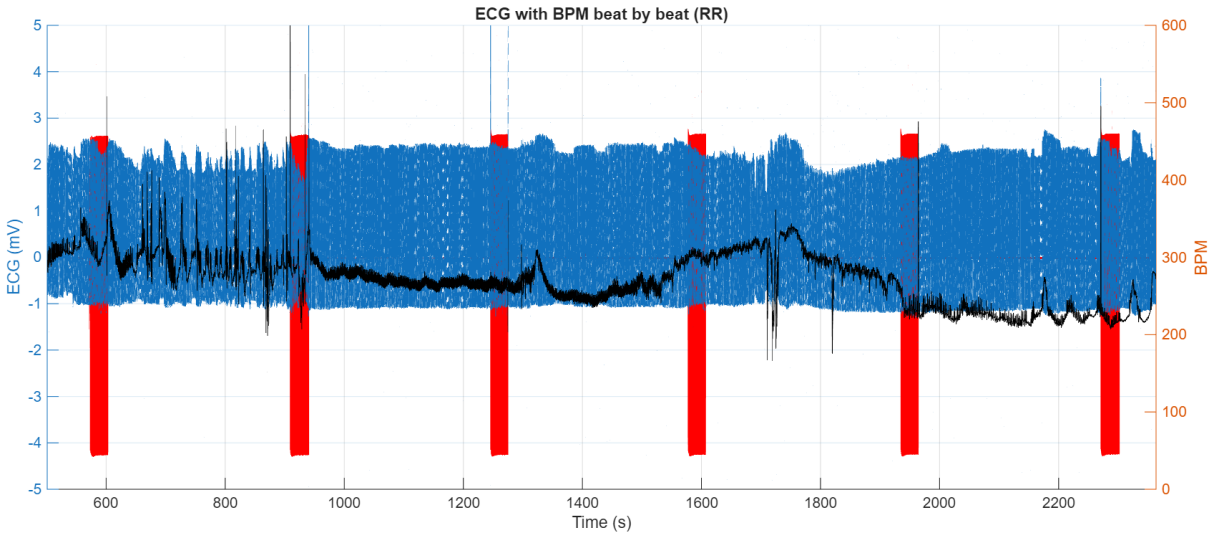
ECG with BPM beat by beat (RR)
ECG (mV)
BPM
Time (s)
5
4
3
2
1
0
-1
-2
-3
-4
-5
600
500
400
300
200
100
0
600
800
1000
1200
1400
1600
1800
2000
2200

EXPERIMENT 003: ANESTHESIA CHANGED

In this set of experiments, stimulation was applied to the auricular branch of the vagus nerve using a non-invasive approach, employing the electrodes shown in Figure 55 B. This is the approach wanted to be used when stimulation is applied in future experiments in STRIKE project. After analyzing the four rodents, the third and the last (Rodent 3 and Rodent 4) may seem to change their beats per minute due to the stimulation in some of the stimulations.

Rodent 1:

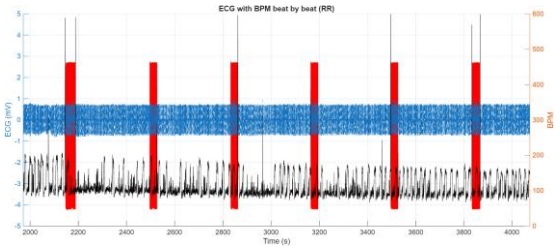

Rodent 3:

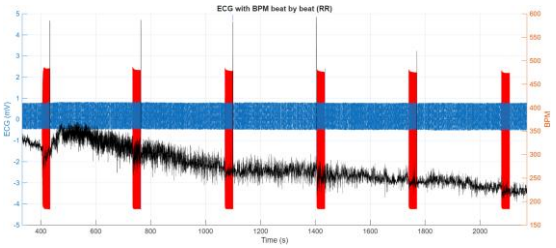

Rodent 2:

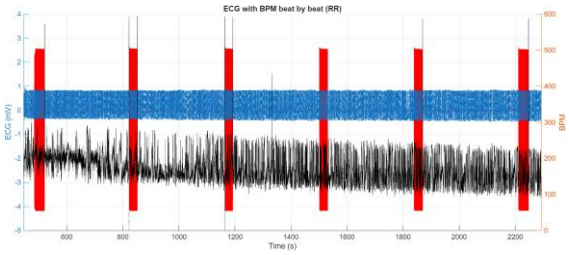

Rodent 4:

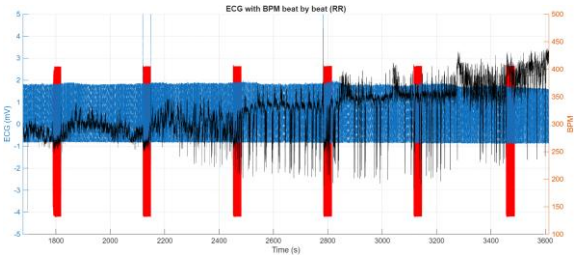

EXPERIMENT 004: AVNS

In this set of experiments, stimulation was applied to the auricular branch of the vagus nerve using a non-invasive approach, employing the electrodes shown in Figure 55 B. This is the approach wanted to be used when stimulation is applied in future experiments in STRIKE project. After analyzing the four rodents, none of the rodents seem to change their beats per minute due to the stimulation in any of the stimulations.

Rodent 1:

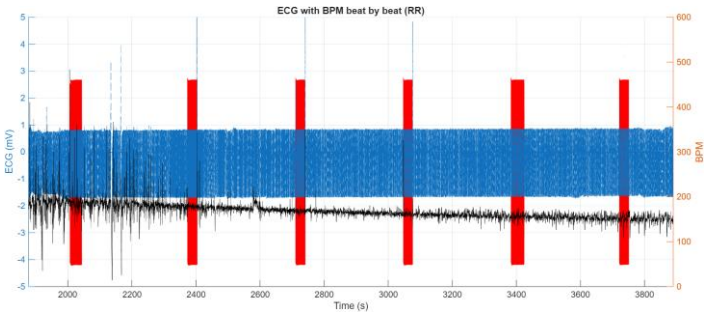

Rodent 3:

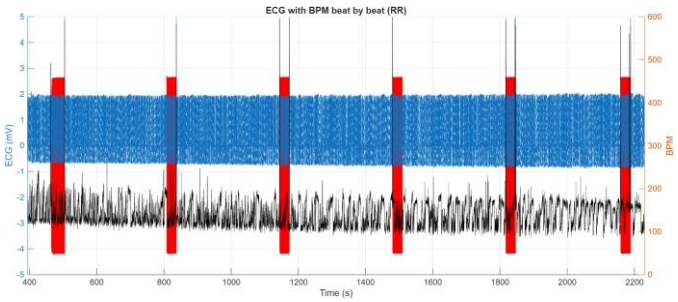

Rodent 2:

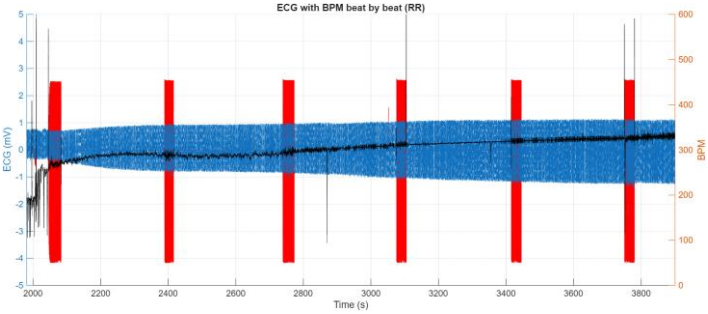

Rodent 4:

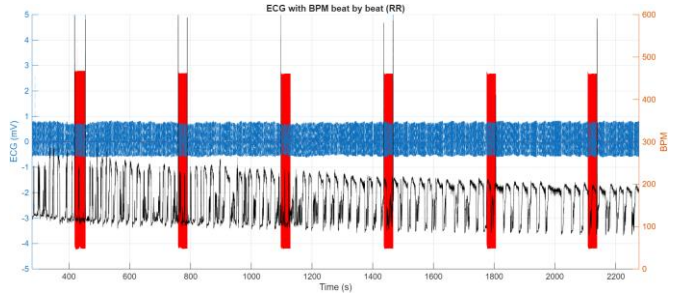

EXPERIMENT 005: AVNS RESTING TIME CHANGE

In this set of experiments, stimulation was applied to the auricular branch of the vagus nerve using a non-invasive approach, employing the electrodes shown in Figure 55 B. This is the approach wanted to be used when stimulation is applied in future experiments in STRIKE project. After analyzing the three rodents, none of the rodents seem to change their beats per minute due to the stimulation in any of the stimulations.

Rodent 1:

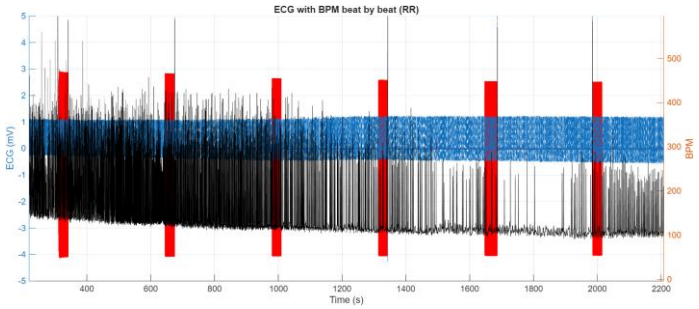

Rodent 3:

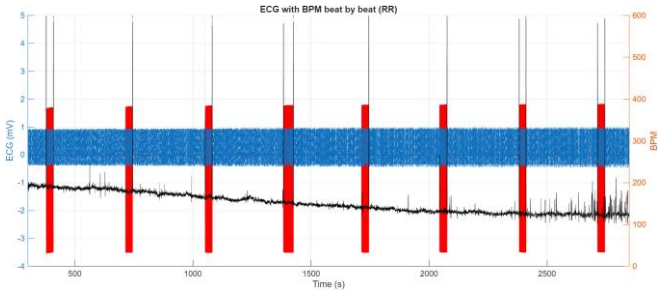

Rodent 2:

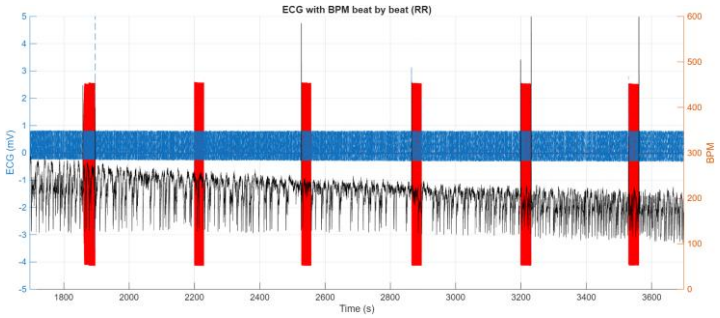

EXPERIMENT 006: MULTIPLE ABVNS

In this set of experiments, stimulation was applied to the auricular branch of the vagus nerve using a non-invasive approach, employing the electrodes shown in Figure 55 B. This is the approach wanted to be used when stimulation is applied in future experiments in STRIKE project. After analyzing the rodent, it does not change its beats per minute due to the stimulation in any of the stimulations. The second rodent used could not be analyses due to the corruption of the file.

Rodent 1:

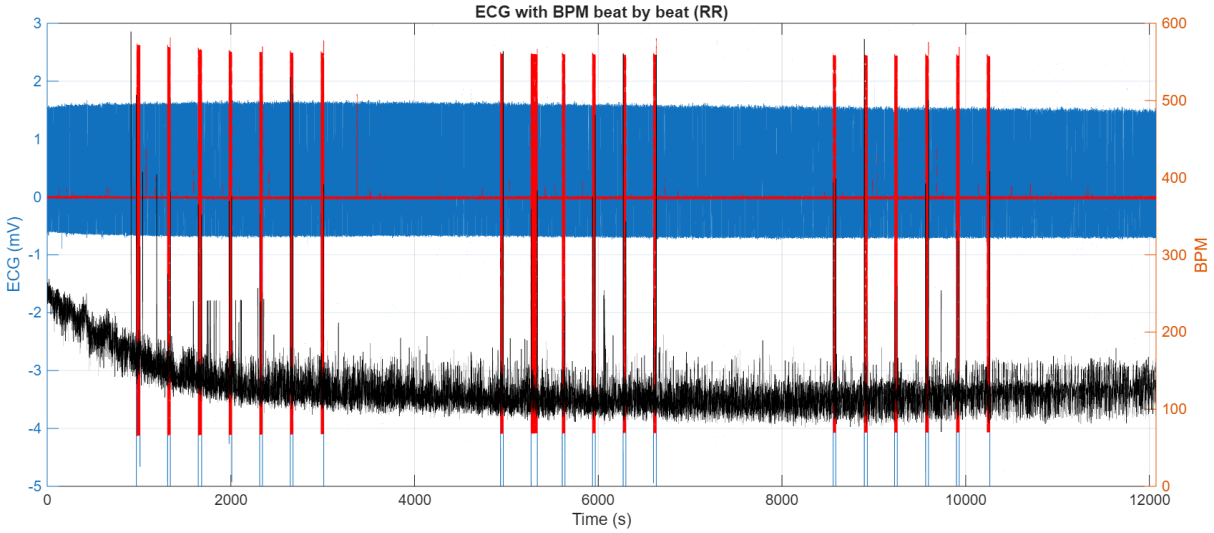

EXPERIMENT 007: AVNS RIGHT EAR

In this set of experiments, stimulation was applied to the auricular branch of the vagus nerve using a non-invasive approach, employing the electrodes shown in Figure 55 B. This is the approach wanted to be used when stimulation is applied in future experiments in STRIKE project. After analyzing the three rodents, none of the rodents seem to change their beats per minute due to the stimulation in any of the stimulations.

Rodent 1 stimulation 1:

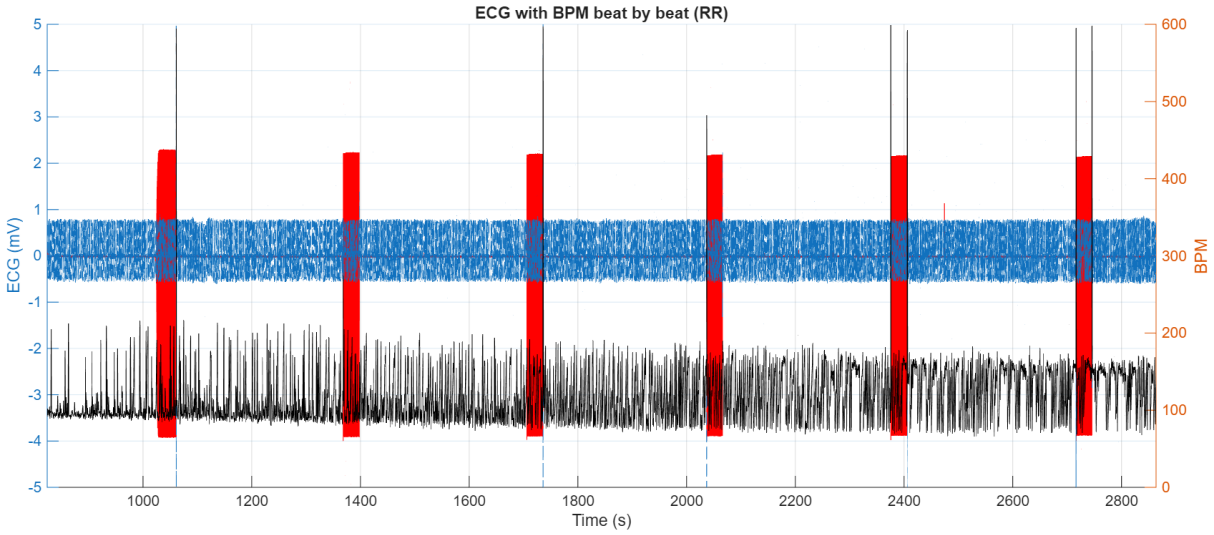

Rodent 1 stimulation 2:

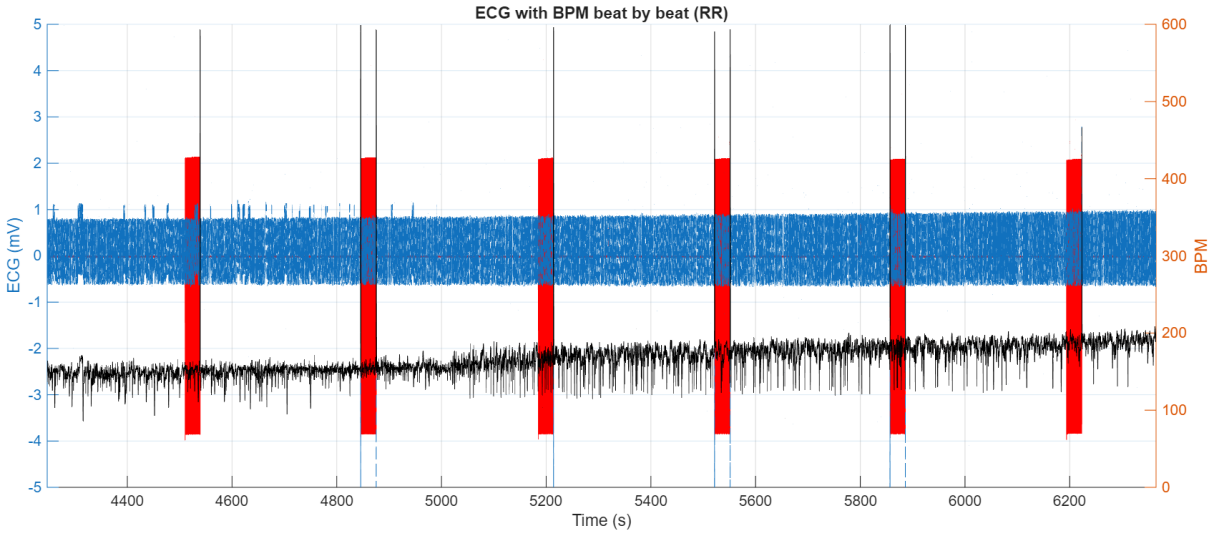

EXPERIMENT 008: AVNS WITH DOPPLER

In this set of experiments, stimulation was applied to the auricular branch of the vagus nerve using a non-invasive approach, employing the electrodes shown in Figure 55 B. This is the approach wanted to be used when stimulation is applied in future experiments in STRIKE project. After analyzing the four rodents, only in one (Rodent 4) changes associated to the stimulation were observed, the rest of rodents did not have any variations on the heart rate while stimulation was applied. As only one had variations, there was a new approach proposed: cervical VNS to check if stimulating the nerve caused the changes that are suggested in the literature.

Rodent 1:

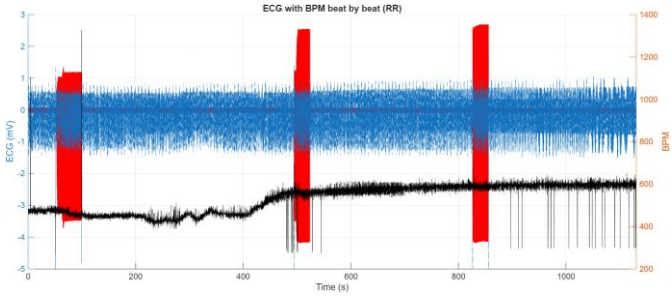

Rodent 3:

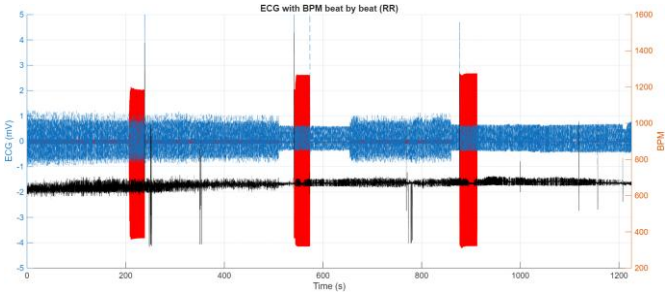

Rodent 2:

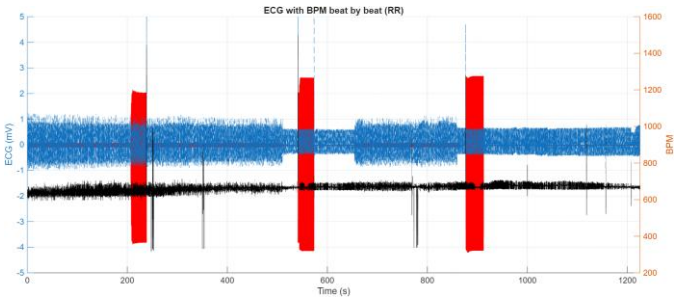

Rodent 4:

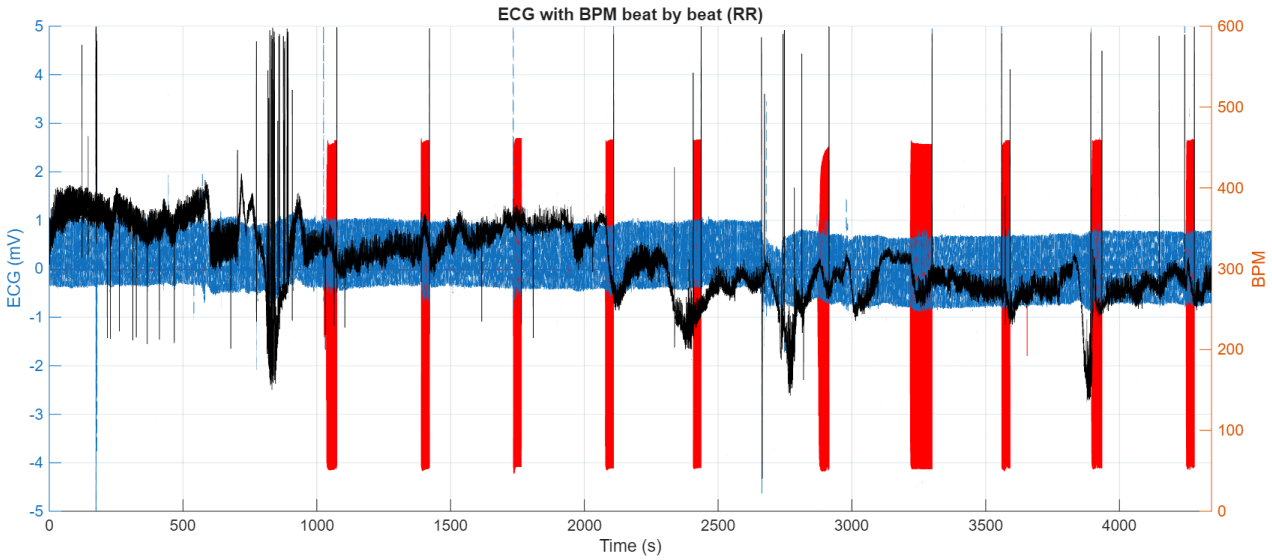

EXPERIMENT 009: CVNS NON INVASIVE

In this set of experiments, stimulation was applied to the cervical branch of the vagus nerve using a superficial (non-invasive) approach, employing the electrodes shown in Figure 55 B. Since the electrode placement was not clearly defined, these experiments were conducted to verify whether correct positioning gad been achieved. However, as observed in the results, no stimulation-related changes were detected, and subsequent analysis confirmed that the electrode position was incorrect. Consequently, these experiments have been excluded from the final analysis.

Rodent 1:

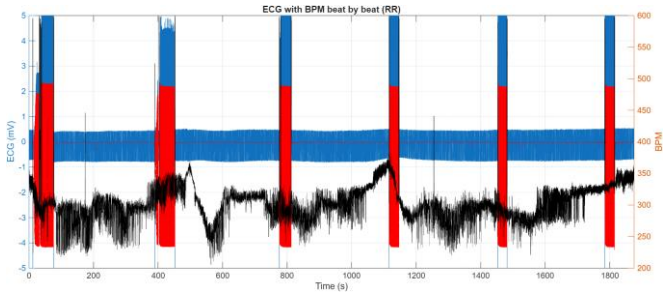

Rodent 4:

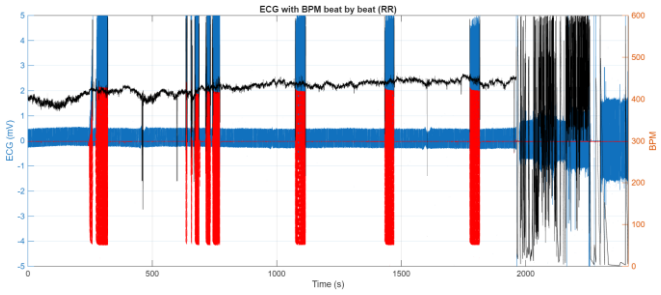

Rodent 2:

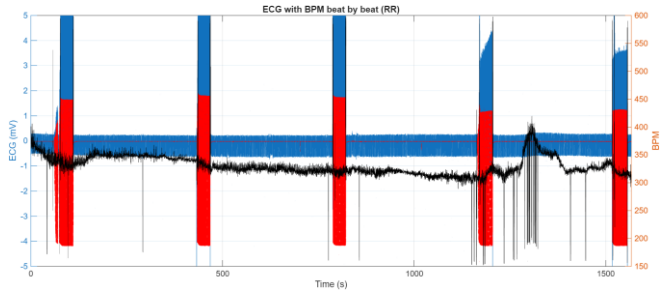

Rodent 5

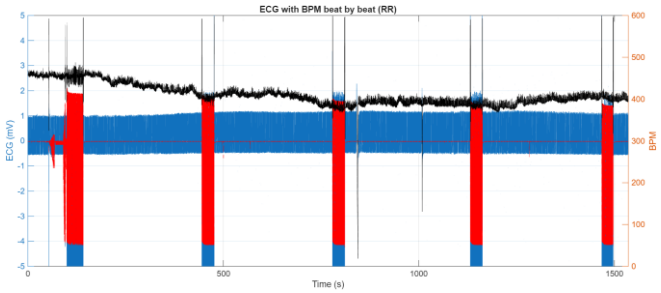

Rodent 3:

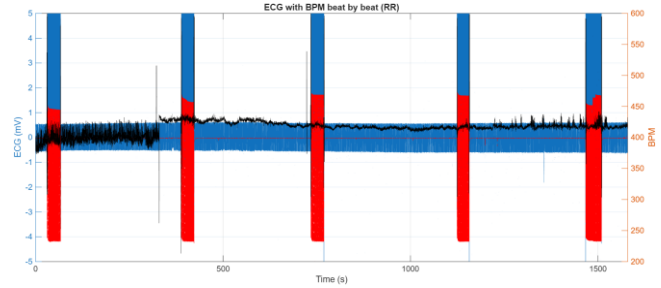

EXPERIMENT 010: CVNS INVASIVE

In this set of experiments, stimulation was applied to the cervical branch of the vagus nerve using a invasive approach, employing the electrodes shown in Figure 55-C and Figure 55-A adapted. The electrodes first employed are very big compared to the animal's complexion therefore an adaptation of those electrodes was done and used in this experiment from rodent 2 onwards.

One of the issues reported by the researcher in charge of doing the experiments was that, while manipulating the nerve, excessive force seemed necessary. Furthermore, analysis of the collected data revealed no changes in heart rate associated with stimulation. Subsequent evaluation confirmed that the manipulation of the nerve may have caused tissue degradation, which led to these results being discarded.

Rodent 1 (right nerve):

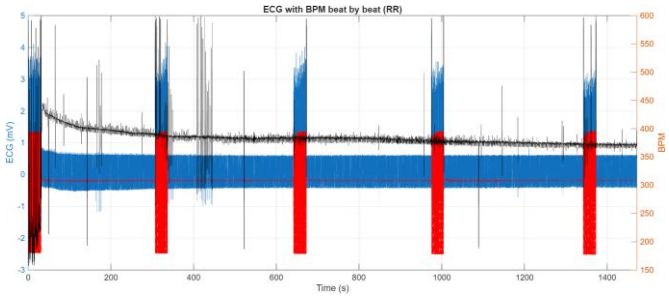

Rodent 3:

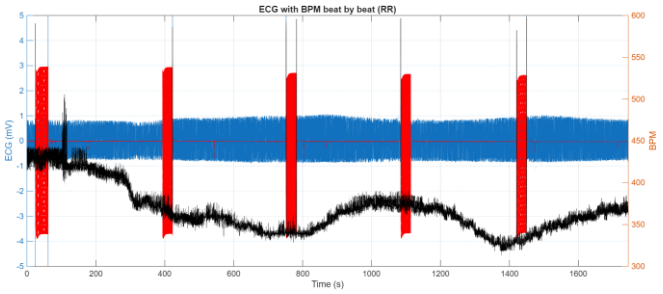

Rodent 1 (left nerve):

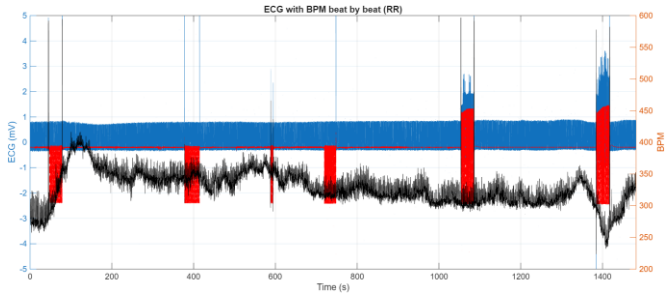

Rodent 4:

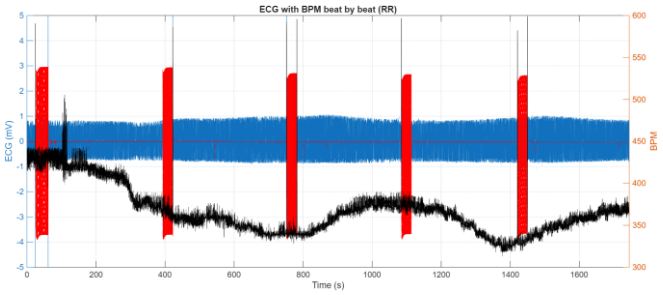

Rodent 2 (right nerve):

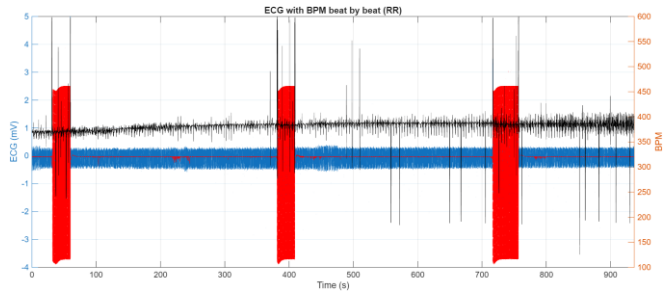

Rodent 5:

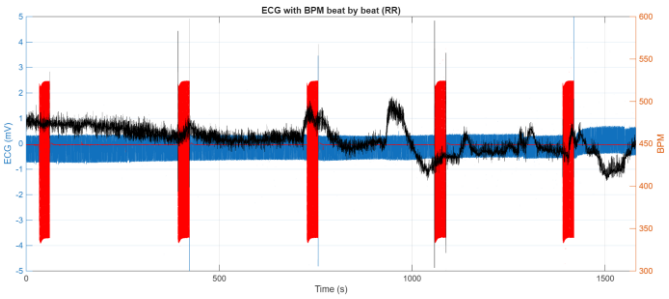

Rodent 2 (left nerve):

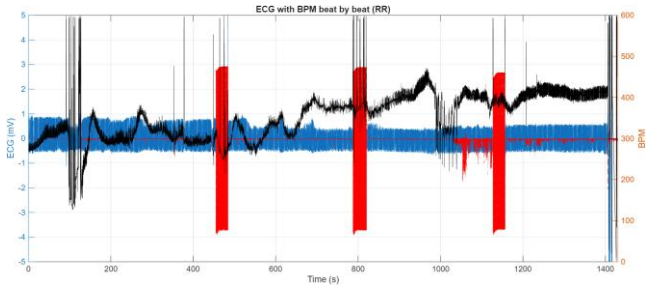

EXPERIMENT 011: CVNS INVASIVE

In this set of experiments, stimulation was applied to the cervical branch of the vagus nerve using an invasive approach, employing the electrodes shown in Figure 55. Those electrodes were specially adapted and made for this experiment, as the previous were too big or too pointy and harmed the tissue around them.

The results of this experiment were favorable in three out of four cases, as variations in heart rate were observed during stimulation. In some instances, these variations were more pronounced, for example, in Rodent 1, where a sharp decrease in heart rate occurred during all stimulation periods. In other cases, the changes were less evident, such as in Rodent 4, where only slight variations in heart rate were detected, potentially associated with stimulation during the first and third intervals.

Rodent 1:

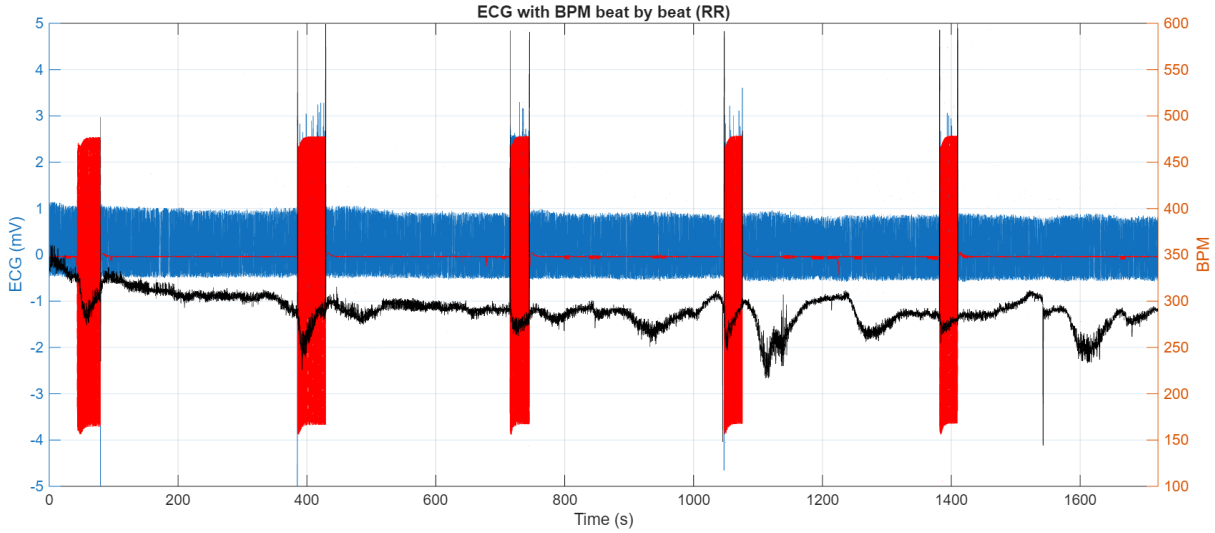

Rodent 2:

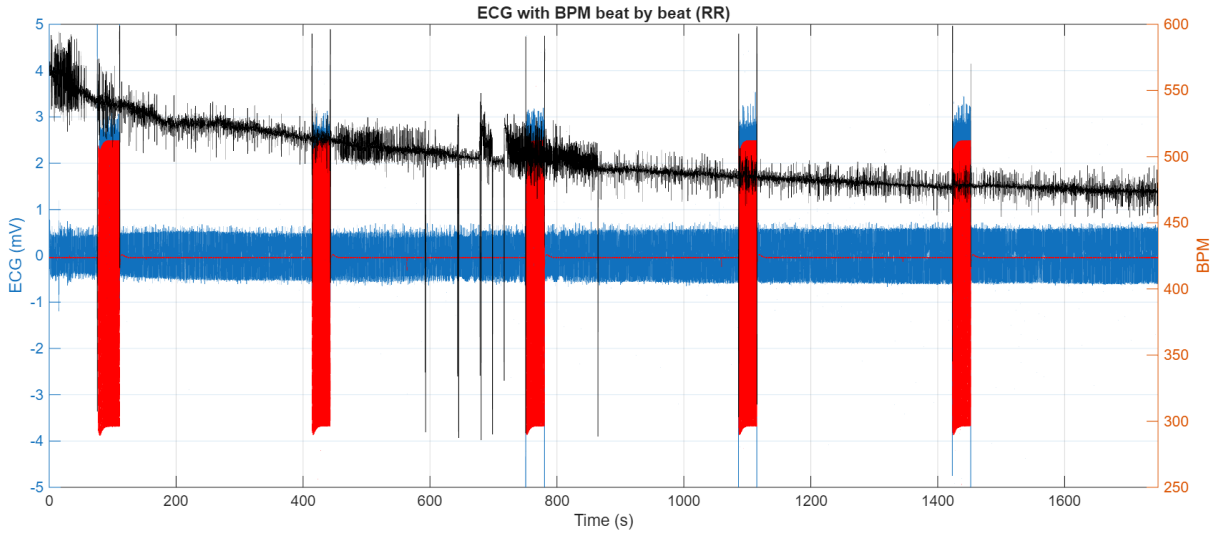

Rodent 3:

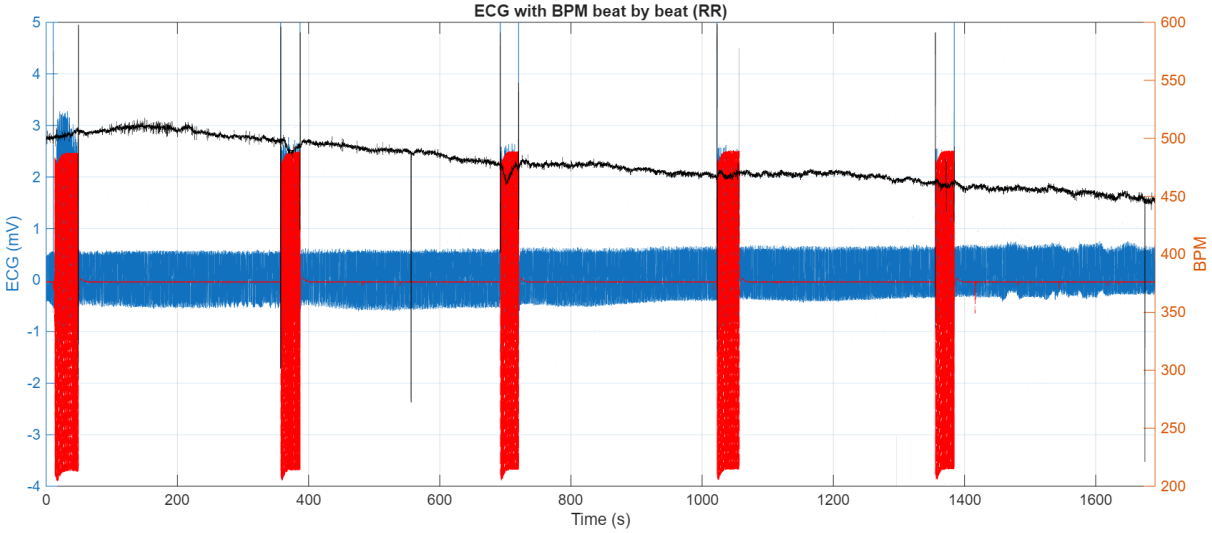

Rodent 4:

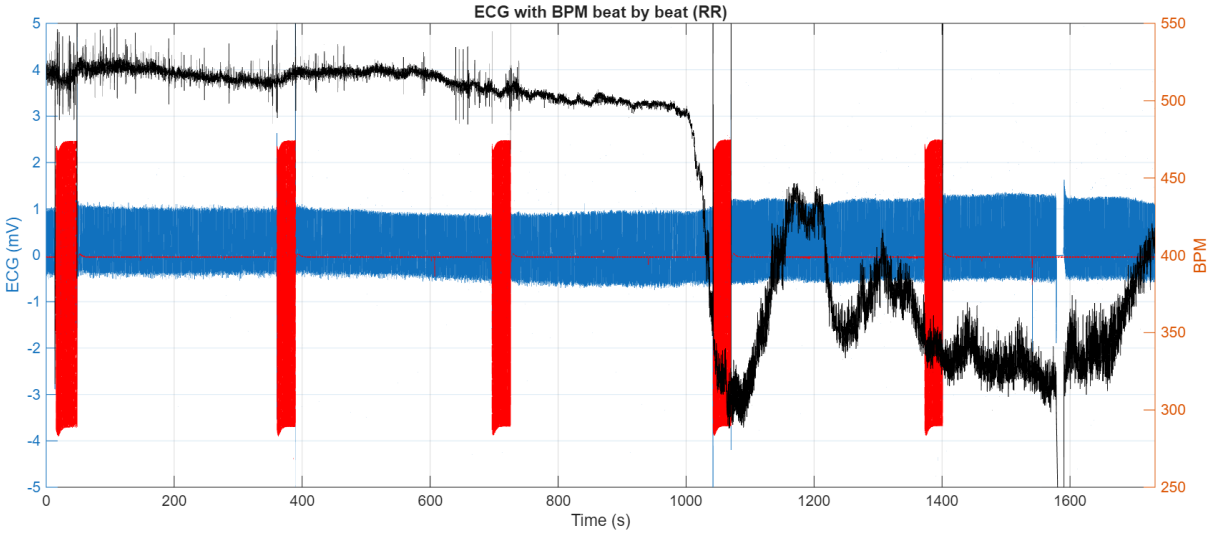

ANNEX E: RESULTS OF THE EXPERIMENTS CONDUCTED FOR THE STIMULATION AND ACQUISITION VALIDATION

To validate the device as a stimulation and acquisition system, several experiments were conducted over two days separated by a one-week interval, the results are presented in this annex. These experiments involved electrical stimulation of the thalamic region and the acquisition of evoked potentials in the visual cortex of four mice. In addition, visual stimulation was also performed, together with the acquisition of the responses generated by this stimulation in the visual cortex.

On the first experimental day, the visual stimulation system was not operating correctly; therefore, only the electrical stimulation experiment was carried out on a single mouse (PEV004). The results of this experiment are presented in section 7.1.2.

On the second experimental day, both electrical and visual stimulation were successfully performed on three different mice. The results of these experiments are presented below. The results are classified into three categories, depending on the type of stimulation applied:

- S: Electrical stimulation in the thalamic region. This type of stimulation may consist of either a single pulse or a pulse train. For differentiating the experiments, as some of the stimulations were carried out with different values of current, an additional notation was created:
    - S1: This kind of experiment corresponds to a single pulse of stimulation with a current value of $10 \cdot 1000 = 10000nA = 10\mu A$.
    - S2: This kind of experiment corresponds to a single pulse of stimulation with a current value of $1 \cdot 1000 = 1000nA = 1\mu A$.
    - S3: This kind of experiment corresponds to a single pulse of stimulation with a current value of $1 \cdot 100 = 100nA$.
    - S4: This kind of experiment corresponds to a train of pulses with a current value of $10 \cdot 1000 = 10000nA = 10\mu A$.
- V: External visual stimulation and acquisition of the resulting signals in the visual cortex.
- C: No visual stimulation is applied; instead, a test is conducted to assess the level of electrical noise introduced into the system due to the activation of the LED screen used in the experiments.

The results obtained from the analysis of these experiments are presented below for each of the aforementioned categories.

ROTENT 1: PEV004

In the experiments done with rodent PEV004, the electrode of the CH2 was not properly connected, so the stimulation result of the analysis is not correct as many noise was detected during the experiment. With this rodent, three types of experiments were done: electrical stimulation, visual stimulation and electrical noise control during visual stimulation.

TYPE S: ELECTRICAL STIMULATION

For electrical stimulation in rodent PEV004, three values of current were used.

S1: 10 μA

For a value of $10\mu A$ of current in the stimulation (only CH1 is valid) it can be observed a similar waveform response to the impulse.

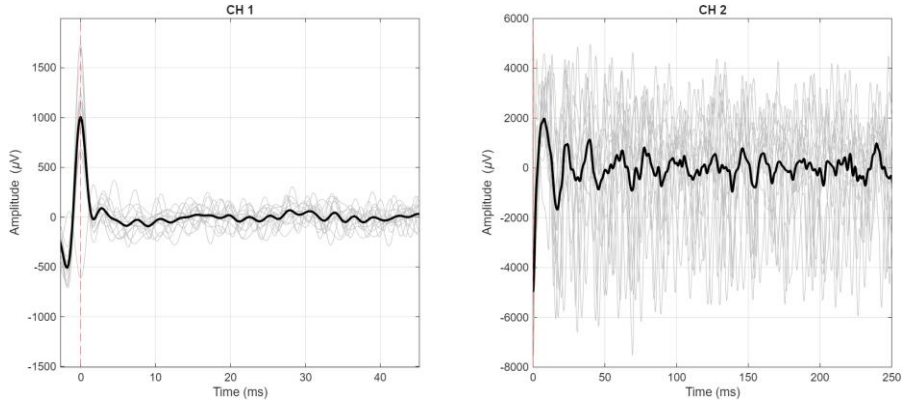

S2: 1 μA

Only the result for the CH1 is presented, as it can be seen that no changes were appreciated during time, at first some stimulation-related changes were noticed but after some time, no changes can be seen.

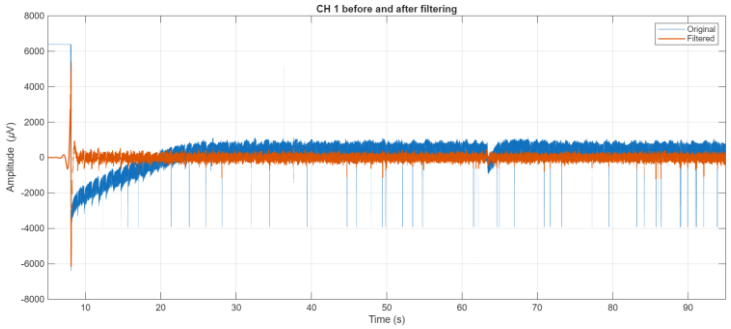

S3: 100 mA

Only the result for the CH1 is presented, as it can be seen that no changes are appreciated during time.

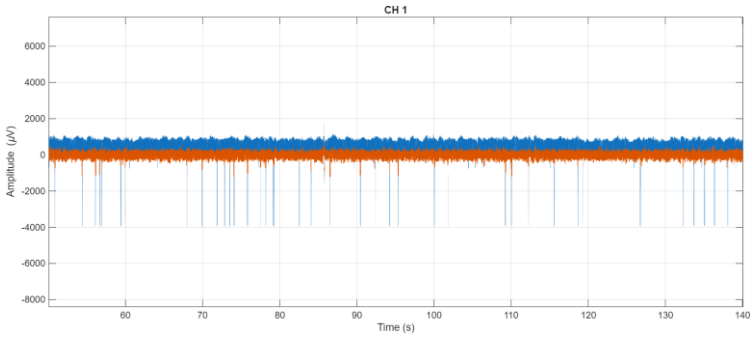

V: VISUAL STIMULATION

In the visual stimulation (as previously mentioned, only the results of CH1 are useful), it can be seen that after 50 ms a peak is detected, this result fits with the results obtained in similar experiments.

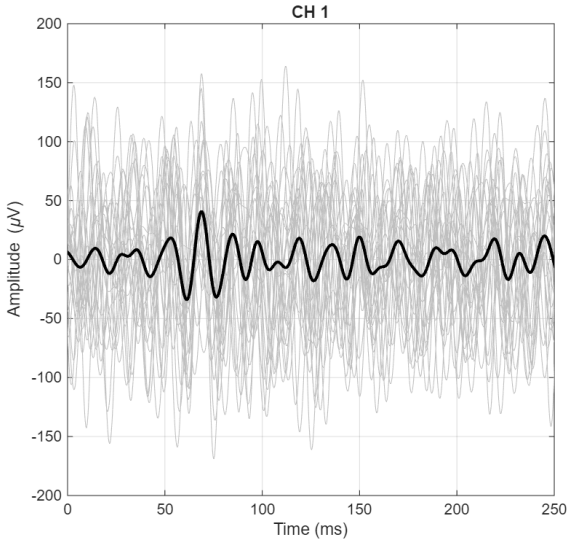

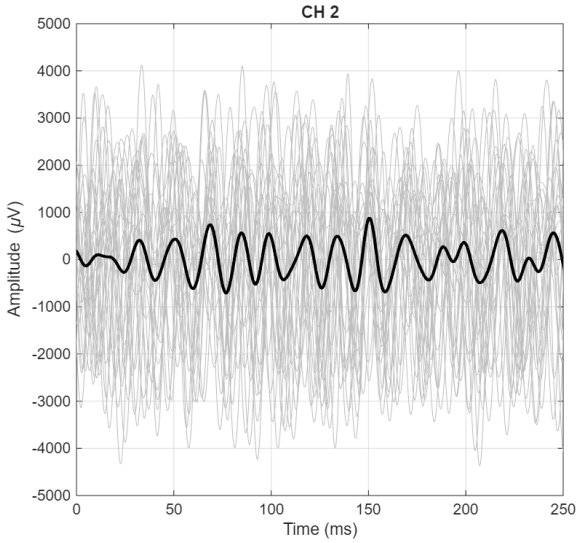

C: CONTROL OF THE ELECTRICAL NOISE

The electrical noise obtained in both electrodes (CH1 and CH2) is very similar, even though the CH2 was not properly connected, its results can be used for justifying the electrical noise.

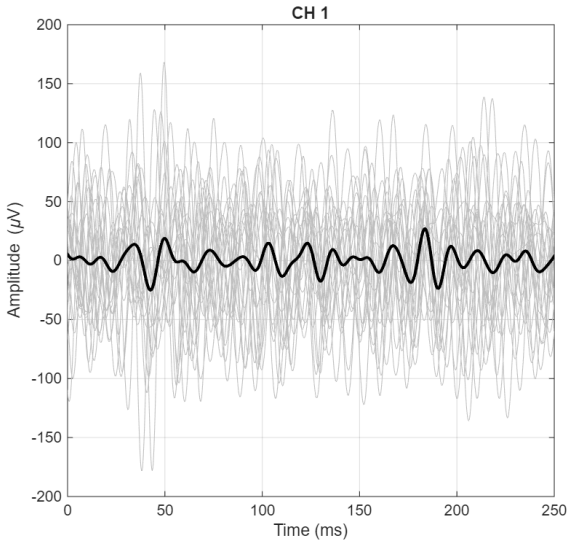

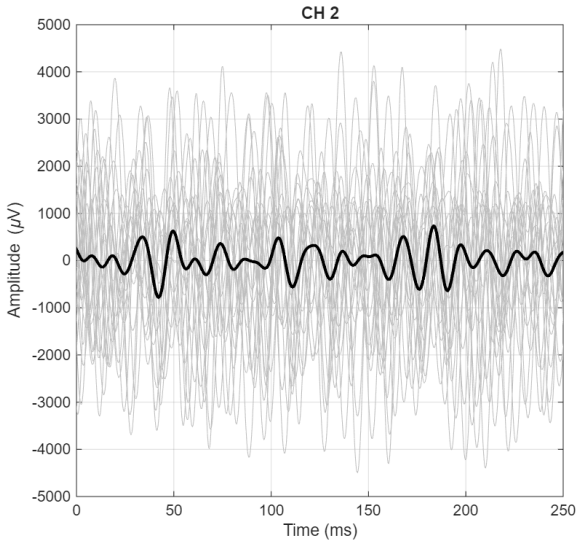

RODENT 2: PEV006

With rodent PEV006 three types of experiments were conducted: electrical stimulation, visual stimulation and electrical noise control during visual stimulation. The results obtained from the reference acquisition system do not present a relation with the obtained result and the visual pattern.

TYPE S: ELECTRICAL STIMULATION

For electrical stimulation in rodent PEV006, three values of current were used.

S1: 10 μA

For a value of $10\mu A$ of current in the stimulation it can be observed in both channels a similar waveform response to the impulse. This presents a response to electrical stimulation but not with a proper waveform.

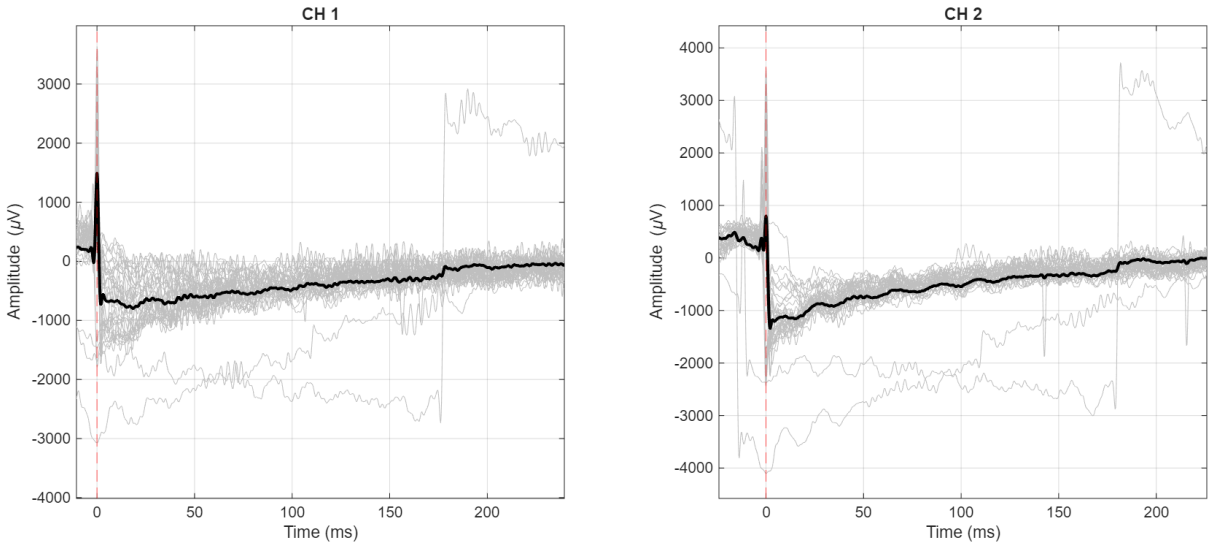

S2: 1 μA

For a value of $1\mu A$ of current in the stimulation it barely can be seen a response to the stimulation.

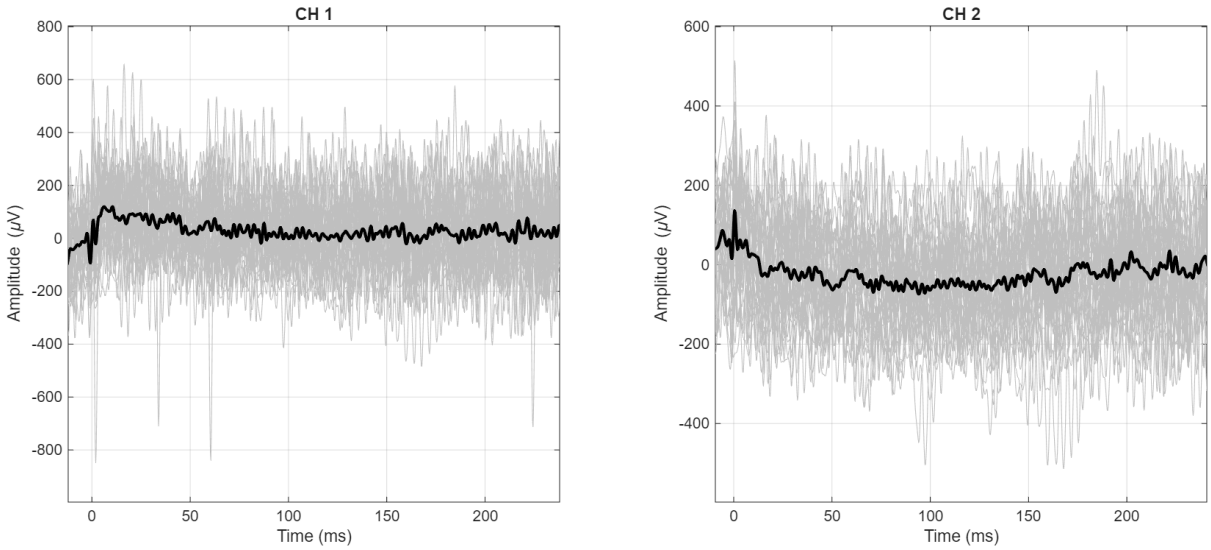

S3: $100mA$

For a value of $100mA$ of current in the stimulation it barely can be seen a response to the stimulation.

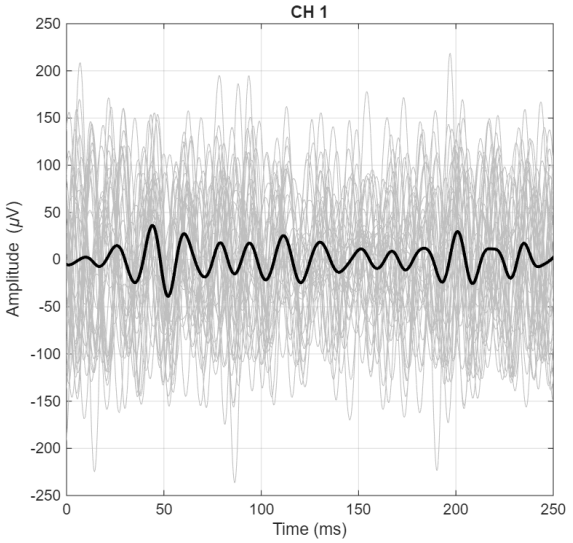

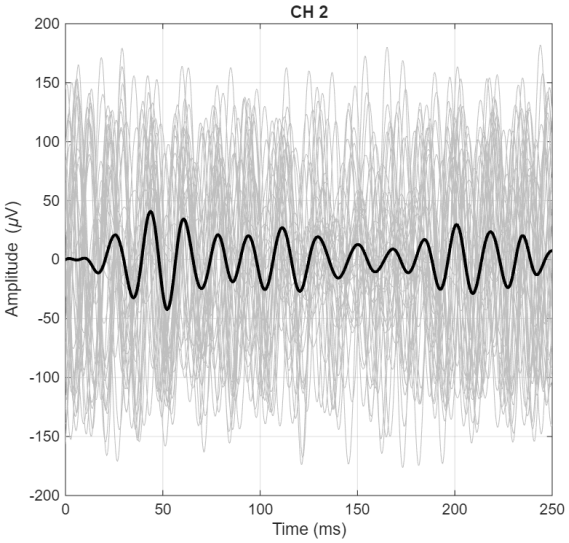

V: VISUAL STIMULATION

In the visual stimulation, no response is noticed, as can be seen in the control of electrical noise, both results seem to be similar.

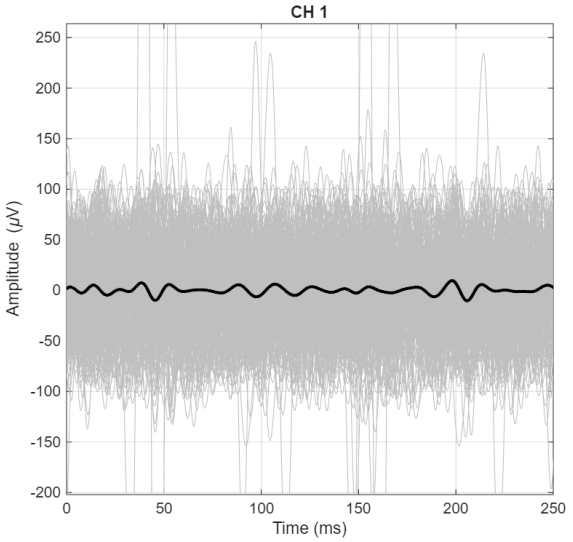

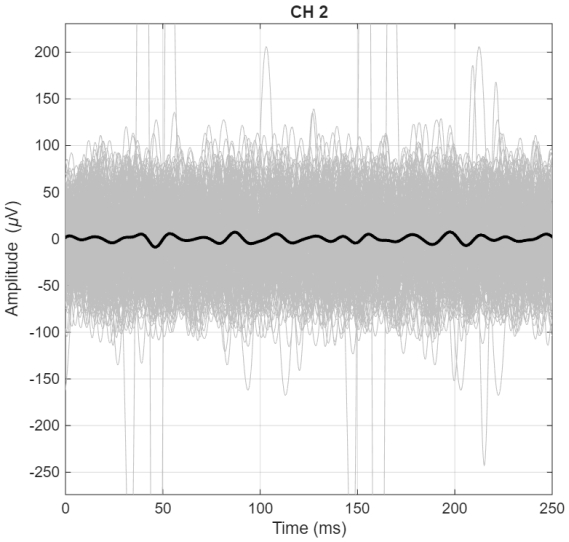

C: CONTROL OF THE ELECTRICAL NOISE

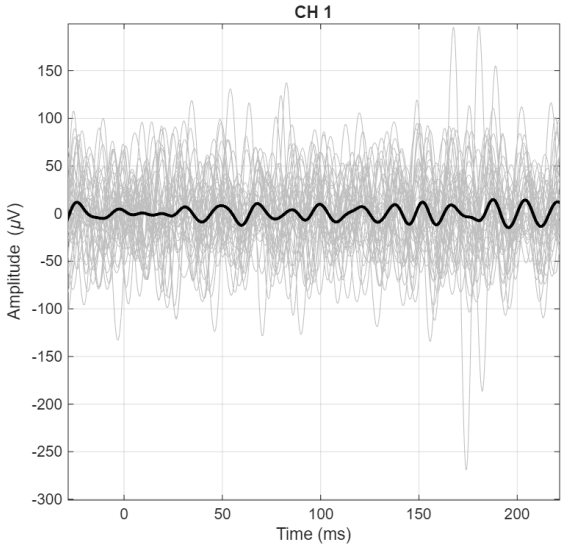

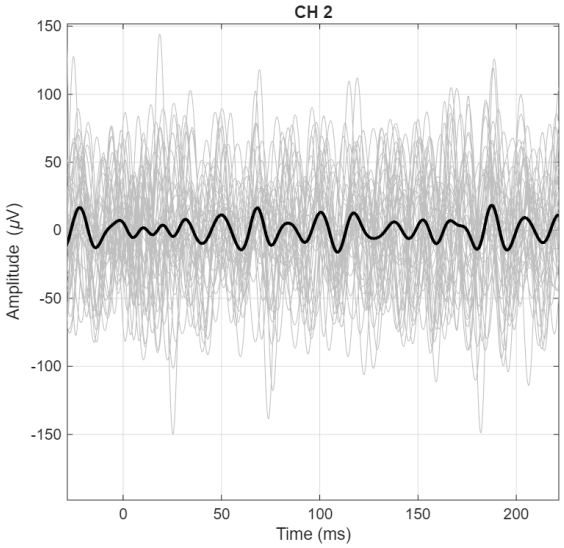

RODENT 3: PEV007

With rodent PEV007 three types of experiments were conducted, but a variation in electrical stimulation was done: electrical stimulation (with a single pulse or with a train of pulses), visual stimulation and electrical noise control during visual stimulation.

TYPE S: ELECTRICAL STIMULATION

For electrical stimulation in rodent PEV007, one value of current ($10\mu A$) is used in two configurations: a single impulse response and a train of pulses.

S1: 10 μA

For a value of $10\mu A$ of current in the stimulation it can be observed that CH1 has a not well defined response to the electrical stimulation while in CH2 a similar waveform response is presented as in other experiments.

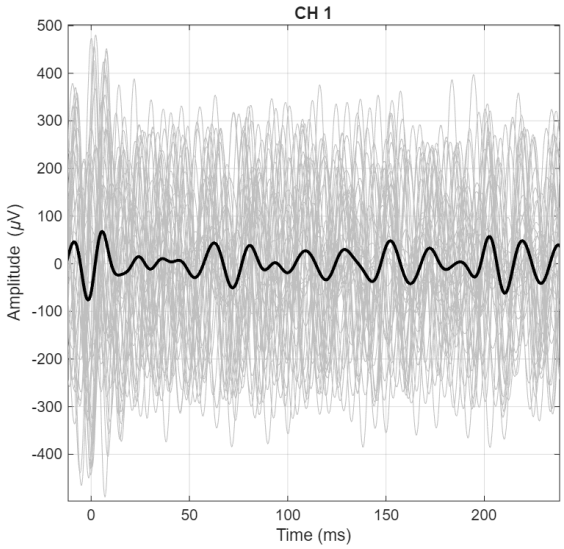

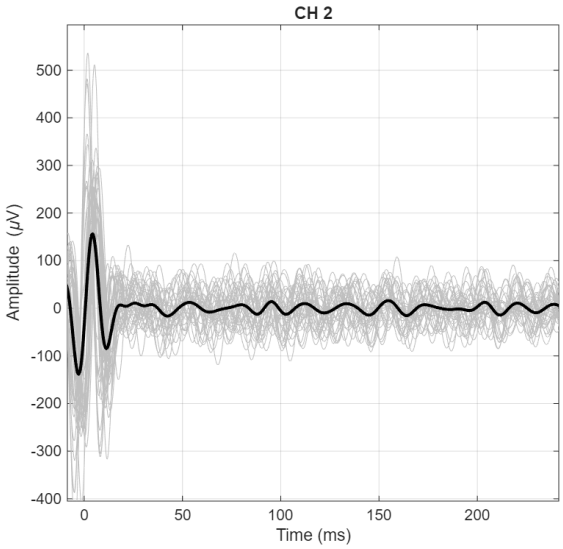

S4: 10 μA PULSE TRAIN

When a $10\mu A$ train of pulses is used, the result obtained in both channels is the one shown in the following graphs. Both channels present a similar waveform, but very noisy an chaotic.

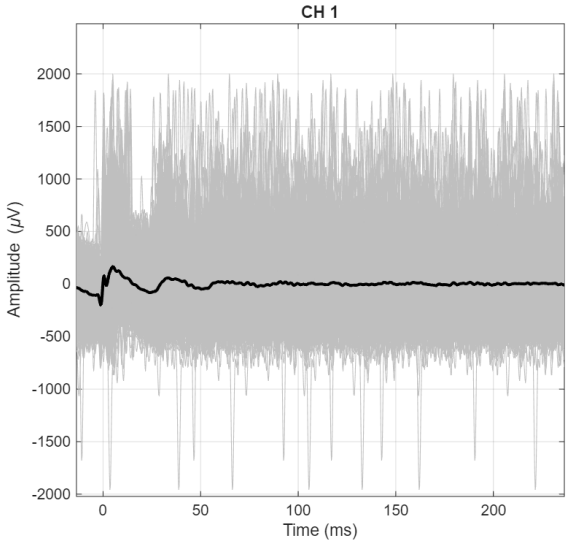

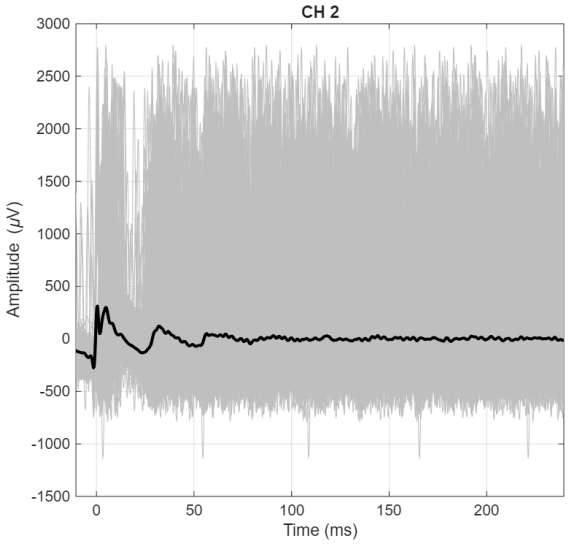

V: VISUAL STIMULATION

In the visual stimulation, no response is noticed, as can be seen in the control of electrical noise, both results seem to be similar.

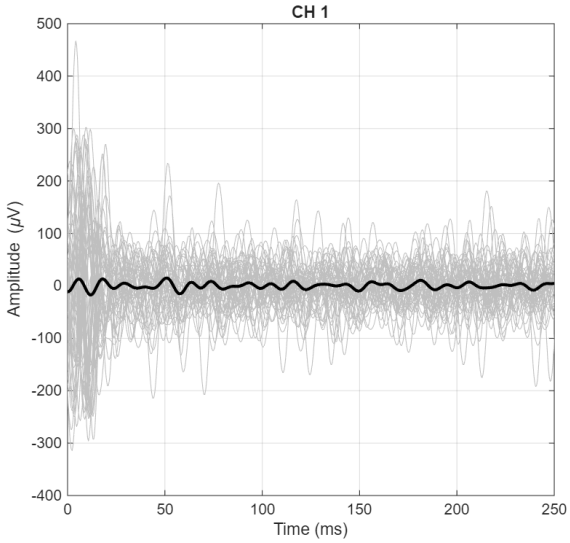

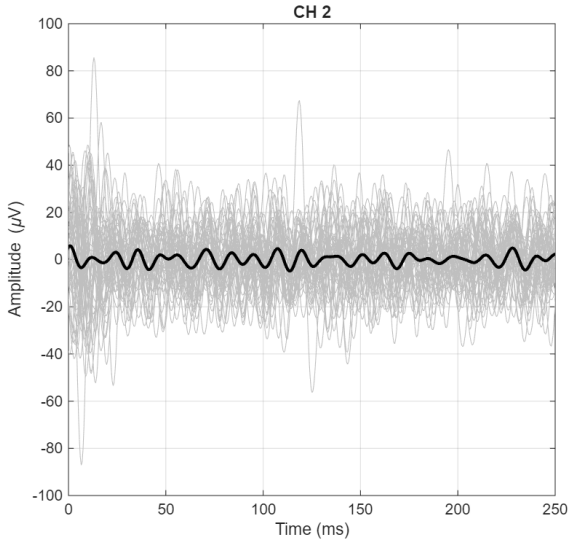

C: CONTROL OF THE ELECTRICAL NOISE